جامعة بيرزيت
BIRZEIT UNIVERSITY

**FACULTY OF GRADUATED STUDIES**

# Computational analysis for the addition reaction of diazoalkanes to alkyne (pentacarbonyl)chromium and the formation of 3H-pyrazole complexes

# تحليل باستخدام الحوسبة الكيميائية لتفاعل إضافة دايأزو ألكان إلى ألكاين-خماسي كربونيل الكروم لتكوين مركبات بيرازول

**A Thesis submitted in partial fulfillment of the requirements for the degree**

**MASTER OF APPLIED CHEMISTRY**

**By**
**Alaa Jarabaa**
**1085345**

**Supervised by: Dr.Hani Awad**

**May, 2011**
**Birzeit, Palestine**

**Computational analysis for the addition reaction of diazoalkanes to alkyne (pentacarbonyl)chromium and the formation of 3H-pyrazole complexes**

## We approve the thesis of Alaa Jarabaa

**Date of Signature**

**.....** **…..……**
**Dr. Hani Awad**
**Supervisor**
**Department of chemistry**
**Birzeit University**

**.....** **…..……**
**Assoc. Prof. Dr. Talal Shahwan**
**Member of the thesis committee**
**Department of chemistry**
**Birzeit University**

**.....** **…..……**
**Dr. Hijazi Abu Ali**
**Member of the thesis committee**
**Department of chemistry**
**Birzeit University**

## ACKNOWLEDGEMENTS

I would like to express my gratitude to my supervisor Dr. Hani Awad for his supervision, help, and guidance.

I also would like to thank the members of the thesis committee, Dr. Talal Shahwan, and Dr. Hijazi Abu Ali, for their help.

I'm very pleased to thank every member of the Department of Chemistry, especially Dr. Talal Shahwan, and Pof. Abdul Latif Abu Hijleh.

Most importantly, I would like to thank my family for their support, understanding and love.

**Birzeit,**
**May, 2011**

**Alaa Jarabaa**

# إهداء

**إلى ربي وهو أجلّ وأعظم..**
**إلى قدوتي رسول الله..**
**إلى الإسلام العظيم ..**
**إلى أمي التي جنتي تحت قدميها..**
**إلى أبي وأخواتي و إخوتي و أحبائي أبنائهم..**
**إلى ديانا..الروح التي تسكن روحي .. فتمدني بالقوة من بين ركام الضعف..**
**إلى إخوتي الذين يسمعون بهذا العالم دون أن يروه خلف قضبان الألم ..**
**إلى كل من أحببتهم في الله و أحبوني في الله..**
**إلى كل من له فضل علي و كل من له حق علي..**
**إلى كل من علمني حرفا..و كل من زرع في خيرا ..**
**إلى كل من تميز ...**

الاء جرابعة

# ABSTRACT

The addition reaction of diazoalkanes to alkyne(pentacarbonyl) chromium leads to the formation of 3H-pyrazole complexes. There are two pathways that can explain this reaction. One path is the addition of diazoalkane to the free alkyne forming the 3H-pyrazole which will react with the solvated $Cr(CO)_5$, the other path is the addition of diazoalkane to the coordinated alkyne with chromium carbonyl followed by rearrangement step to give the 3H-pyrazole complex.

The aim of present work is to assign which of the two pathways is more thermodynamically favorable. Computational calculations are done for all compounds in both paths, based on the hyprid density function theory (B3LYP), supplemented by high accuracy basis set (6-311++g (3df,pd)).

The obtained results show that the reaction prefers to proceed by the addition of the diazoalkane to the coordinated alkyne followed by rearrangement, since a lower energy barrier exist for the formation of the 3H-pyrazole. The bonding interaction type of each compound is also explained by these computational calculations.

As a result, chromium carbonyls act as a catalyst, that reduces the activation energy for the reaction to proceed faster.

## ملخص

تفاعل إضافة دايأزو ألكانات إلى ألكاين-خماسي كربونيل الكروم يؤدي إلى تكوين مركبات بيرازول .و يوجد هناك طريقين لحدوث التفاعل.

الهدف من هذه الدراسة هو تحديد أي الطريقين أفضل من حيث استهلاك الطاقة باستخدام الحوسبة الكيميائية. بحيث تمت دراسة الأشكال وكيفية الترابط و الطاقة لكل المركبات في كلا الطريقين في حالتيها المستقرة و الانتقالية.

أيدت النتائج مرور التفاعل عن طريق إضافة الدايأزو ألكان إلى ألالكاين المرتبط مع خماسي كربونيل الكروم متبوعا بإعادة ترتيب الروابط، و ذلك لأن هذا الطريق يحتاج طاقة تنشيط أقل للوصول إلى النواتج. كما أوضحت النتائج كيفية الترابط في كل مركب من هذه المركبات.

من الممكن استنتاج أن مركبات كربونيل الكروم تلعب دورا مهما كعامل مساعد لإتمام التفاعل بسرعة عن طريق تقليل طاقة التنشيط اللازمة للتفاعل.

# TABLE OF CONTENTS

# LIST OF FIGURES

**Figure** **Page**

## List of Figures cont.

**Figure** **Page**

## List of Figures cont.

**Figure** **Page**

# LIST OF TABLES

**Table** **Page**

## List of Tables cont.

**Table** **Page**

## List of Tables cont.

**Table** **Page**

# CHAPTER ONE

## PROBLEM STATEMENT

Computational chemistry is a branch of chemistry that uses computers to assist in solving chemical problems based on the principle of quantum mechanics (*1*). Computational chemistry can be used to calculate molecular geometry the shapes of molecules, bond lengths, bond angles, energies of molecules and transition states, chemical reactivity, spectroscopic data such as IR, UV, and NMR, and other properties (*2*).

Computational chemistry opens the door for chemists to model a molecular system prior to the synthesis of that molecule in the laboratory. This is very useful information because synthesizing a single compound could require months of labor and raw materials, and generate toxic waste (*3*). Furthermore, chemists can study some properties of a molecule that can be obtained computationally more easily than by experimental means (*3*).

Metal-carbon multiple bonds complexes play an important role in organometallic chemistry. They are involved in a variety of chemical

transformation, including catalytic processes such as alkenes and alkynes isomerization, hydrogenation, and epoxidation (*4,5*).

The metal-carbon multiple bond complexes are usually discussed by Dewar-Chatt-Duncanson model, which considers two synergistic bonding interactions. One is σ donation, in which the π HOMO of unsaturated ligand donates electron density to the metal's empty LUMO forming a σ bond. The second one is π-back donation, in which a metal donates electron density from its d-orbitals HOMO into the ligand's empty π* LUMO of the same symmetry (*6*).

1,3-Dipolar cycloaddition involves the reaction of the dipolarophile (π-component, like; alkenes, alkynes, carbonyls) with a 1,3-dipolar compound (three atom π-electron system with four π-electrons delocalized over the three atoms, like; ozone, azides, diazoalkanes) to produce five membered cyclic compound, as shown in Figure 1.1 (*7,8*).

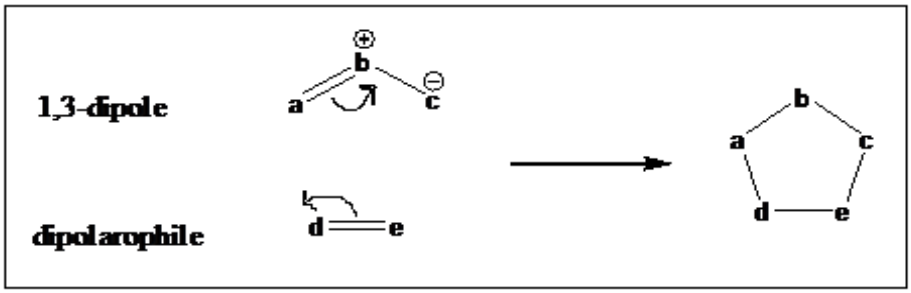


Figure 1.1: 1, 3-dipolar cycloadditon (*7*).

1,3-Dipolar cycloaddition is a powerful kind of reaction for the preparation of functionalized five member heterocyclic compounds (*7,9*). Moreover, it is highly stereospecific and stereoselective (*7,10*). Transition metal-alkyne complexes have been used as dipolarophile (*11*). 1,3-Dipolar cycloaddition reaction of diazo compounds with alkynes represents a standard method for the preparation of pyrazoles (*12*). It is controlled for simple diazoalkanes by HOMO (dipole) →LUMO (dipolarophile), which is enhanced by conjugation and electron withdrawing substituents at the dipolarophile (*7,12*).

When the dipolarophile is a metal-alkyne complex, it will have low energy LUMO, due to the electron acceptor character of the complex, and hence, reacts with electron-rich diazoalkane dipole of high HOMO energy (*7,9*). The favored interaction must be of correct orbital match, closer in energy, and sterically feasible (*7,8*).

Only very few alkyne(pentacarbonyl) complexes having terminal alkyne ligands have been isolated. Moreover, in solutions these complexes are present in a rapid equilibrium with their vinylidene tautomer (*13*).

The reaction of diazoalkanes with alkyne(pentacarbonyl)chromium to form 3H-pyrazole is proposed by Abd-Elzaher et al. (*13*) to proceed by either one of two pathways **a**, or **b** as shown in (Figure1.2) .

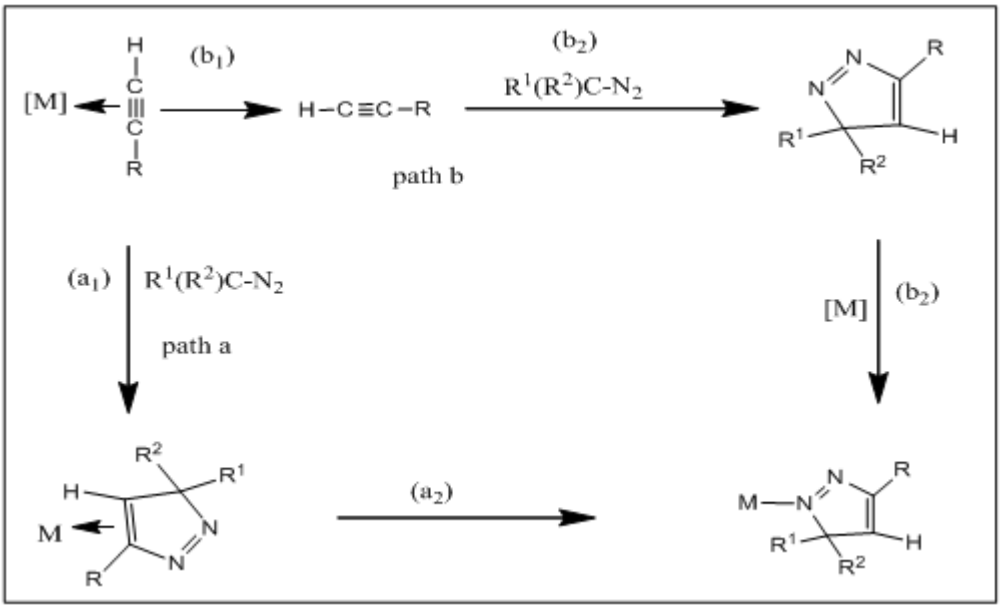


Figure 1.2: Proposed mechanisms for the addition reaction of diazoalkanes to alkyne (pentacarbonyl)chromium (*13*).

Path **a** involves the addition of the diazo compound to the coordinated alkyne (step $\mathbf{a_1}$) followed by rearrangement (step $\mathbf{a_2}$). While path **b** involves dissociation of the coordinated alkyne from alkyne(pentacarbonyl) chromium complex (step $\mathbf{b_1}$) which will lead to the formation of non-coordinated alkyne. The formed non-coordinated alkyne will react with the diazo compound (step $\mathbf{b_2}$) forming the 3H-pyrazole. Finally, the 3H-pyrazole will react with $Cr(CO)_5$(solvent)

forming the 3H-pyrazole chromium complexes. The authors of this work then concluded that path **a** is the preferred path (*13*).

Pyrazoles and their derivatives are very important class of compounds, which are applicable in many areas (*14*,*15*). They are applied for the metal ion extraction, used in agricultural herbicides, in industry as catalyst for hydrogenation of alkenes and as starting materials for synthesis of fused ring system, pharmaceutical as anti-inflammatory, antibacterial, antifungal, antitumor, and antidepressants (*14*,*15*,*16*,*17*). Furthermore, they are widely used as pigments for the synthetic leather, vinyl polymers, food, cosmetic, and drugs (*16*,*18*,*19*). Although, natural products containing pyrazole derivatives are rare, one of them occurs in watermelon seeds (*17*,*19*). As a result they have to be produced synthetically (*17*). In this study the addition reaction of 3-diazopentane to $\eta^2$-methyl prop-2-ynoate(pentacarbonyl)chromium complex to generate pentacarbonyl(3,3-diethyl-5-methoxycarbonyl-3H-pyrazol-$N_2$)chromium(0) is considered by studying bonding nature and energy of each step in both proposed mechanisms by means of computational methods. As a result, determination of which of the two pathways is more thermodynamically favorable can be assigned.

# CHAPTER TWO

# INTRODUCTION

## A) Computational background

### A.2.1) Schrödinger equation

The Schrödinger Equation is the fundamental equation of quantum mechanics (*20*). Energy and other related properties of particles can be obtained by solving it; many different wave functions are the solutions of the equation (*21*). The general form of Schrödinger equation is formulated as eigenvalue problem (*20*):

$$\hat{H}\psi = E\,\psi \qquad (2.1)$$

Where H is the Hamiltonian operator, and is equal to the sum of kinetic energy and potential energy operators for electron in the atom (*21*):

$$\hat{H} = T + V \qquad (2.2)$$

It operates on the wavefunction ψ that describes the electron, to give E the energy of the electron (eigenvalue) and set of wavefunction (eigenfunctions) ψ (*20, 21*).

### A.2.2) Schrödinger equation for hydrogen atom

The hydrogen atom is of great interest for chemists because it is the smallest atom with one electron, and can give prototype for more complex systems (*20*).

Hydrogen atom is pictured as a fixed proton at the origin and an electron of mass $m_e$, the interaction between them is through a columbic potential (*20*) as shown in Figure 2.1

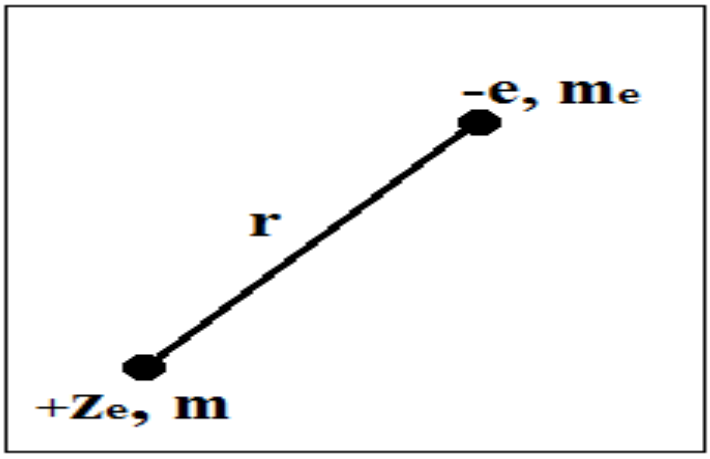


Figure 2.1: The hydrogen system.

The columbic potential is giving by:

$$V = V(r) = -\frac{Ze^2}{4\pi\varepsilon_0 r} \qquad (2.3)$$

Where **e** is the charge on the proton, $\boldsymbol{\varepsilon_0}$ is the permittivity of free space, and **r** is the distance between the electron and proton (*22*).

The Hamiltonian operator for hydrogen atom is:

$$\hat{H} = -\frac{\hbar^2}{2m}\nabla^2 - \frac{Ze^2}{4\pi\varepsilon_0 r} \qquad (2.4)$$

Where $m$ is the mass of electron, $\hbar = \frac{\boldsymbol{h}}{\boldsymbol{2\pi}}$ . Because of the spherical symmetry of the atom, it is convenient to use spherical coordinates (r, θ,Φ), where $\nabla^2$ becomes (*22*):

$$\nabla^2 = \frac{1}{r^2}\frac{\partial}{\partial r}\left(r^2\frac{\partial}{\partial r}\right) + \frac{1}{r^2}\left\{\frac{1}{\sin\theta}\frac{\partial}{\partial\theta}\left(\sin\theta\frac{\partial}{\partial\theta}\right) + \frac{1}{sin^2\theta}\frac{\partial^2}{\partial\emptyset^2}\right\} \qquad (2.5)$$

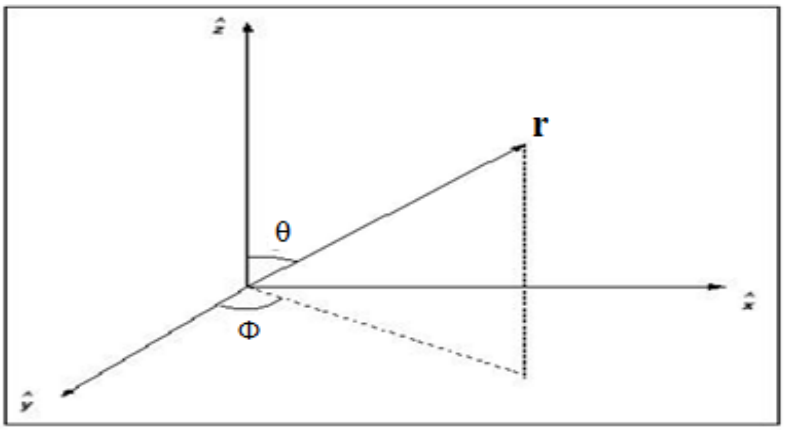


Figure 2.2: Spherical polar coordinates.

The advantage of using spherical coordinates lies in the fact that it allows to separate radial from angular coordinates (*22*).

When we substitute, eqn. 2.5 and eqn. 2.4 in eqn. 2.1, then Schrödinger equation for the hydrogen atom becomes:

$$-\frac{\hbar^2}{2m}\frac{1}{r^2\sin\theta}\left[\sin\theta\frac{\partial}{\partial r}\left(r^2\frac{\partial\psi}{\partial r}\right) + \frac{\partial}{\partial\theta}\left(\sin\theta\frac{\partial\psi}{\partial\theta}\right) + \frac{1}{\sin\theta}\frac{\partial^2\psi}{\partial\emptyset^2}\right] + V(r)\psi(r,\theta,\emptyset) = E\psi(r,\theta,\emptyset) \qquad (2.6)$$

Equation 2.6 can be solved exactly by using the separation of variables method, to give hydrogen wavefunctions in the form of (*23*):

$$\psi_{nlm} = R_{nl}(r)Y_l^m(\theta, \emptyset) \qquad (2.7)$$

Where $n$ is the principal quantum number, $l$ is the azimuthal quantum number (angular momentum), and $m$ is the magnetic quantum number.

For $n$=1, $l$ =0, $m$ =0,

$$\psi_{1s} = \frac{1}{\pi^{1/2}}\left(\frac{Z}{a}\right)^{3/2} e^{-Zr/a} \qquad (2.8)$$

The quantity Z is the atomic number of the nucleus, and $a_0$ is Bohr radius (*20*).

$$a_0 = \frac{4\pi\varepsilon_0\hbar^2}{m_e e^2} \qquad (2.9)$$

The second wavefunction is for 2s is given by:

$$\psi_{2s} = \frac{1}{4(2\pi)^{\frac{1}{2}}}\left(\frac{Z}{a}\right)^{\frac{3}{2}}\left(2 - \frac{Zr}{a}\right)e^{-Zr/2a} \qquad (2.10)$$

According to the solution of Schrödinger equation, the energy (eigenvalues) must be quantized, which is in agreement with Bohr model for hydrogen atom (*20*).

$$E_n = -\frac{Zm_e e^4}{32\pi^2\varepsilon_0{}^2\hbar^2 n^2} = -\frac{Ze^2}{8\pi\varepsilon_0 a_0 n^2} \qquad \text{n = 1,2,…} \qquad (2.11)$$

### A.2.3) Schrödinger equation for helium atom

The helium system can be pictured as a nucleus of mass **m** at the origin and two electrons of mass $\mathbf{m_e}$ interacting with the proton and with each other through a columbic potential.

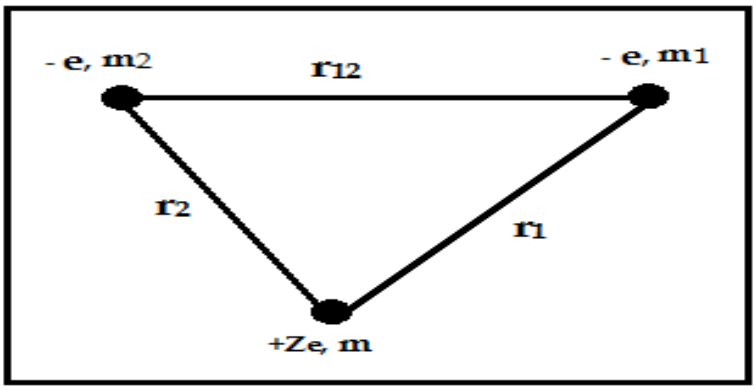


Figure 2.3: Helium system.

The Hamiltonian operator of helium system is giving by:

$$\hat{H} = -\frac{\hbar^2}{2m}\nabla^2 - \frac{\hbar^2}{2m_{e1}}\nabla_1^2 - \frac{\hbar^2}{2m_{e2}}\nabla_2^2 - \frac{2e^2}{4\pi\varepsilon_0 r_1} - \frac{2e^2}{4\pi\varepsilon_0 r_2} + \frac{2e^2}{4\pi\varepsilon_0 r_{12}} \qquad (2.12)$$

Then the Schrödinger equation for helium is expressed as

$$\left(-\frac{\hbar^2}{2m}\nabla^2 - \frac{\hbar^2}{2m_e}\nabla_1^2 - \frac{\hbar^2}{2m_e}\nabla_2^2 - \frac{2e^2}{4\pi\varepsilon_0 r_1} - \frac{2e^2}{4\pi\varepsilon_0 r_2} + \frac{2e^2}{4\pi\varepsilon_0 r_{12}}\right)\psi(r_1, r_2, r_{12}) = E\psi(r_1, r_2, r_{12}) \qquad (2.13)$$

$\nabla^2$ is the laplacian operator with respect to the position of nucleus,$\nabla_1^2$ and $\nabla_2^2$ are the laplacian operators with respect to electrons positions (*20,24*).

Equation 2.13 can be simplified by the use of Born-Oppenheimer approximation since m»$m_e$, so that the nucleus can be assumed to be stationary and the kinetic energy operator for the nucleus is thus taken as zero. Consequently, the Schrödinger equation becomes,

$$\left(-\frac{\hbar^2}{2m_e}\nabla_1^2 - \frac{\hbar^2}{2m_e}\nabla_2^2 - \frac{2e^2}{4\pi\varepsilon_0 r_1} - \frac{2e^2}{4\pi\varepsilon_0 r_2} + \frac{2e^2}{4\pi\varepsilon_0 r_{12}}\right)\psi(r_1, r_2) = E\psi(r_1, r_2) \quad (2.14)$$

Even with this simplification, the equation cannot be solved exactly, since the interelectronic repulsion given by the term $\frac{2e^2}{4\pi\varepsilon_0 r_{12}}$.

Equation (2.14) without the interelectronic term looks as the sum of two hydrogenlike atoms (*20*,*24*). To solve equation (2.14) approximation methods should be used, and this will be covered in section 2.5.

**A.2.4) Schrödinger equation for molecules**

Hydrogen molecule is the simplest molecule, and for simplicity it can be taken as example of other molecules.

The Hamiltonian operator for hydrogen molecule is given by

$$\hat{H} = -\frac{\hbar^2}{2M}(\nabla_A^2 + \nabla_B^2) - \frac{\hbar^2}{2m_e}(\nabla_1^2 + \nabla_2^2) - \frac{e^2}{4\pi\varepsilon_0 r_{1A}} - \frac{e^2}{4\pi\varepsilon_0 r_{1B}} - \frac{e^2}{4\pi\varepsilon_0 r_{2A}} - \frac{e^2}{4\pi\varepsilon_0 r_{2B}} + \frac{e^2}{4\pi\varepsilon_0 r_{12}} + \frac{e^2}{4\pi\varepsilon_0 R} \quad (2.15)$$

Here M is the mass of each of hydrogen atom nucleus, $m_e$ is the electron mass, r is the distance, the subscripts A and B refer to the nuclei of the individual atoms, the subscripts 1 and 2 refer to the individual electrons. The distances used are given in Figure 2.4 (*20*,*24*).

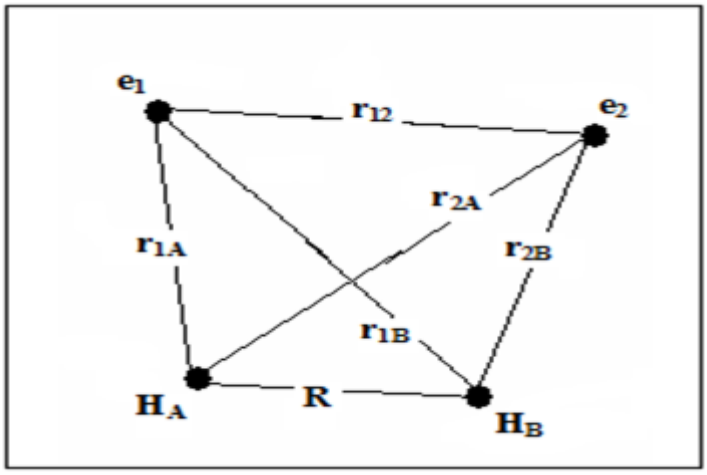


Figure 2.4: Hydrogen molecule system.

Equation 2.15 can be broken into the following terms;

* $[-\frac{\hbar^2}{2M}(\nabla_A^2 + \nabla_B^2)]$: the kinetic energy of the two nuclei.

* $[-\frac{\hbar^2}{2m_e}(\nabla_1^2 + \nabla_2^2)]$: kinetic energy of the two electrons.

*$[-\frac{e^2}{4\pi\varepsilon_0 r_{1A}} - \frac{e^2}{4\pi\varepsilon_0 r_{1B}} - \frac{e^2}{4\pi\varepsilon_0 r_{2A}} - \frac{e^2}{4\pi\varepsilon_0 r_{2B}}]$: potential energy arising from the attraction between the nuclei and electrons.

*$[+\frac{e^2}{4\pi\varepsilon_0 r_{12}} + \frac{e^2}{4\pi\varepsilon_0 R}]$: potential energy arising from the electron-electron, and nuclear-nuclear repulsions (*20*).

Based on the Born-Oppenheimer approximation, which neglects the nuclear motion , the term of nuclear kinetic energy in the Hamiltonian operator can be dropped out as shown in equation 2.16 (*20*,*24*).

$$\widehat{H} - \frac{\hbar^2}{2m_e}(\nabla_1^2 + \nabla_2^2) - \frac{e^2}{4\pi\varepsilon_0 r_{1A}} - \frac{e^2}{4\pi\varepsilon_0 r_{1B}} - \frac{e^2}{4\pi\varepsilon_0 r_{2A}} - \frac{e^2}{4\pi\varepsilon_0 r_{2B}} + \frac{e^2}{4\pi\varepsilon_0 r_{12}} + \frac{e^2}{4\pi\varepsilon_0 R} \quad (2.16)$$

It is obvious that the increase in the number of electrons and nuclei in the system will increase and complicate the number of terms of repulsions and make it more difficult to solve the equation directly. Approximation methods must be used to give an approximate solution for each system (*20*,*24*).

**A.2.5) Approximation methods**

As we have seen in previous sections that Schrödinger equation cannot be solved exactly for any atom or molecule more complicated than the hydrogen atom (*20*). So approximation methods are needed to solve the equation for those complicated systems. The two basic methods of approximation are variation and perturbation theories (*25*). In variation theory, an initial guess is made for wavefunction, which is then optimized to approximate the true wavefunction for the problem (*25*).

Alternatively, in the perturbation theory Schrödinger equation is separated into parts, at which a solution of previously solved model problem is used as a starting point to approximate the true wavefunction for the Schrödinger equation of interest (*25*).

**A.2.5.1) Variation method**

The basic idea of the variational method is to guess a trial wavefunction, which consists of some adjustable parameters called "variational parameters" These parameters are adjusted until the energy of the trial wavefunction is minimized. The resulting trial wavefunction and its corresponding energy are variational method approximations to the exact wavefunction and energy (*26*).

To illustrate variational principal a system at the ground state, with $\psi_0$ the ground state function and the energy $E_0$ which satisfy the Schrödinger equation shall be considered

$$\hat{H}\psi_0 = E_0\psi_0 \qquad (2.17)$$

Multiply equation 2.19 by $\psi_0^*$ and integrate over all space and rearrange it we get

$$E_0 = \frac{\int \psi_0^* \hat{H} \psi_0 d\tau}{\int \psi_0^* \psi_0 d\tau} \qquad (2.18)$$

Where dτ is volume element (*20,24*).

If we choose any normalized acceptable function ∅ (trail function) for $\psi_0$ (*27*),

$$E_{\emptyset} = \frac{\int \emptyset^* \hat{H} \emptyset \, d\tau}{\int \emptyset^* \emptyset \, d\tau} \quad (2.19)$$

Then $E_{\emptyset}$ calculated by equation 2.19 is greater than $E_0$, ground state energy, this is a variational principal (*20*,*24*).

$$E_{\emptyset} \geq E_0 \quad (2.20)$$

Which means that an upper limit on $E_0$ can be calculated by using any trail function with appropriate electronic and nuclear coordinates to be operated upon by the Hamiltonian (*20*,*24*,*28*). The equality occurs if the trail function is identical to the ground state wavefunction of the system (*29*).

∅ can be chosen such that it depends on parameters, called variational parameters, so as $E_{\emptyset}$ depend on them too, $E_{\emptyset}(\alpha, \beta, \gamma \ldots)$ (*20*,*24*).

$E_{\emptyset}$ then can be minimize with respect to each of the variational parameters and thus approach ground state energy $E_0$ (*20*,*24*).

It is possible to use a trail function as a linear combination of functions equation 2.21

$$\emptyset = \sum_{n=1}^{N} c_n f_n \quad (2.21)$$

$c_n$ are variational parameters and $f_n$ the functions (*20*,*23*,*24*).

Taking N = 2 for simplicity,

$$\emptyset = c_1 f_1 + c_2 f_2 \tag{2.22}$$

Then substitute in the numerator of equation 2.19,

$$\int \emptyset \, \widehat{H} \, \emptyset \, d\tau = \int (c_1 f_1 + c_2 f_2) \widehat{H} (c_1 f_1 + c_2 f_2) \, d\tau$$

$$= c_1^2 \int f_1 \widehat{H} f_1 d\tau + c_1 c_2 \int f_1 \widehat{H} f_2 d\tau + c_1 c_2 \int f_2 \widehat{H} f_1 d\tau \; + \; c_2^2 \int f_2 \widehat{H} f_2 d\tau$$

$$= c_1^2 H_{11} + c_1 c_2 H_{12} + c_1 c_2 H_{21} + c_2^2 H_{22} \tag{2.23}$$

Where

$$H_{ij} = \int f_i \widehat{H} f_j \, d\tau \tag{2.24}$$

And $H_{ij} = H_{ji}$ because Hamiltonian operator $\widehat{H}$ is Hermitian (*20,23,24*),

Then

$$\int \emptyset \widehat{H} \emptyset \, d\tau = c_1^2 H_{11} + 2 c_1 c_2 H_{12} + c_2^2 H_{22} \tag{2.25}$$

Applying the same, by substituting equation 2.22 in the denominator of equation 2.19 we have (*20, 23, 24*)

$$\int \emptyset^2 d\tau = c_1^2 S_{11} + 2 c_1 c_2 S_{12} + c_2^2 S_{22} \tag{2.26}$$

Where

$$S_{ij} = S_{ji} = \int \emptyset_i \emptyset_j \, d\tau \tag{2.27}$$

Putting them together into equation 2.19, where $H_{ij}$ and $S_{ij}$ called matrix element, will give

$$E(c_1, c_2) = \frac{c_1^2 H_{11} + 2c_1 c_2 H_{12} + c_2^2 H_{22}}{c_1^2 S_{11} + 2c_1 c_2 S_{12} + c_2^2 S_{22}} \quad (2.28)$$

A necessary condition for minimum in a function $E(c_1, c_2, \ldots.)$ of several variables is that partial derivative with respect to each of the variables must be zero at the minimum, so differentiating equation 2.28 with respect to $c_1$ and then with respect to $c_2$ give equation 2.29 and 2.30 respectively (20,23,24),

$$c_1(H_{11} - ES_{11}) + c_2(H_{12} - ES_{12}) = 0 \quad (2.29)$$

$$c_1(H_{12} - ES_{12}) + c_2(H_{22} - ES_{22}) = 0 \quad (2.30)$$

These two equations formed a pair of linear algebraic equations for $c_1$ and $c_2$. From the linear algebraic theorem there is a solution for them other than trivial solution $c_1 = c_2 = 0$, the determinant of the coefficients must vanish, at N = 2, we have (20,23,24)

$$\begin{vmatrix} H_{11} - ES_{11} & H_{12} - ES_{12} \\ H_{12} - ES_{12} & H_{22} - ES_{22} \end{vmatrix} = 0 \quad (2.31)$$

This is called secular determinant, from it we can obtain a quadratic equation called secular equation which gives two values for E, the smaller can be taken as the approximation for the ground state energy (20,23,24).

A trial function with many parameters gives almost accurate results. Hence using a linear combination of N functions, will give us N× N

determinant 2.32, with the $N^{th}$ order polynomial in E, and so $N^{th}$ order secular equation, then the smallest root of $N^{th}$ order solution is chosen as the approximation to the energy, which should be more accurate approximation (*20,23,24*). However, it is difficult to solve this numerically or graphically, instead, computers with special software packaged do this (*20,24*)

$$\begin{vmatrix} H_{11}-ES_{11} & H_{12}-ES_{12} & \cdots & H_{1N}-ES_{1N} \\ H_{21}-ES_{21} & H_{22}-ES_{22} & \cdots & H_{2N}-ES_{2N} \\ \vdots & \vdots & \vdots & \vdots \\ H_{N1}-ES_{N1} & H_{N2}-ES_{N2} & \cdots & H_{NN}-ES_{NN} \end{vmatrix} = 0. \qquad (2.32)$$

The variational method lies behind the Hartree-Fock theory (HF) and the configuration interaction method (CI) for the electronic structure of atoms and molecules (*26*).

**A.2.5.2) Perturbation method**

Perturbation theory is the second most widely used approximation method in quantum chemistry (*30*). The idea behind the perturbation theory is to split the Hamiltonian into a part we know how to solve unperturbed Hamiltonian, and a part we don't know how to solve the perturbation (*31*).

To solve a problem of equation 2.1 for a system of interest using first order perturbation theory (*20,24*)

$$\hat{H}\psi = E\,\psi \tag{2.1}$$

Hamiltonian operator should be split to give unperturbed Hamiltonian denoted by $\hat{H}^{(0)}$ and perturbation Hamiltonian denoted by $\hat{H}^{(1)}$, then it can be written as

$$\hat{H} = \hat{H}^{(0)} + \hat{H}^{(1)} \tag{2.33}$$

Where the Schrödinger equation with known solution is given by

$$\hat{H}^{(0)}\psi^{(0)} = E^{(0)}\psi^{(0)} \tag{2.34}$$

And ψ and E should be in the form

$$\psi = \psi^{(0)} + \Delta\psi \tag{2.35}$$

$$E = E^{(0)} + \Delta E \tag{2.36}$$

Where $\psi^{(0)}$ and $E^{(0)}$ are given by the solution of the unperturbed problem, and $\Delta\psi, \Delta E$ are small quantities (*20*,*24*). Substituting equations 2.33, 2.35 and 2.36 into equation 2.1 one obtains

$$\hat{H}^{(0)}\psi^{(0)} + \hat{H}^{(1)}\psi^{(0)} + \hat{H}^{(0)}\Delta\psi + \hat{H}^{(1)}\Delta\psi = E^{(0)}\psi^{(0)} + \Delta E\psi^{(0)}$$

$$+E^{(0)}\Delta\psi + \Delta E\Delta\psi \tag{2.37}$$

Since $\hat{H}^{(0)}\psi^{(0)} = E^{(0)}\psi^{(0)}$, the first term in each equation side is cancelled, and since $(\hat{H}^{(1)}\Delta\psi)$ and $(\Delta E\Delta\psi)$ are small quantities they can be neglected in first order perturbation theory (*20*,*24*), so the equation with unknown $\Delta\psi$ and $\Delta E$ becomes

$$\hat{H}^{(1)}\psi^{(0)} + \hat{H}^{(0)}\Delta\psi = \Delta E\psi^{(0)} + E^{(0)}\Delta\psi \qquad (2.38)$$

Rewriting this equation and multiplying both sides by $\psi^{(0)*}$ and integrating over all space gives

$$\int \psi^{(0)*}\left[\hat{H}^{(0)} - E^{(0)}\right]\Delta\,\psi\, d\tau + \int \psi^{(0)*}\hat{H}^{(1)}\psi^{0}\, d\tau = \Delta E \int \psi^{(0)*}\psi^{(0)} d\tau \qquad (2.39)$$

$\int \psi^{(0)*}\psi^{(0)} d\tau = 1$ (Normalization).

$\int \psi^{(0)*}\left[\hat{H}^{(0)} - E^{(0)}\right]\Delta\,\psi\, d\tau = \int\{\left[\hat{H}^{(0)} - E^{(0)}\right]\psi^{(0)}\}^{*}\Delta\psi\, d\tau = 0\, \hat{H}^{(0)} - E^{(0)}$

Hermitian, then integrand vanishes.

Then equation 2.39 becomes (*20*,*24*),

$$E^{(1)} = \int \psi^{(0)*}\hat{H}^{(1)}\psi^{(0)}\, d\tau \qquad (2.40)$$

Which is a first order correction to $E^{(0)}$, then the energy to the first order is given by

$$E = E^{(0)} + \int \psi^{(0)*}\hat{H}^{(1)}\psi^{(0)}\, d\tau + higher - order\ terms \qquad (2.41)$$

If we want to calculate higher order terms for energy and wave functions computers, with special software packaged are needed (*20*,*24*). The perturbation method lies behind Møller–Plesset perturbation theory (MP) for the electronic structure of atoms and molecules (*21*).

## A.2.6) Basis set

A basis set is mathematical functions (basis functions) that used in ab-initio method, and DFT method calculations to describe the shape of

the orbitals within a system. Which in turn combine to approximate the total electronic wavefunction (*3*,*32*). They are expanded as a linear combination of such functions with coefficients; usually these functions are atomic orbitals. A mathematical description for linear combination of atomic orbitals (LCAO) is

$$\psi_i = c_{1i}\chi_1 + c_{2i}\chi_2 + \cdots + c_{ni}\chi_n \quad (2.42)$$

Or

$$\psi_i = \sum_{\mu}^{n} c_{\mu i}\chi_\mu \quad (2.43)$$

Where $\psi_i$ is a molecular orbital represented as the sum of n atomic orbitals $\chi_\mu$, each multiplied by a corresponding coefficient $c_{\mu i}$. The coefficients are the weights of the contributions of the n atomic orbitals to the molecular orbital (*28*).

Number and type of basis set influence the accuracy of approximation. The larger the basis set, the more accurate representation (*33*).

**A.2.6.1) Functional form**

The basis orbitals commonly used in electronic structure calculations fall into two classes: Slater Type Orbitals (STO) and Gaussian Type Orbitals (GTO) (*33*).

Slater type orbitals are proposed by J.C.Slater in 1930, as a kind of modification of mathematical functions for hydrogen orbitals to fit many-electron system (*34*).

STOs are described by the function depending on spherical coordinates

$$S_{\zeta,n,l,m}(r,\theta,\emptyset) = \chi_{\zeta,n,l,m}(r,\theta,\emptyset) = N_{\zeta,n,l,m} r^{n-1} e^{-\zeta r} Y_l^m(\theta,\emptyset) \quad (2.44)$$

STO are characterized by quantum numbers $n, l, and\ m$, the symbol $N_{\zeta,n,l,m}$ denotes the normalization constant, $Y_l^m$ are spherical harmonics, r is the radius in angstroms, $\zeta$ (zeta) is orbital exponent gives the radial orbital size which control the width of the STO, and it can be calculated by

$$\zeta = \frac{Z-s}{n^*} \quad (2.45)$$

The term **s** is the shielding constant and **n*** is a parameter that varies with the principal quantum number **n**, and **Z** the atomic number (*24*,*25*,*32*,*33*,*35*).

Unfortunately, Slater orbitals are not suitable for fast calculations, because it is difficult to evaluate necessary integrals over these STOs, especially integrals involving more than one nuclear center because of its dependence of rapid exponential function (*20*,*32*,*33*).

Frank Boys, in 1950s suggested a modification to the wavefunction by introducing Gaussian type functions, which contain the exponential $e^{-\zeta r^2}$, rather than the $e^{-\zeta r}$ of the STOs, such functions are very easy to evaluate (*32*). Gaussian type orbitals can be written in terms of polar or Cartesian coordinates as shown in equation 2.46,

$$G_{\zeta,n,l,m}(r,\theta,\emptyset) = \chi_{\zeta,n,l,m}(r,\theta,\emptyset) = N_{\zeta,n,l,m} r^{n-1} e^{-\zeta r^2} Y_l^m(\theta,\emptyset) \quad (2.46a)$$

$$G_{\zeta,l_x,l_y,l_z}(X,Y,Z) = \chi_{\zeta,l_x,l_y,l_z}(X,Y,Z) = N_{\zeta,l_x,l_y,l_z} X^{l_x} Y^{l_y} Z^{l_z}\ e^{-\zeta r^2} \quad (2.46b)$$

Where $l_x$, $l_y$ and $l_z$ the angular shape and direction of the orbital, the sum of $l_x$, $l_y$ and $l_z$ determines the type of orbital (for example $l_x + l_y + l_z = 1$ is a p-type orbital, $l_x + l_y + l_z = 2$ is d-type orbital) (*28*,*30*,*32*,*33*). Although GTOs are used conveniently, they have many deficiencies. GTOs have a problem representing a proper behavior near nucleus, since they have a zero slope at r = 0, in contrast with STOs which has a cusp at r = 0 (discontinuous derivative), which is a characteristic of hydrogenlike solutions (*28*,*33*,*35*). In addition, GTOs depend on $e^{-r^2}$, while STOs depend on $e^{-r}$ which results in reduction in amplitude with distance for GTOs (*28*,*33*).

**A.2.6.2)Contracted Gaussian Functions and minimal basis set**

To overcome this weakness of GTOs, It is common to combine the best feature of GTOs (computational efficiency) with that of STOs

(proper radial shape) (*28,32,35*). The resultant functions are the sum of GTOs fitting STO (*28*), the fit improving with N, the number of GTOs used in combination.

$$\varphi^{CGTO}_{(x,y,z,\zeta,l_x,l_y,l_z)} = \sum_{a=1}^{N} d_a \, \emptyset^{GTO}_{(x,y,z,\zeta_a,l_x,l_y,l_z)} \qquad (2.47)$$

$d_a$ chosen to optimize the shape of the basis function sum and ensure normalization. This linear combination of GTOs is called "Contraction basis functions", while the individual Gaussian is called "primitive" (*28*). In a basis set of contracted GTOs, each basis function is defined by the contraction coefficients d and exponents ζ of each of its primitives (*28*).

Since N GTOs are used to represent one Slater orbital it is commonly called STO-NG basis set (*20*). It was discovered that the optimum fit when N = 3, Figure 2.5 illustrate different combination of GTOs that fit STO for 1s orbital (*20,28*).

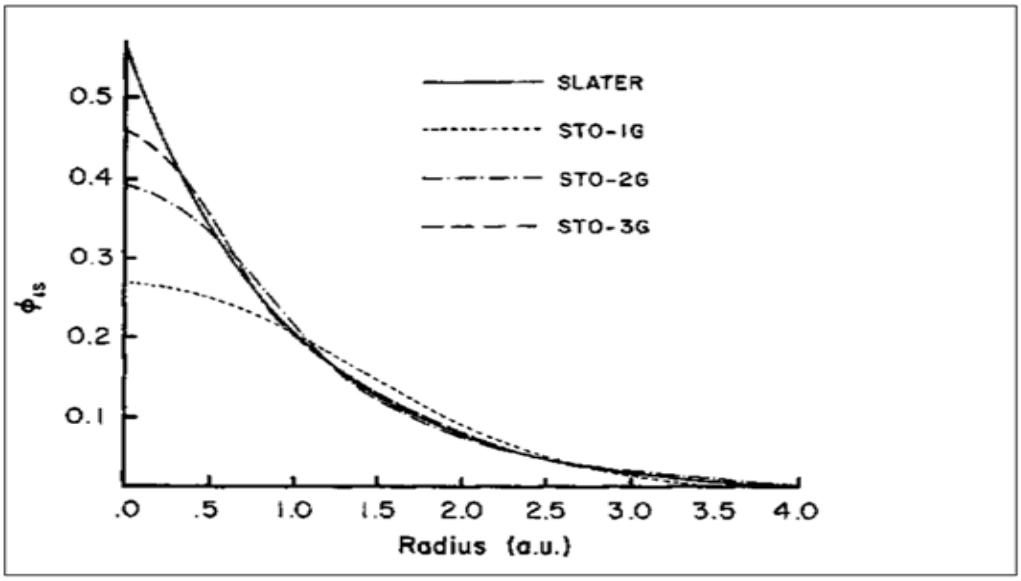


Figure 2.5: Comparison of the quality of the least-squares fit of a 1s Slater function ($\zeta = 1.0$) obtained at the STO-1G, STO-2G, and STO-3G levels (*20*).

The smallest basis sets used, which called minimal basis set is the STO-NG (N = 1, 2, 3,….), at which only one basis function defined for the atomic orbital, the number of STO-NG or the CGTO is equal to the number of core and valence atomic orbitals in the atom (*3*,*28*,*35*), for example carbon atom has five atomic orbital (1s, 2s, $2p_x$, $2p_y$, $2p_z$) which can be described by five STO-3G, while the number of primitive GTOs is fifteen.

**A.2.6.3) Multiple Zeta(ζ), and split valence**

Minimal basis set has some problems, the atomic orbitals use fixed exponent ζ, so all orbitals of given type are identical in size (*20*). Furthermore, it is unable to reproduce the anisotropic charge

distribution (*20*). To solve these problems computational chemists introduced Multiple Zeta basis sets (*20*).

Multiple Zeta basis set includes double zeta (DZ), triple zeta (TZ), Quadruple Zeta (QZ) and Pentuple Zeta (PZ) (*33*). The term zeta stems from the fact that the exponent of STO basis functions is often denoted by the Greek letter $\zeta$ (*28*). Double Zeta basis set is made of two functions for each AO, Triple Zeta basis set is formed of three functions for each AO, and so on ..

In Double Zeta an atomic orbital is expressed as sum of two STOs that differ only in the value of their exponent $\zeta$. For example, 2s is written as

$$\emptyset_{2s}(r) = \emptyset_{2s}^{STO}(r, \zeta_1) + d\emptyset_{2s}^{STO}(r, \zeta_2) \qquad (2.48)$$

This means that an atomic orbital whose size can range between that specified by $\emptyset_{2s}^{STO}(r, \zeta_1)$ and $\emptyset_{2s}^{STO}(r, \zeta_2)$ by varying the constant d (*20,28*).

In Triple Zeta an atomic orbital is expressed as sum of three STOs that differ only in $\zeta$.

Since the chemical bonding occurs between valence orbitals, then the core orbitals are weakly affected by chemical bonding. Valence orbitals, on the other hand, can vary widely as a function of chemical

bonding (*28,33*). So that, only the valence orbitals are expressed by multiple zeta (*20*).

Split valence basis sets describe the core electrons by a single Slater orbital and the valence electrons by the sum of Slater orbitals, each STO could be expressed as linear combination of GTOs (*20*).

Amongst the most widely used split-valence basis sets are those of Pople *et al*. .These basis sets include 3-21G, 6-21G, 4-31G, 6-31G, and 6-311G. The first number indicates the number of primitive Gaussian functions used to describe contracted core functions, the hyphen indicates that we have split valence basis set, the numbers after the hyphen indicate the numbers of primitives used to describe the valence functions; if there are two such numbers, it is a valence-double-$\zeta$ basis, if there are three, valence-triple-$\zeta$ (*20,28*).

For example, carbon atom described by a 6-31G,where 6 tells that 1s orbital on the core orbital is giving by a sum of 6 primitive Gaussian functions. The hyphen indicates a split valence basis set, telling that 2s and 2p orbitals are each represented by a pair of Slater orbitals. One of these Slater orbitals is represented by a sum of three Gaussian functions, and the other is represented by a single Gaussian function. i.e. nine atomic orbitals with twenty two GTOs (*20*).

### A.2.6.4) Polarization functions

Polarization functions can be added to basis sets to try to model the polarization effect (atomic orbitals distortion) as two atoms are brought close together. The electron cloud on one atom introduces a distortion in the shape of the electron cloud in the neighboring atom. Polarization functions basically consist of adding functions of a higher $l$ quantum number than are usually present for the atom (*20,28,36*). Thus, for a second-row atom, the most useful polarization functions are d GTOs, and for hydrogen, p GTOs. Figure 2.6 illustrates how a d function on oxygen can polarize a p function to improve the description of the O–H bonds in the water molecule (*20,28*).

Pople and co-workers introduced a simple notation to indicate the presence of these functions, addition of d orbitals to the second row elements in the periodic table denoted by an asterisk *. A double asterisk to denote for addition of p orbital to hydrogen and helium (*20,28*). (d, p) and ** are synonymous, .i.e. 6-31G** is equivalent to 6-31G (d,p) (*33*).

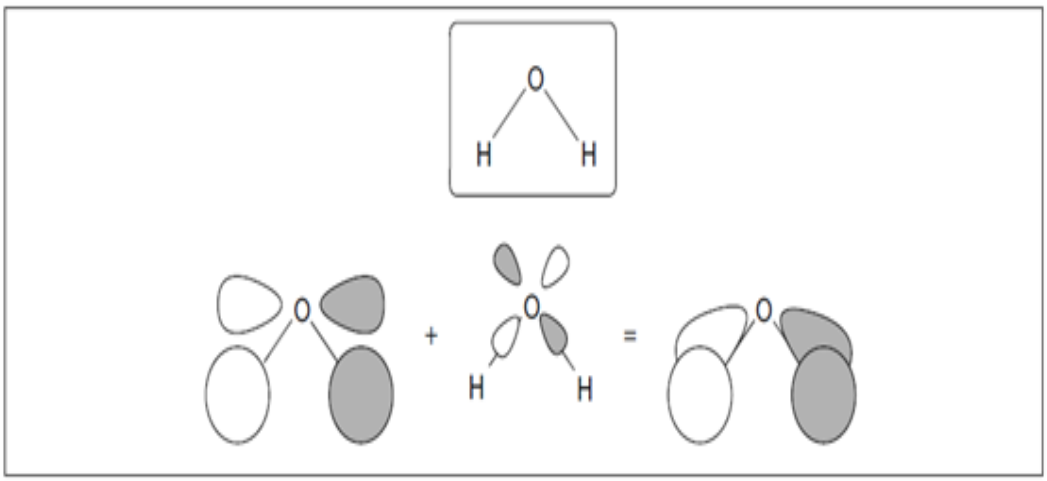


Figure 2.6: The MO formed by interaction between the antisymmetric combination of H 1s orbitals and the oxygen $p_x$ orbital. Bonding interactions are enhanced by mixing a small amount of O $d_{xz}$ character into the MO (*28*).

### A.2.6.5) Diffused functions

Diffuse functions are basis functions with a larger spatial extent than the normal ones. These functions are particularly important in the modeling of anions, or excited states, lone pairs, loose supermolecular complexes, and other systems where electrons are relatively far from the nucleus (*21,28,36*). Errors in energies and other molecular properties can occur, when a basis set does not have the flexibility necessary to allow a weakly bound electron to localize far from the remaining density (*28*), so diffused functions are added to the basis set. In the Pople notation, a single set of diffuse functions are added to heavy atoms by adding a "+" after the digits representing the number of valence functions. Thus for example, 6-31+G (3df,2p) designates

the 6-31G basis set supplemented by diffuse functions, 3 sets of d functions and one set of f functions on heavy atoms, and supplemented by 2 sets of p functions on hydrogen's. A second "+" represents a single set of diffuse functions added to H and He atoms. Thus, 6-31++G basis set has a single set of diffuse functions added to heavy atoms and H and He atoms (*21*,*28*,*33*,*37*).

**A.2.6.6) Effective core potential (ECP)**

For very heavy elements (4th period and up) calculations using atomic orbital based basis sets become very time consuming due to the number of electrons (and hence number of basis functions) involved in the calculation (*36*). To overcome this problem, the core electrons and their basis functions are replaced in the wave function by a potential term in the Hamiltonian. This is called core potentials, effective core potentials (ECP) (*3*). A key issue in the construction of ECPs is just how many electrons to include in the core, 'large-core' ECPs include everything other than the outermost (valence) shell, while 'small-core' ECPs scale back to the next lower shell (*28*). For example, silver with an atomic number of 47, one may consider two different choices of core size, where the electrons replaced by an ECP are indicated in *italic* and the remaining electrons in bold:

• “Large-core” ECP: 11 electrons considered explicitly:

$(1s)^2\ (2s)^2\ (2p)^6\ (3s)^2\ (3p)^6\ (4s)^2\ (3d)^{10}\ (4p)^6\mathbf{(4d)^{10}\ (5s)^1}$

• “Small-core” ECP: 19 electrons considered explicitly:

$(1s)^2\ (2s)^2\ (2p)^6\ (3s)^2\ (3p)^6\mathbf{(4s)^2}(3d)^{10}\mathbf{(4p)^6\ (4d)^{10}\ (5s)^1}$

• All-electron ECP: 47 electrons considered explicitly:

$\mathbf{(1s)^2\ (2s)^2\ (2p)^6\ (3s)^2\ (3p)^6\ (4s)^2\ (3d)^{10}\ (4p)^6\ (4d)^{10}\ (5s)^1}$ (*33*).

### A.2.7) Electronic Structure calculation Methods

Solving Schrödinger equation and determining the electronic structure of atoms and molecules are primary goals in molecular quantum mechanics (*29*). In polyatomic molecules, the presence of several nuclei makes quantum mechanical calculations harder. Because the electronic wavefunction depends on several parameters, bond distances, bond angles, and dihedral angles of rotation about single bond. Thus the full theoretical treatment of a polyatomic molecule involves calculation of the electronic wavefunction for range of each of these parameters (*23*).

There are three main approaches to calculate molecular properties via solving Schrödinger equation, ab-initio methods, density functional method, semiempirical methods (*23*,*29*).

### A.2.7.1) Ab-initio methods

The term “ab initio” comes from Latin meaning from the beginning.

This name is given to computations that are derived directly from theoretical principles using as input only the values of fundamental constants and atomic numbers of the nuclei, with no inclusion of experimental data. This is an approximate quantum mechanical calculation (*3*,*25*,*29*). The accuracy of this approach is determined by the model chosen for the wavefunction (basis set) (*29*). The first assumption in ab-initio methods is the Born-Oppenheimer approximation which reduces the Hamiltonian for molecular system to only the electronic motion as shown before in helium atom and hydrogen molecule (*25*).

#### A.2.7.1.1) Hartree-Fock self-consistent field method(HF-SCF)

The most common type of ab-initio calculation is called a Hartree-Fock method, it is the starting point of many other ab-initio methods (*3*,*29*). It was first introduced by D.R. Hartree as self-consistent field (SCF). It was further improved by including electron exchange by V. Fock and J.C. Slater. The orbitals obtained by a combination of these procedures are called Hartree-Fock self consistent field orbitals (*25*).

The primary approximation is that the Columbic electron-electron repulsion is taken into account, the second approximation in HF calculations is due to the fact that the wavefunction must be described by some mathematical function (basis set) (*3*). An advantage of this method is that it breaks the many-electron Schrödinger equation into many simpler one-electron equations. Each one electron equation is solved to yield a single-electron wave function, called an orbital, and an energy, called an orbital energy. The orbital describes the behavior of an electron in the net field of all the other electrons (*3*).

It was assumed that electrons don't interact with each other, then the two electron wavefunction is written as a product of orbitals, for example helium atom,

$$\psi(r_1, r_2) = \emptyset(r_1)\emptyset(r_2) \qquad (2.49)$$

Which is known as Hartree product, but this product fails to satisfy Pauli exclusion principal, which states that the total wavefunction must be antisymmetric with respect to the interchange of any pair of electrons. To do so, spin function must include with the spatial function.

$$\psi(x, y, z, \sigma) = \psi(x, y, z)\alpha(\sigma) \qquad or \qquad \psi(x, y, z)\beta(\sigma) \qquad (2.50)$$

Where the complete one electron wavefunction ψ is called (spin orbital), $\alpha(\sigma)$ and $\beta(\sigma)$ are spin functions, $\sigma$ is called spin variable and has no classical analog (*20*,*24*).

Again for helium,

$$\psi(1,2) = \psi_{1s}\alpha(1)\psi_{1s}\beta(2) \qquad (2.51)$$

1 and 2 denote all four coordinates $(x, y, z, \sigma)$ of electrons 1 and 2. But the electrons are indistinguishable from each other, then the wavefunction

$$\psi(2,1) = \psi_{1s}\alpha(2)\psi_{1s}\beta(1) \qquad (2.52)$$

Is equivalent to equation (2.51). The linear combinations of equation (2.51) and equation (2.52) are

$$\boldsymbol{\psi_1 = \psi(1,2) + \psi(2,1) = \psi_{1s}\alpha(1)\psi_{1s}\beta(2) + \psi_{1s}\alpha(2)\psi_{1s}\beta(1)} \qquad (2.53)$$

$$\boldsymbol{\psi_1 = \psi(1,2) - \psi(2,1) = \psi_{1s}\alpha(1)\psi_{1s}\beta(2) - \psi_{1s}\alpha(2)\psi_{1s}\beta(1)} \qquad (2.54)$$

Both $\psi_1$ and $\psi_2$ describe states in which there are two indistinguishable electrons, and both appear to be acceptable wavefunction for the ground state of helium, but experimentally only $\psi_2$ describes the ground state of helium atom since it has a property that it changes sign when two electron are interchanged, so $\psi_2(1,2)$ is antisymmetric wavefunction (*20*,*24*,*29*).

Antisymmetric wavefunctions can be represented by Slater determinants,

$$\psi(1,2) = \frac{1}{\sqrt{2}}\begin{vmatrix}\psi_{1s}\alpha(1) & \psi_{1s}\beta(1)\\ \psi_{1s}\alpha(2) & \psi_{1s}\beta(2)\end{vmatrix} \tag{2.55}$$

$\frac{1}{\sqrt{2}}$ is normalization constant for two electrons (*20*,*24*).

To generalize this development for an N-electron system, N × N determinant is used with normalization constant ($\frac{1}{\sqrt{N!}}$),

$$\psi(1,2,\dots,N) = \frac{1}{\sqrt{N!}}\begin{vmatrix}u_1(1) & u_2(1) & \dots & u_N(1)\\ u_1(2) & u_2(2) & \dots & u_N(2)\\ \vdots & \vdots & & \vdots\\ u_1(N) & u_2(N) & \dots & u_N(N)\end{vmatrix} \tag{2.56}$$

Where the u's are spin orbitals (*20*,*24*).

For simplicity, a closed shell system of 2N electron is used to show how HF method proceeds, the Hamiltonian operator for 2N electron atom in atomic units is

$$\hat{H} = -\frac{1}{2}\sum_{j=1}^{2N}\nabla_j^2 - \sum_j^{2N}\frac{Z}{r_j} + \sum_{i=1}^{2N}\sum_{j>i}\frac{1}{r_{ij}} \tag{2.57}$$

And the wavefunction is

$$\psi(1,2,\dots 2N) = \frac{1}{\sqrt{N!}}\begin{vmatrix}\emptyset_1\alpha(1) & \emptyset_1\beta(1) & \dots & \emptyset_N\alpha(1) & \emptyset_N\beta(1)\\ \emptyset_1\alpha(2) & \emptyset_1\beta(2) & \dots & \emptyset_N\alpha(2) & \emptyset_N\beta(2)\\ \vdots & \vdots & & \vdots & \vdots\\ \emptyset_1\alpha(2N) & \emptyset_1\beta(2N) & \dots & \emptyset_N\alpha(2N) & \emptyset_N\beta(2N\end{vmatrix} \tag{2.58}$$

And energy is given by

$$E = \int dr_1 d\sigma_1 \dots dr_{2N} d\sigma_{2N} \psi^*(1,2,\dots,2N)\widehat{H}\ \psi(1,2,\dots,2N) \qquad (2.59)$$

And can be written as

$$E = 2\sum_{j=1}^{N} I_J\ +\ \sum_{i=1}^{N}\sum_{j=1}^{N}(2J_{ij} - K_{ij}) \qquad (2.60)$$

Where

$$I_j = \int dr_j \emptyset_j^*(r_j)\left(-\frac{1}{2}\nabla_j^2 - \frac{Z}{r_j}\right)\emptyset_j(r_j) \qquad (2.61)$$

$$J_{ij} = \iint dr_1 dr_2 \emptyset_i^*(r_1)\emptyset_j^*(r_2)\frac{1}{r_{12}}\emptyset_i(r_1)\emptyset_j(r_2) \qquad (2.62)$$

And

$$K_{ij} = \iint dr_1 dr_2 \emptyset_i^*(r_1)\emptyset_j^*(r_2)\frac{1}{r_{12}}\emptyset_i(r_2)\emptyset_j(r_1) \qquad (2.63)$$

Where $I_j$ are the overall orbitals energies of the occupied molecular orbitals, the factor 2 is needed because there are two electrons in each molecular orbital, N electron with $\alpha$ spin function, and N with $\beta$ spin function. The $J_{ij}$ integrals are called coulomb integrals is the energy of the Columbic interaction between an electron in orbital i with an electron in orbital j. And $K_{ij}$ integrals are called exchange integrals, it has no physical interpretation but it account for the fact that the two electrons exchange their positions from the left to the right of the integrand (*20,24,25*).

The spatial orbitals $\emptyset_i(r_i)$ are determined by applying variational principal to equation 2.59. The following equations are obtained as a result for applying the variational principal

$$\widehat{F}_i\emptyset_i = \varepsilon_i\emptyset_i \qquad i = 1,2,\dots,N \tag{2.64}$$

Where $\widehat{F}_i$ is Fock operator and is given by

$$\widehat{F}_i = \widehat{f}_i + \sum_j(2\widehat{J}_j - \widehat{K}_j) \tag{2.65}$$

Where

$$\widehat{f}_i = -\frac{1}{2}\nabla_i^2 - \frac{Z}{r_i} \tag{2.66}$$

$$\widehat{J}_j(r_1)\emptyset_i(r_1) = \emptyset_i(r_1)\int dr_2\emptyset_j^*(r_2)\frac{1}{r_{12}}\emptyset_j(r_2) \tag{2.67}$$

And

$$\widehat{K}_j(r_1)\emptyset_i(r_1) = \emptyset_j(r_1)\int dr_2\,\emptyset_j^*(r_2)\frac{1}{r_{12}}\emptyset_i(r_2) \tag{2.68}$$

Fock operator depends on all the orbitals and cannot be evaluated through equation 2.65 to 2.68 until all the orbitals are known (*20,24,25*).

The Hartree-Fock orbitals are a set of N coupled equations, which can be solved by iterative procedure called a self-consistent field procedure (SCF) in which an initial guess of set of orbitals $\emptyset_i(r_i)$, are assumed, the one-electron wave functions are approximated by Various basis sets, most of which are composed of Gaussian

functions, then initial set of Fock operators are calculated, then equation 2.64 can be solved using the calculated Fock operators to find a new set of orbitals. These new orbitals are used to calculate a new set of Fock operator, which in turn are used to calculate a new set of orbitals. This cyclic procedure is continued until the orbitals of one cycle are essentially the same as those of next cycle or, in other words, until they are self-consistent, the self-consistent orbitals are called Hartree-Fock orbitals, the eigenvalues $\varepsilon_i$ are called orbital energies (*3*,*20*,*24*).

A variation on the HF procedure is the way that orbitals are constructed to reflect paired or unpaired electrons. If the molecule has a single spin, then the same orbital spatial function can be used for both the $\alpha$ and $\beta$ spin electrons in each pair. This is called the restricted Hartree-Fock method (RHF) (*3*,*29*).

There are two techniques for constructing HF wave functions of molecules with unpaired electrons (open shell). One technique is to use two completely separate sets of orbitals for the $\alpha$ and $\beta$ electrons. This is called an unrestricted Hartree-Fockwave function (UHF). This means that paired electrons will not have the same spatial distribution.

This introduces an error into the calculation, called spin Contamination (*3*,*29*).

Another way of constructing wave functions for open-shell molecules is the restricted open shell Hartree-Fock method (ROHF). In this method, the paired electrons share the same spatial orbital; thus, there is no spin contamination (*3*,*29*).

One of the limitations of HF calculations is that they do not include electron correlation. This means that HF takes into account the average affect of electron repulsion, but does not consider the instantaneous columbic interaction between electrons. Within HF theory the probability of finding an electron at some location around an atom is determined by the distance from the nucleus but not the distance to the other electrons as shown in Figure 2.7.

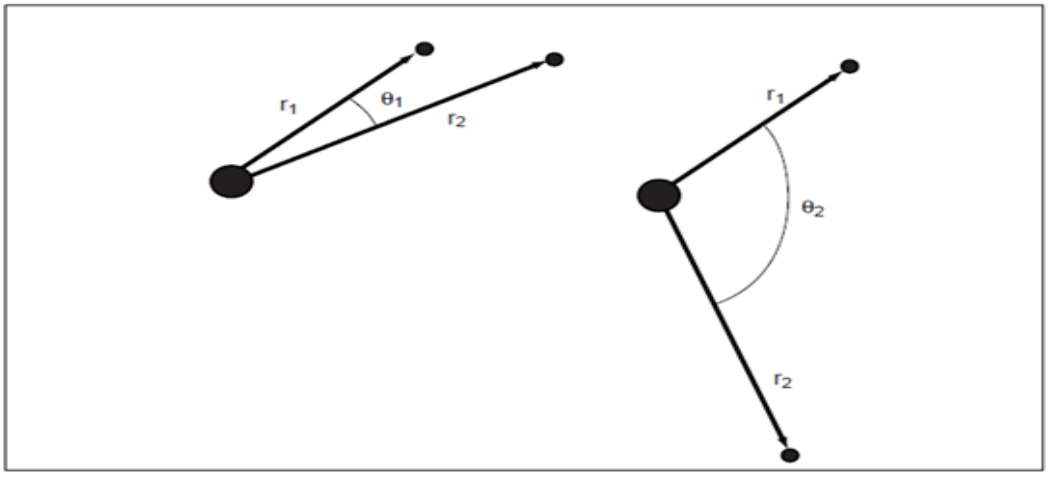


Figure 2.7: Two arrangements of electrons around the nucleus of an atom having the same probability within HF theory, but not in correlated calculations (*3*).

Correlation is important for many different reasons. Including correlation generally improves the accuracy of computed energies and molecular geometries (*3*).

A number of types of calculations begin with a HF calculation and then correct for correlation. Some of these methods are Moller-Plesset perturbation theory (MPn, where n is the order of correction), configuration nteraction (CI), etc…(*3*,*25*).

**A.2.7.1.2) Configuration Interaction (CI)**

Configuration Interaction a method assumes that the exact wavefunction ψ cannot be expressed as single determinant, as HF theory assume. Instead it proceeds by construction multiple-determinant wavefunction by promoting electrons from the occupied to unoccupied orbitals (*3*,*21*).

Then the electron correlation is considered by taking a linear combination of the HF ground-state wavefunction with a large number of excited configurations. The expansion coefficients are then varied using a Variational approach until a minimum energy is achieved (*25*). Some of the common ones include the following: Configuration Interaction Single excitations (CIS) only, Configuration Interaction

Double excitations (CID) only, and Configuration Interaction Single and Double excitations (CISD) only, the configuration interaction calculation with all possible excitations is called a full CI (*3*,*21*,*25*).

**A.2.7.1.3) Moller-Plesset Perturbation Theory**

Correlation can be added as a perturbation from the Hartree-Fock wave function, at which higher excitations to HF theory as non iterative correction. A Moller-Plesset computation to a second-order energy correction is called an MP2 computation, and higher-order energy corrections are called MP3, MP4, and so on (*3*,*21*,*25*).

The most significant advantages of using correlated models is to obtain reliable thermodynamic information, and is fast calculation however, it has a disadvantage that it is not variational, a non-Variational result is not, in general, an upper bound of the true ground-state energy (*3*,*25*).

**A.2.7.2) Semiempirical method**

Because of the difficulties of applying the ab-initio methods to large molecules, semiempirical methods were developed. The earliest semiempirical methods proposed by E. Huckel, in 1930, treated only the π electrons in conjugated systems. Semiempirical methods are based on HF calculations, but use a simpler Hamiltonian than the

correct one which is used in HF, and use parameters whose values are adjusted to fit experimental data. Even though semiempirical methods are fast and widely popular, they have limitation to the accuracy because of the approximations inherent in their formulations, and the accuracy of the experimental data used to obtain the parameters (*3,23,29*).

**A.2.7.3) Density Functional Theory (DFT)**

The Ab-initio and semiempirical approaches are to use the electrons wavefunctions. However, a wavefunction is not a measurable feature of a molecule or atoms (*2*).

In 1964, an alternative approach is introduced, density functional methods, the origins for density functional theory (DFT) is the proof of P. Hohenberg and W. Kohn (*23,33*), that for molecules with nondegenerate ground state, the ground state molecular energy, wavefunction, and all other molecular electronic properties are uniquely determined by the ground state electron probability density $\rho(r)$ (*23*).

Since ab-initio methods based on HF-SCF approximation have difficulty for performing accurate calculations with large basis set on

many atoms and many electros systems (*29*). DFT are attractive because it begins with the concept of the electron probability density, and it include the effects of electron correlation (*21*,*29*), using electron density makes the integrals for coulomb repulsion needed to be done only over three-dimensional function which results in faster and more accurate calculations than HF calculation (*3*).

A functional is a function of a function (*3*), it takes a function and provides a number, and it is usually written with the function in square brackets (*32*). In DFT the electronic energy E is written in terms of electron probability density and E is said to be functional of the electron density and is denoted E[($\rho(r)$], which means that for a given density functional $\rho(r)$ there is one and just one energy value (*29*).

Unfortunately, Hohenberg-Kohn theorem proves only that there is functional dependence of energy on the density, but does not tell the form of this dependence (*29*).

The DFT methods developed by Kohn and Sham, they suggested that a variational approach might yield a way to calculate the energy and electron density which in turn could be used to calculate other properties, at which variational approach led to Kohn-Sham (KS) equations (*2*,*29*,*38*), which have the form

$$\left\{-\frac{\hbar^2}{2m_e}\nabla_1^2 - j_0\sum_{I=1}^{N}\frac{Z_I}{r_{I1}} + j_0\int\frac{\rho(r_2)}{r_{12}}dr_2 + V_{XC}(r_1)\right\}\psi_i(r_1) = \varepsilon_i\psi_i(r_1) \qquad (2.69)$$

Where $\varepsilon_i$ are the KS orbital energies and the exchange-correlation potential, $V_{XC}$ , is the functional derivative of the exchange-correlation energy, and given by

$$V_{XC}[\rho] = \frac{\delta E_{XC}[\rho]}{\delta\rho} \qquad (2.70)$$

And

$$\rho(r) = \sum_{i=1}^{n}|\psi_i(r)|^2 \qquad (2.71)$$

Is the exact ground-state electronic density, the sum is over all the occupied Kohn-Sham (KS) orbitals (*23*,*29*), which are obtained when the KS equations are solved in a self-consistent fashion (*29*). Initially, the electron density is guessed, and by using some approximation for the functional $E_{XC}[\rho]$, $V_{XC}[\rho]$ computed as a function of r (*29*,*38*). Then a set of KS equation is solved to obtain an initial set of KS orbitals, this initial guess is then used to refine these orbitals, in a manner similar to that used in the HF SCF method. The final KS orbitals are used to calculate an electron density that in turn is used to calculate the energy, which is written as

$$E[\rho] = -\frac{\hbar^2}{2m_e}\sum_{i=1}^{n}\int\psi_i^*(r_1)\nabla_1^2\psi_i(r_1)dr_1 - j_0\sum_{I=1}^{N}\frac{Z_I}{r_{I1}}\rho(r_1)dr_1 +$$

$$\frac{1}{2}j_0\int\frac{\rho(r_1)\rho(r_2)}{r_{12}}dr_1dr_2 + E_{XC}[\rho] \qquad (2.72)$$

Where the one electron spatial orbitals $\psi_i$ $(i = 1,2,\dots,n)$ are the Kohn-Sham orbitals, the first term represents the kinetic energy of electrons, the second represents the electron-nucleus attraction and the sum is overall N nuclei with index I and atomic number $Z_I$, the third represents the coulomb interaction between the total charge distribution summed over all KS orbitals at $r_1 \, and \, r_2$, the last represents the exchange-correlation energy of the system, which is also a functional of the density and takes into accounts the remaining part of electron-electron interactions (*21*,*29*).

The KS orbitals are expressed in terms of basis functions (different basis sets), which are exactly the same basis functions used as in wavefunction theory (ab-initio and semiempirical methods) (*2*,*29*).

There are different DFT methods which differ in the choice of functional form for the exchange–correlation energy (*33*). And these Density functionals can be broken down into several classes (*3*). The simplest is $X_\alpha$method, which was introduced by J. C. Slater, in this method electron exchange is included and correlation is not included (*3*). The simplest approximation to $E_{XC}[\rho]$ is within the local density approximation (LDA), which assumes that the density locally can

be treated as a uniform electron gas, or equivalently that the density is a slowly varying function (2,*3*,*33*). And when $\alpha$ and $\beta$ densities are not equal (open shell system) then LDA replaced by the Local Spin Density Approximation (LSDA), which gives Better results than with the LDA, but for closed shell systems, LSDA is equal to LDA (*2*,*33*).

Improvements over the LSDA approach must consider a non-uniform electron gas (*33*). At which the exchange and correlation energies dependent not only on the electron density but also on its gradient, these functionals are called gradient-corrected, or generalized-gradient approximation (GGA) (*2*,*33*). Most popular GGA functionals are Proposed by A. D. Becke, Lee, Yang and Parr, and J. P. Perdew and coworkers (*33*).

There are also hybrid methods that combine density functionals correlation and exchange with Hartree-Fock corrections, usually the exchange integrals (*3*,*29*). Becke 3 parameter functional (B3) methods is example of such hybrid models, with the popular B3LYP method which is a combination of Becke 3 (B3) with the Lee, Yang and Parr method (LYP), which is defined by equation 2.73 shown below(*3*,*23*,*29*,*33*).

$$E_{XC}^{B3LYP} = (1-a)E_X^{LSDA} + aE_X^{exact} + b\Delta E_X^{B88} + (1-c)E_C^{LSDA} + cE_C^{LYP} \quad (2.73)$$

At which the exchange energy is defined as a combination of LSDA, B88 (Becke), and exact change comes from the use of HF definition. a, b and c parameters were chosen to give good fit to experimental data, with typical values $a\sim 0.2, b\sim 0.7, and\ c\sim 0.8$ (*23*,*33*,*38*).

Due to the newness of DFT, its performance is not completely known and continues to change with the development of new functionals. However, a number of commonly used functionals are listed in Table 2.1 (*3*).

Table 2.1: Density functionals (*3*).

| Acronyms | Name | Type |
|---|---|---|
| Xα | X alpha | Exchange only |
| HFS | Hartree–Fock Slater | HF with LDA exchange |
| VWN | Vosko, Wilks, and Nusair | LDA |
| BLYP | Becke correlation functional with Lee, Yang, Parr exchange | Gradient-corrected |
| B3LYP, Becke3LYP | Becke 3 term with Lee, Yang, Parr exchange | Hybrid |
| PW91 | Perdue and Wang 1991 | Gradient-corrected |
| G96 | Gill 1996 | Exchange |
| P86 | Perdew 1986 | Gradient-corrected |
| B96 | Becke 1996 | Gradient-corrected |
| B3P86 | Becke exchange, Perdew correlation | Hybrid |
| B3PW91 | Becke exchange, Perdew and Wang correlation | Hybrid |

## B) Chemical background

Coordination compounds are formed by coordination covalent bond between metal atom or ion; as an electron pair acceptor, with the surrounding atoms or groups each donating its electron density to an empty orbital on the metal atom or ion. These electron donors groups are called ligands (*39,40*). When these ligands are organic compounds, coordination covalent bond is between metal and carbon, or metal and hydrogen, while the compound formed is called organometallic compound. Typical organic ligands that usually bind to metals are carbonyls, alkenes, alkynes, etc..(*5*).

Alfred Werner was the first who interpreting bonding and reaction of coordination compounds in 1893 (*5,40*). The organometallic compounds are of great interest since they are useful catalyst for industrial processes and for organic synthesis (*5*).

### B.2.1) Metal carbonyl complexes

Metal carbonyl complexes are coordination compounds that contain carbon monoxide as a ligand bonded to transition metals (*41*). Even carbon monoxide has lower basicity; it forms thousands of complexes with strong interactions with the transition metals (*40,41*). This is due to the type of interaction between the metal and carbon monoxide

orbitals, molecular orbital of both carbon monoxide and octahedral metal-ligand complex are shown in Figure 2.8.

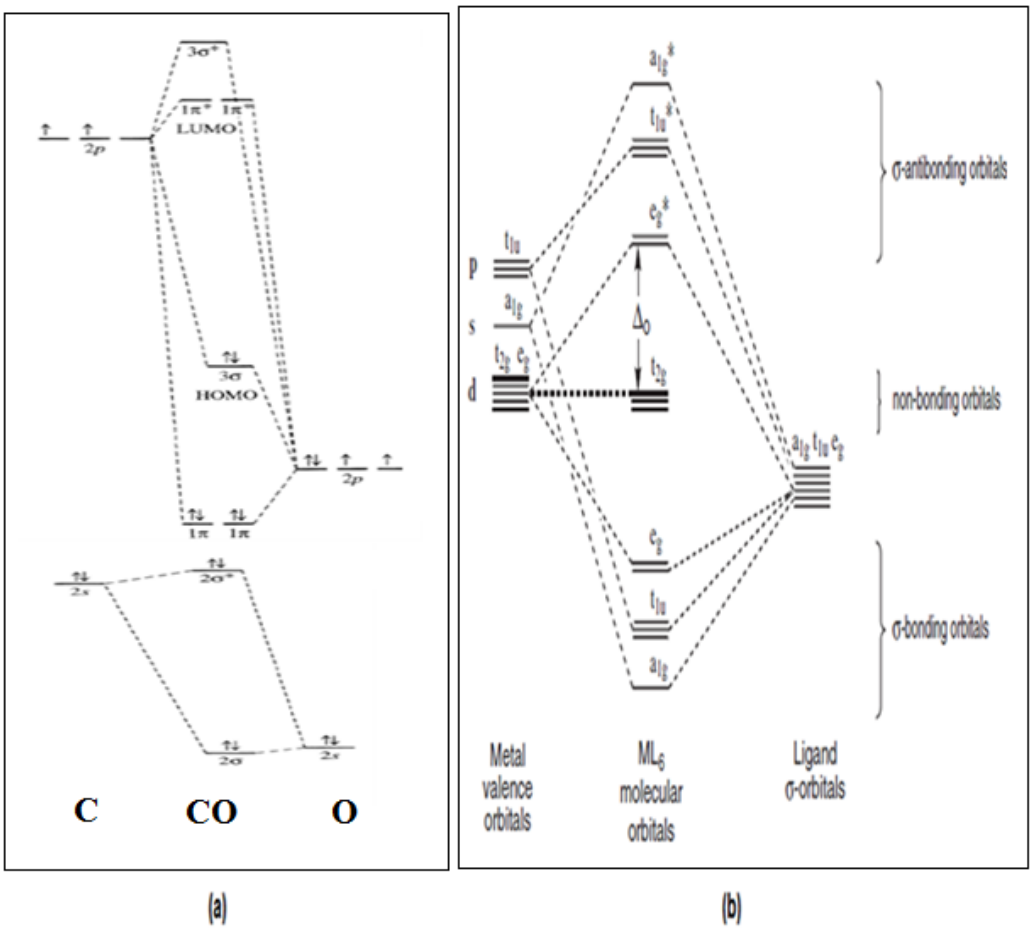


Figure 2.8: Molecular orbital diagram for (a) carbon monoxide (*40*) and (b) octahedral $ML_6$ complex (*39*).

The interaction of the CO group orbitals, with the transition metal orbitals can be described as a combination of two components:

1) The HOMO of CO (σ orbital) which possesses a lone pair, interacts with an appropriate metal orbital (such as an unfilled d

or hybrid orbital) in a bonding M-L σ and antibonding M-L $\sigma^*$ (*40,41*).

2) The LUMO of CO are two degenerate empty $\pi^*$ orbitals, the overlap of the higher energy LUMO of CO with the lower energy metal $t_2g$ orbitals ($d_{xy}$, $d_{yz}$, $d_{xz}$), results in one filled bonding orbital lower in energy than initial metal $t_2g$ orbitals, and one empty antibonding orbital that is higher in energy than the σ antibonding orbital as shown in Figure 2.9 (*4,39-42*).

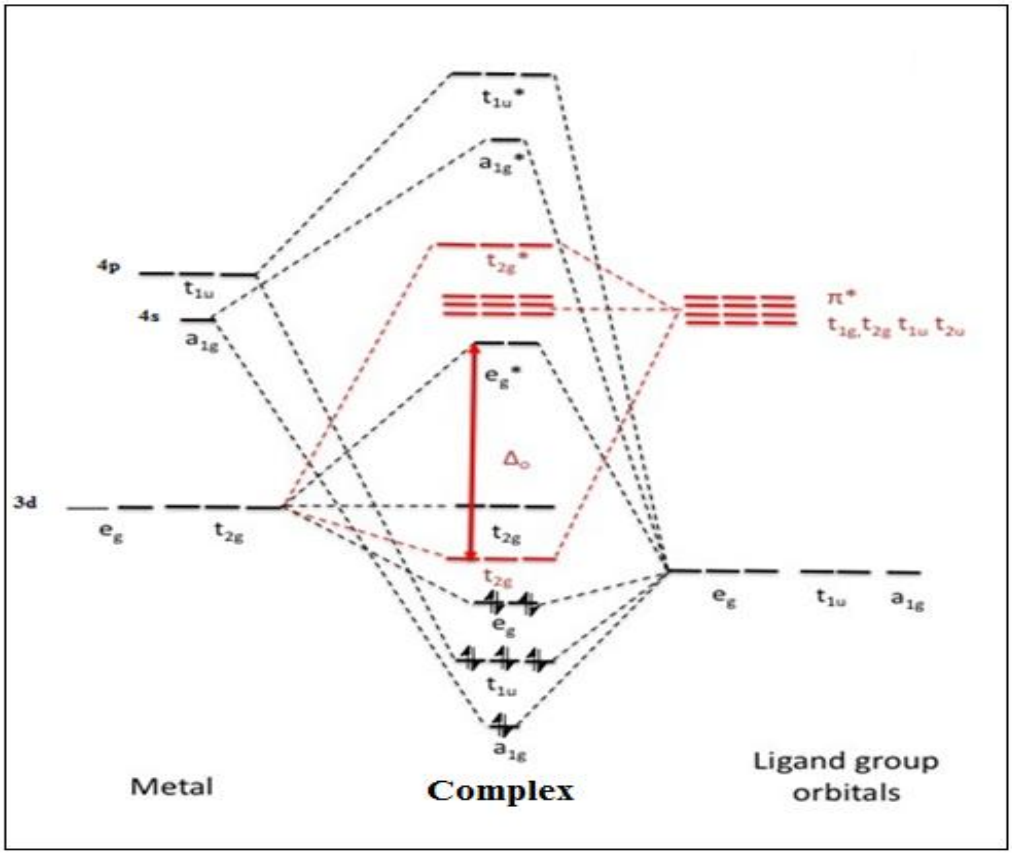


Figure 2.9: Approximate partial MO diagram for metal-ligand π-bonding in an octahedral complex, with a π-acceptor ligand (*42*).

As a result, the value of $\Delta_0$ is larger and hence bonding strength is increased, the d electrons donated back to the CO $\pi^*$ orbitals, in a phenomena called M→L $\pi$ bonding (also called back bonding) as shown in Figure 2.10 (*4,39-42*).

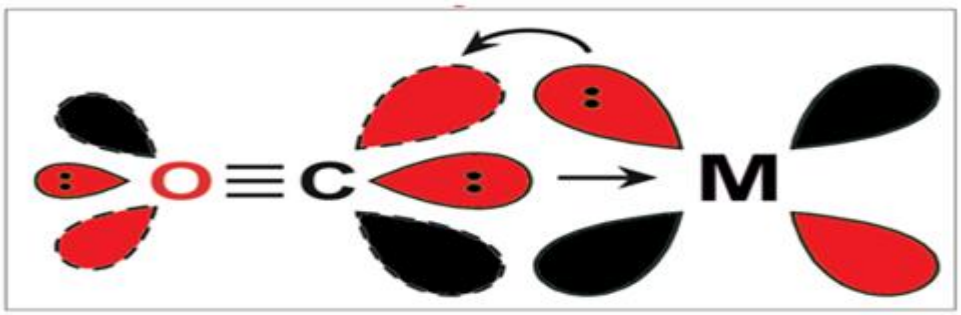


Figure 2.10: Metal- to – ligand $\pi$ back-bonding (*4*).

The occupation of the $\pi^*$ orbital of the CO leads to a decrease in C-O bond order, which causes lengthening of the C-O bond compared with free CO, therefore carbonyl stretching frequency is lower than in free CO (*4,39*). Free CO absorbs at ~2143 $cm^{-1}$, while coordinated CO absorbs in the range 1840-2120 $cm^{-1}$ (39).

**B.2.2) Trans effect**

Trans effect is "the effect of a coordinated group L on the rate of substitution reactions of ligands trans to itself X (*43*) as shown below:

$$L\text{-}M\text{-}X \rightarrow L\text{-}M + X$$

Where X is the leaving group and M is the metal center. The concept of trans effect was first introduced by Chernyaev, in 1926 (*40*). Trans

effect has a particular importance in ligand-replacement reaction of square planner complexes, and octahedral complexes reactions also show trans effect (*44*). To explain the trans effect, the effects of L on the activation energy of the reaction should be considered (*45*). The Lowering of activation energy for the substitution reaction occurs by destabilizing the ground state of the complex or by stabilizing the transition state or both (*40,44*).

The trans effect term is used to cover two types of effects;

***Structural trans–effect (STE):** STE is also termed Trans influence, STE is a ground state effect used to describe the tendency of a bonded ligand (L) to selectively weaken the bond of the ligand trans to it (X) (*45,46*). STE is a thermodynamic effect that contributes to the overall kinetic result by changing the reactant ground state energy (*40*). The STE is caused by π-acceptor ability of the ligand, since the ligand (L) withdraws metal electrons into its own empty $\pi^*$ orbitals, which causes weakening of the trans M-X bond (*44,46*). As a result, the energy of complex ground state become higher and leads to smaller activation energy (*40,45,46*).

*** Kinetic trans-effect (KTE)**: Kinetic phenomenon depends on both ground state and transition state factors, and describes the effect on the

liability of a trans ligand (*45,46*). In octahedral complexes, σ-donor ligands are able to stabilize the 5-coordinate transition state intermediate and hence favor dissociation of a *trans* ligand X (*46,47*). Since octahedral complexes are generally undergoing dissociative activated ligand substitution, there is often a close correlation between STEs and KTEs (*46*).

According to the combination of the two effects it was found that the overall trans effect decrease in the order:

$CO \sim CN^- \sim C_2H_4 > PR_3 \sim H^- > CH_3^- \sim SC(NH_2)_2 > C_6H_5^- >$

$NO_2^- \sim SCN^- \sim I^- > Br^- > Cl^- > py\ , NH_3 \sim OH^- \sim H_2O$ (*41,46*).

**B.2.3) Metal-alkene complexes**

Bonding between alkene and transition metal is described by Dewar-Chatt-Duncanson model (model that explains bonding between an unsaturated ligand and a metal forming a π complex) (*6,41*). Bonding takes place with transition metal as $\eta^2$ –alkenyl, i.e. bonding to the face of alkene, at which bonding is assumed to consist of two components as shown in Figure 2.11.

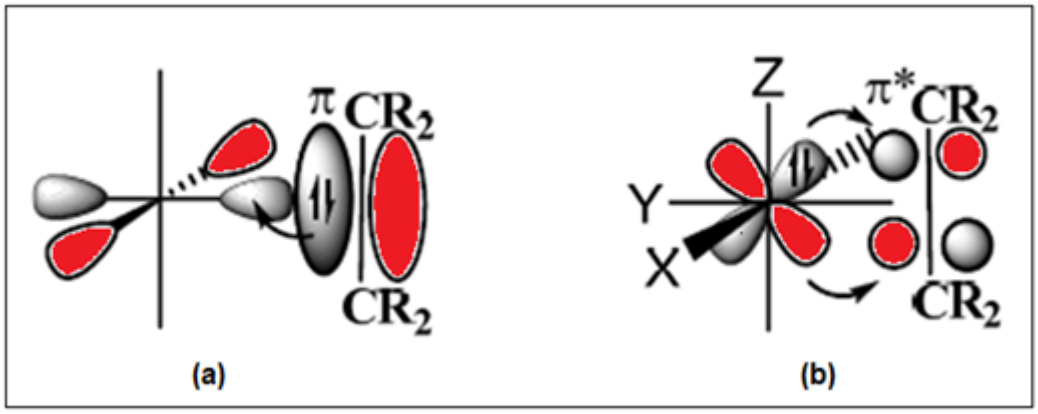


Figure 2.11: Bonding in alkene complexes. (a) Donation from filled π orbital to vacant metal orbital. (b) Back-bonding from filled metal orbital to $\pi^*$ orbitals (*44*).

- Donation of π- electron density of the HOMO filled alkene orbital to $sp^3d^2$ hybrid orbital (or $dz^2$) of σ-type acceptors on the metal atom (*6,41,44*).
- Back donation of electron density from the filled $t_{2g}$ d orbital of suitable symmetry to the LUMO π- antibonding orbital on the carbon atom (*6,40,41,44*).

Alkenes are considered to be stronger σ-donors but weaker π-acceptors than CO (*46*). Alkene complexes tend to be more stable if a withdrawing group or heteroatom is attached to alkenes. This is due to the energy lowering of the π-antibonding orbital, so increasing of both back-bonding and C-C interaction bond (*40,41*).

**B.2.4) Metal-alkyne complexes**

Metal-alkyne complexes are of great interest because of their important role in organometallic chemistry. They are involved in many transformations, including catalytic processes such as alkyne polymerization, metathesization, hydrogenation, epoxidation, cyclization, and synthesis of a variety of organic compound (*4-6,13,48, 49*).

Since these transformations may include formation or cleavage of the metal-alkyne bond, it is necessary to understand the metal-alkyne interaction (*6*).

The bonding in metal-alkyne complexes can be described by Dewar-Chatt-Duncanson model (*4,6,50*). Alkynes have two bonding and two antibonding π orbitals that can interact with metal d orbitals. These molecular orbital interactions are assumed to consist of four components as shown in Figure 2.12 (*49*).

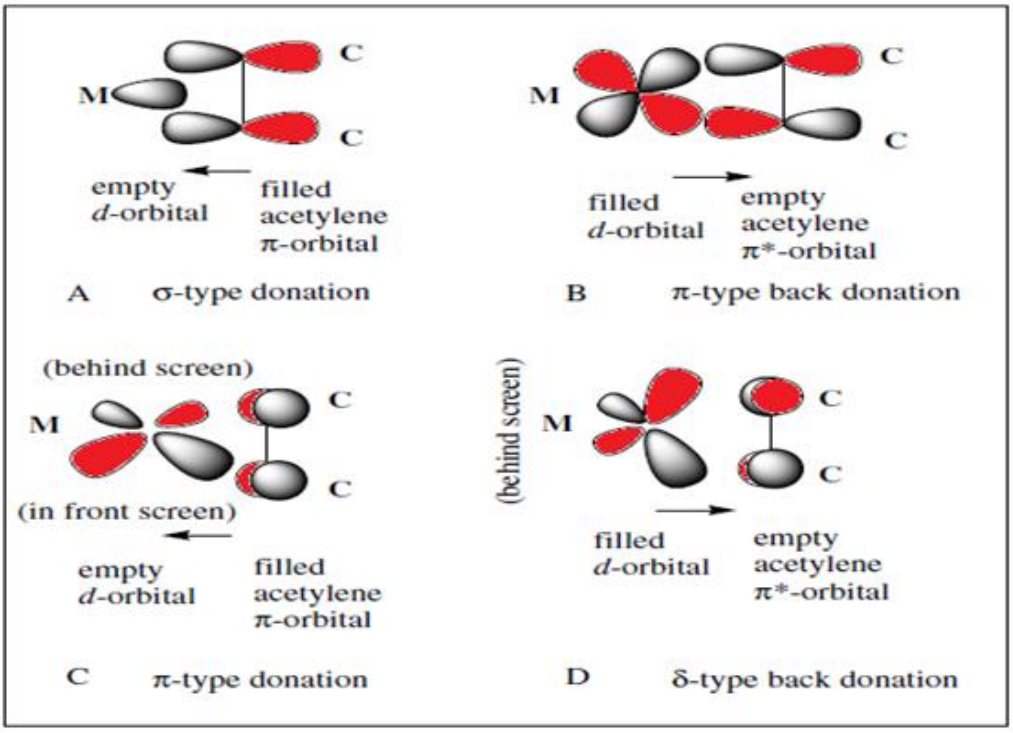


Figure 2.12: Molecular orbital interactions between metal and alkyne (*49*).

A) σ-type donation from the alkyne occupied in plane π-orbital into empty d orbital of σ-type acceptor (s, $p_z$, $d_z^2$, $dx^2$-$y^2$) in a metal as shown in Figure 2.13 (*4,49*).

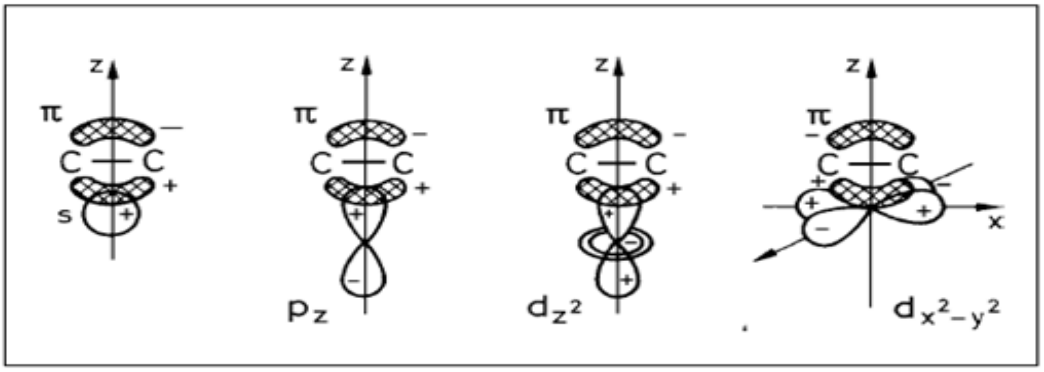


Figure 2.13: Participation of various orbitals in σ-type donation of alkyne complexes (*49*).

B) π- Back donation from the filled $p_x$ or $d_{xz}$ orbitals in the metal into the empty antibonding $\pi^*$ in alkyne, as seen in Figure 2.14 (*4,49*).

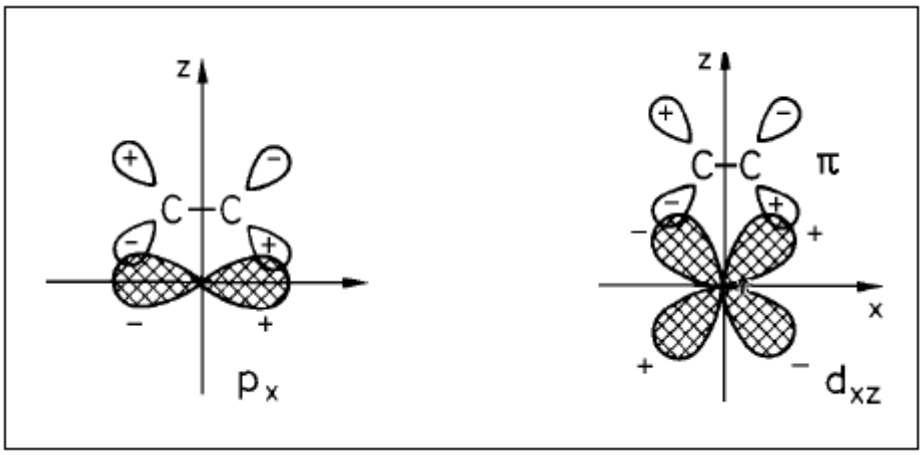


Figure 2.14: π- Back donation in alkyne complexes (*49*).

Alkynes also have another orthogonal C-C π bond, and hence can make

C) π–type donation from the filled alkyne π-orbital into the empty d-orbital in the metal.

D) δ-type back donation from filled d-orbitals in the metal into the empty antibonding $\pi^*$ (*4,49,51*).

The perpendicular π donor bond has a good overlap and must be considered. However, δ-type back donation can be ignored since the perpendicular empty antibonding can only overlap with metal d-orbital in the xy-plane (*49*).

Bonding in alkyne complexes may vary according to the attached metal, and the alkyne substituent. Thus, affecting the contribution of each type of donation mentioned above (A-D) (*50*).

When sufficient π-back donation into the parallel π-acceptor orbital, it creates a structure described as a "Metallacyclopropene" as shown in Figure 2.15 This would strengthen the metal–alkyne bond, weaken the C-C bond, and the substituent groups are bent away from the metal (*4*).

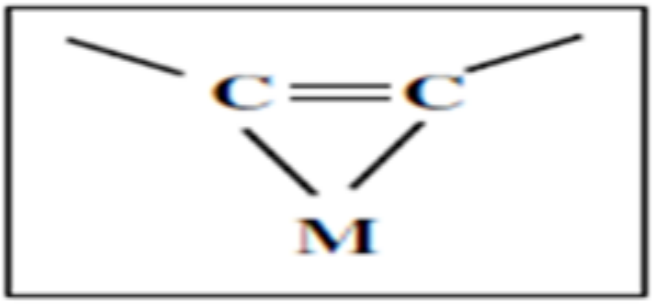


Figure 2.15: Metallacyclopropene structure (*49*).

One of applicable alkyne complexes is alkyne (pentacarbonyl) complexes, which can be prepared through photochemical reaction between metal hexa-carbonyl with alkyne (*13,48*). But there are only very few of these alkyne(pentacarbonyl) complexes that have been isolated and fully characterized having terminal alkyne ligand (*13, 52*). Whenever these terminal alkyne complexes are generated, they are exist in equilibrium with their vinylidene tautomer by 1,2-hydrogen shift, as shown in Figure 2.16 (*13,48, 53*).

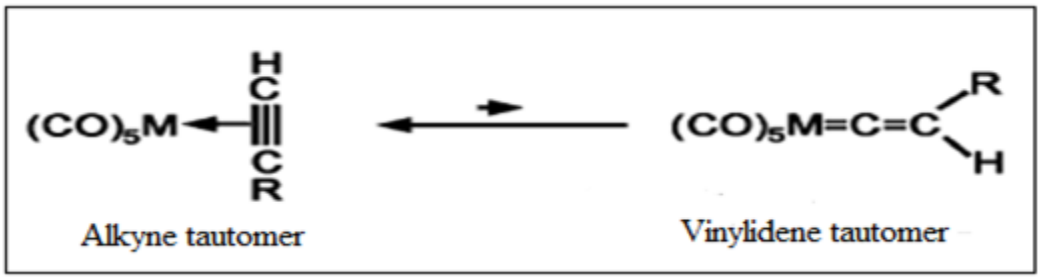


Figure 2.16: Tautomerization of alkyne complexes (*13*).

The reaction of the equilibrium (alkyne/vinylidene)pentacarbonyl complex depends on the substrate type, as some of them prefer to react with the vinylidene complex tautomer; others prefer to react with alkyne complex tautomer (*13*). Diazoalkanes tend to react with the terminal alkyne complex tautomer (*13*).

# CHAPTER THREE
# METHODS, RESULTS, AND DISCUSSION

## 3.1) Methods

Structure and energy calculations were carried on DELL PRECISION 490 workstation with quad processors, and memory of 4GB, however the Gaussian uses just 1GB. The model of the molecules is drawn by Gaussian view Version 3.07, at which Gaussian 03 software (*54*) can read these files format and perform the required calculations.

The job type option used is the combination of optimization and frequency; it first optimizes the structure to a minimum at ground state calculations then, calculates the frequency. DFT method with hybrid type B3LYP method is used. The split valence triple zeta 6-311 basis set is used, supplemented by diffuse functions 3sets of “d” functions and one set of “f” functions on heavy atoms, and supplemented by one set of “p” functions and one set of “d” functions on hydrogen atoms. So the full statement in the input file becomes: “opt freq b3lyp/6-311++g (3df, pd)”.

## 3.2) Results and discussion:

### 3.2.1) Molecular Geometry Analysis:

#### 3.2.1.1) Pentacarbonyl(3,3-diethyl-5-methoxycarbonyl-3H-pyrazol-$N_2$)chromium(0)

The optimized structure of the pentacarbonyl(3,3-diethyl-5-methoxycarbonyl-3H-pyrazol-$N_2$)chromium(0) is shown in Figure 3.1a, which is in a good agreement with the X-ray molecular structure determinations shown in Figure 3.1b (*13*). The data listed in Table 3.1 and Table 3.2.

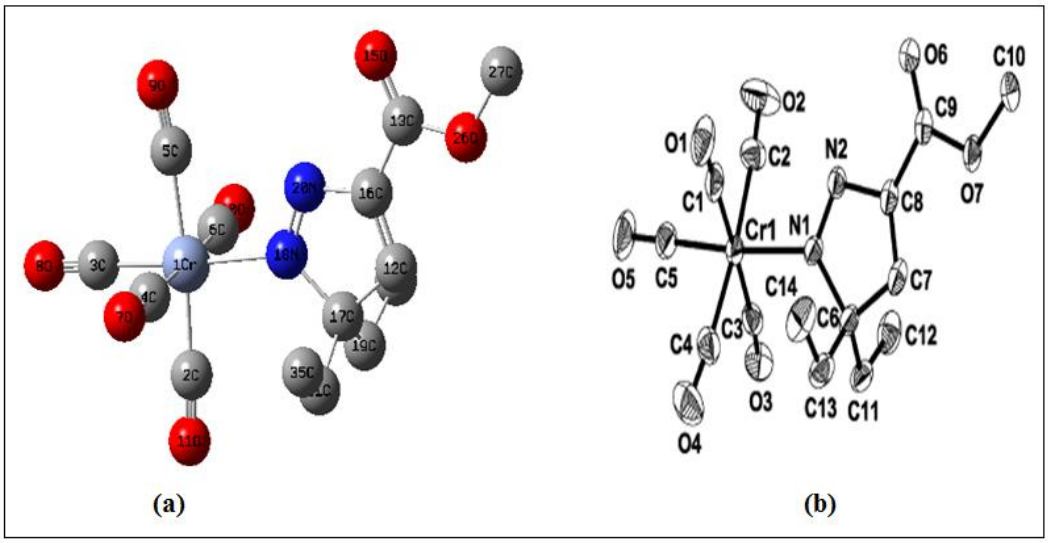


Figure 3.1: (a) Optimized structure of pentacarbonyl(3,3-diethyl-5-methoxycarbonyl-3H-pyrazol-$N_2$)chromium(0), (b) X-ray structure (*13*). (Red balls: oxygen atoms, gray balls: carbon atoms, dark blue balls: nitrogen atoms, light blue ball: chromium atom, hydrogen atoms are omitted for simplicity).

Table 3.1: Selected bond lengths (Å) compared to X-ray analysis data of pentacarbonyl(3,3-diethyl-5-methoxycarbonyl-3H-pyrazol-$N_2$)chromium(0).

| | **BOND LENGTH** | **B3LYP** |
|---|---|---|
| **BOND** | **Experimental ( Å ) (*13*)** | **Calculated ( Å )** |
| Cr1-N1 | 2.138 | 2.17213 |
| N1-N2 | 1.272 | 1.25929 |
| N1-C6 | 1.509 | 1.50673 |
| N2-C8 | 1.438 | 1.41574 |
| C6-C7 | 1.485 | 1.48567 |
| C7-C8 | 1.334 | 1.33744 |
| C8-C9 | 1.489 | 1.48223 |
| O6-C9 | 1.204 | 1.20088 |
| O7-C9 | 1.342 | 1.34626 |
| O7-C10 | 1.45 | 1.43785 |
| Cr-C1 | | 1.94276 |
| C1-O1 | | 1.13760 |
| Cr-C2 | | 1.92143 |
| C2-O2 | | 1.14247 |
| Cr-C3 | | 1.90173 |
| C3-O3 | | 1.14706 |
| Cr-C4 | | 1.92143 |
| C4-O4 | | 1.14247 |
| Cr-C5 (trans) | | 1.87247 |
| C5-O5 (trans) | | 1.14713 |

Table 3.2: Selected bond angles ($^0$) compared to X-ray analysis data of pentacarbonyl(3,3-diethyl-5-methoxycarbonyl-3H-pyrazol-$N_2$)chromium(0).

| | **BOND ANGLES** | **B3LYP** |
|---|---|---|
| **ANGLE** | **Experimental (*13*)** | **Calculated** |
| N2-N1-C6 | 110.81 | 110.381 |
| N2-N1-Cr1 | 119.13 | 118.64 |
| C6-N1-Cr1 | 130.05 | 130.979 |
| N1-N2-C8 | 109.26 | 110.394 |
| C7-C6-N1 | 101.57 | 101.497 |
| N2-C8-C9 | 119.08 | 119.267 |
| C7-C8-N2 | 110.26 | 110.185 |
| C7-C8-C9 | 130.63 | 130.547 |
| O6-C9-C8 | 125.18 | 124.813 |
| C8-C7-C6 | 108.1 | 107.542 |

The bond distances and bond angles calculated for the complex are similar to those of X-ray data. The Cr-N1 bond length calculated is 2.17213Å, which is similar to the bond length from X-ray data 2.1384 Å (*13*), and it indicates bonding between nitrogen atom adjacent to the $sp^3$ carbon and chromium (*13*). The calculated N1-N2 bond distance is 1.259Å which is also similar to that obtained from X-ray data 1.272 Å, indicating $sp^2$ N=N double bond (*13*). A bond angle data are also similar to those obtained by X-ray analysis as shown in Table 3.2. Comparison of the CΞO bond distances in cis and trans to the pyarzole ligand shows that the cis CΞO bond length is (1.1424Å) (average of the four cis carbonyls) is shorter than the trans CΞO bond length (1.1471Å). On the other hand, the Cr-C bond length for the cis carbonyl is 1.9218 Å (average of the four cis carbonyls), while the trans Cr-C bond length is (1.8725Å). This is shorter than the cis arrangement. These facts can be explained by electron-back donation from the metal center to the trans carbonyl which is caused by a donor ligand from the trans position of the CO. Hence, the trans CΞO bond is elongated, and the Cr-C bond length is shortened. The experimental and calculated IR frequencies of the Pentacarbonyl(3,3-diethyl-5-methoxycarbonyl-3H-pyrazol-N2)chromium (0) are listed in Table

3.3. The IR spectrum of the optimized structure is also shown in Figure 3.2.

Table 3.3: Comparison of experimental IR frequencies and calculated of pentacarbonyl(3,3-diethyl-5-methoxycarbonyl-3H-pyrazol-$N_2$)chromium(0) ***(13)***.

| **Experimental CO frequencies $cm^{-1}$** | **Calculated** | **Scaled (0.9646)** |
|---|---|---|
| 2069 carbonyls (m) | 2138.38 | 2062.68 |
| 1997 carbonyls (m) | 2072.49 | 1999.12 |
| 1950 carbonyls (vs) | 2031.58 | 1959.66 |
| 1942 carbonyls (s) | 2027.11 | 1955.35 |
| 1922 carbonyls (s) | 2009.11 | 1937.99 |
| 1745 (C=O) methoxy group (m) | 1801.45 | 1737.68 |

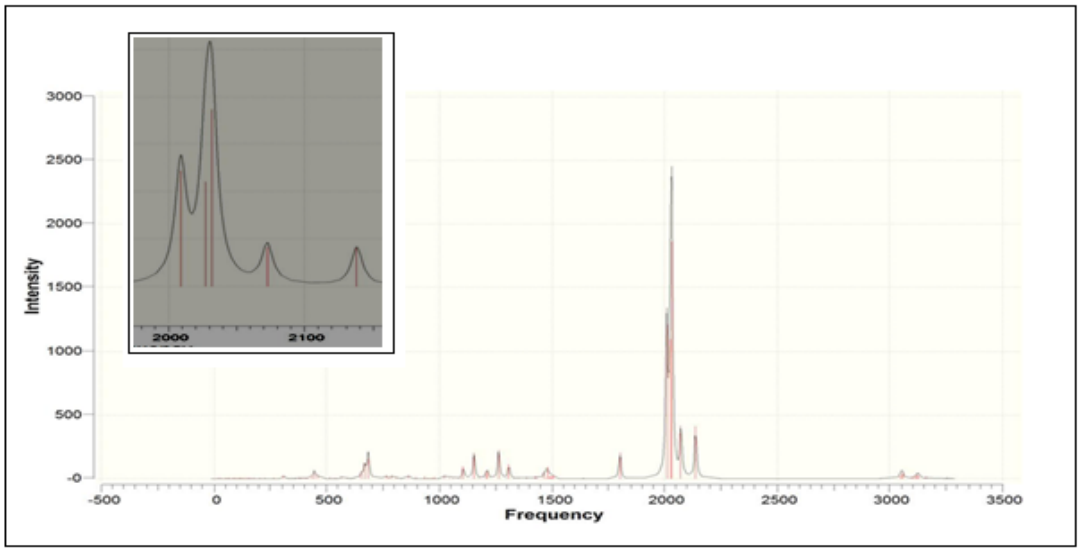


Figure 3.2: Infra red spectrum of pentacarbonyl(3,3-diethyl-5-methoxycarbonyl-3H-pyrazol-$N_2$)chromium(0).

It has been known that the calculated IR frequencies are always higher than the experimental, so that a scale factor (0.9646) (*21*) is

multiplied by the calculated frequencies for comparison purposes as shown in Table 3.3.

Optimization of the transition state of the complex is also carried out, the structure is shown in Figure 3.3, and selected bond lengths and bond angles compared to the ground state structure are also shown in Tables 3.4, and Table 3.5 respectively. IR frequencies of both ground state and transition state are supplemented in Table 3.6.

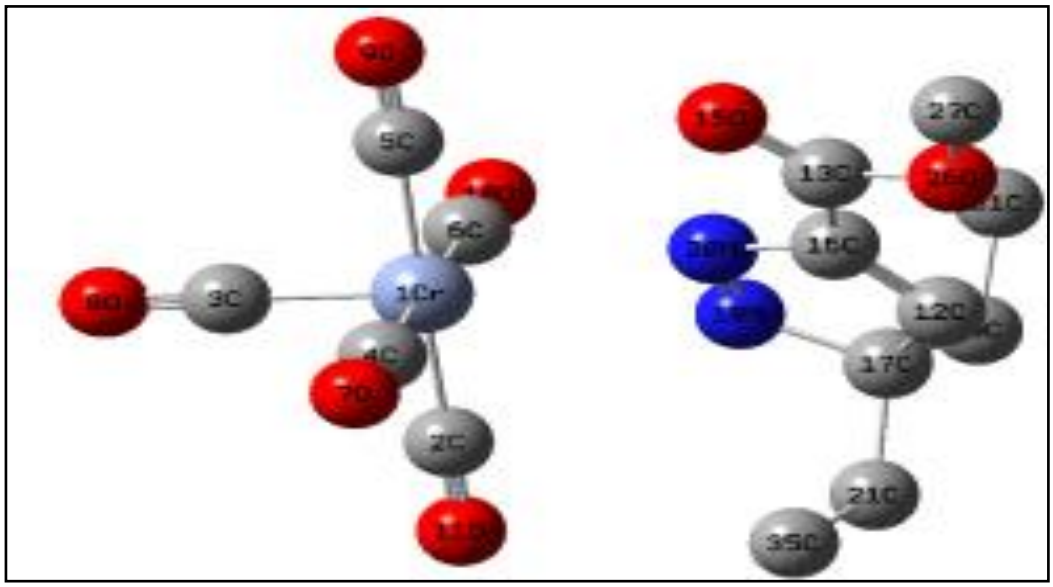


Figure 3.3: Optimized transition state of pentacarbonyl(3,3-diethyl-5-methoxycarbonyl-3H-pyrazol-$N_2$)chromium(0). (Hydrogen atoms are omitted for simplicity).

Table 3.4: Comparison between bond lengths (Å) of pentacarbonyl(3,3-diethyl-5-methoxycarbonyl-3H-pyrazol-$N_2$)chromium(0) in transition state and ground state.

| | **BOND LENGTH B3LYP** | |
|---|---|---|
| **BOND** | **Ground state** | **Transition state** |
| Cr1-N1 | 2.17213 | 2.93150 |
| N1-N2 | 1.25929 | 1.25132 |
| N1-C6 | 1.50673 | 1.48101 |
| N2-C8 | 1.41574 | 1.43435 |
| C6-C7 | 1.48567 | 1.48857 |
| C7-C8 | 1.33744 | 1.33755 |
| C8-C9 | 1.48223 | 1.47999 |
| O6-C9 | 1.20088 | 1.20173 |
| O7-C9 | 1.34626 | 1.34561 |
| O7-C10 | 1.43785 | 1.43829 |
| Cr-C1 | 1.94276 | 1.93500 |
| C1-O1 | 1.13760 | 1.13862 |
| Cr-C2 | 1.92143 | 1.92144 |
| C2-O2 | 1.4247 | 1.14186 |
| Cr-C3 | 1.90173 | 1.191266 |
| C3-O3 | 1.14706 | 1.14386 |
| Cr-C4 | 1.92143 | 1.92137 |
| C4-O4 | 1.14247 | 1.14201 |
| Cr-C5 (trans) | 1.87247 | 1.84626 |
| C5-O5 (trans) | 1.14713 | 1.14955 |

Table 3.5: Comparison of bond angles ($^0$) of pentacarbonyl(3,3-diethyl-5-methoxycarbonyl-3H-pyrazol-$N_2$)chromium(0) in ground state and transition state.

| | **BOND ANGLES B3LYP** | |
|---|---|---|
| **ANGLE** | **Ground state** | **Transition state** |
| N2-N1-C6 | 110.381 | 111.063 |
| N2-N1-Cr1 | 118.64 | 78.283 |
| C6-N1-Cr1 | 130.979 | 161.523 |
| N1-N2-C8 | 110.394 | 110.171 |
| C7-C6-N1 | 101.497 | 102.120 |
| N2-C8-C9 | 119.267 | 119.563 |
| C7-C8-N2 | 110.185 | 109.307 |
| C7-C8-C9 | 130.547 | 131.129 |
| O6-C9-C8 | 124.813 | 124.507 |
| C8-C7-C6 | 107.542 | 107.336 |

Table 3.6: Comparison of IR frequencies ($cm^{-1}$) of pentacarbonyl(3,3-diethyl-5-methoxycarbonyl-3H-pyrazol-$N_2$)chromium(0) in ground state and transition state.

| **B3LYP** | **Ground state** | | **Transition state** | |
|---|---|---|---|---|
| **Bond** | **IR Calculated** | **IR Scaled (0.9646)** | **IR Calculated** | **IR scaled (0.9646)** |
| C=O | 1801.45 | 1737.68 | 1796.75 | 1733.15 |
| Carbonyl | 2009.11 | 1937.99 | 2005.59 | 1934.60 |
| Carbonyl | 2027.11 | 1955.35 | 2032.74 | 1960.78 |
| Carbonyl | 2031.58 | 1959.66 | 2034.57 | 1962.55 |
| Carbonyl | 2072.49 | 1999.12 | 2070.4 | 1997.11 |
| Carbonyl | 2138.38 | 2062.68 | 2149.34 | 2073.25 |
| C=C | 1641.43 | 1583.32 | 1643.47 | 1585.29 |
| N=N | 1478.37 | 1426.04 | 1533.52 | 1479.23 |

The Cr-N1 bond distance in the transition state becomes longer than in the ground state, while N1-N2 bond distance in the transition state is shorter than the ground state. As expected, the bond distance in the transition state has weaker interaction between the Cr-N1, which results in stronger interaction between the two nitrogen atoms (N1-N2). The N2-N1-Cr1 bond angle in the ground state is ($118.64^0$), while it is ($78.28^0$) in the transition state. So there is a distortion in the structure of the complex in the transition state in addition to Cr-N1 bond breakage. The trans C≡O bond distance in the transition state becomes longer than in the ground state and trans Cr-C bond distance in the transition state becomes shorter than in ground state. These observations can suggest that the pyrazole ligand is able to donate more electrons in the transition state than in the ground state, which

can be explained by assuming that the pyrazole ligand has back bonding ability with the metal complex in the ground state structure, this back bonding is lost in the transition state. Moreover, the electron withdrawing methoxy carbonyl group stabilizes the Cr-N1 in the ground state by enhancing the pyrazole back bonding. In the transition state and the pyrozole becomes a σ-donor ligand only. In the ground state, both pyrazole and trans carbonyl occupy the same orbital of the metal that is involved in carbonyl and pyrazole back bonding (*55*), while this does not occur in the transition state. The bond angle of N2-N1-Cr1 is changed from $118.64^0$ in the ground state to $78.28^0$ in the transition state, which could be the reason for the loss of back bonding in the transition state

**3.2.1.2) Methyl prop-2-ynoate**

The optimized structure of methylprop-2-ynoate is shown in Figure 3.4, and selected bond distances and bond angles are listed in Table 3.7, and Table 3.8 respectively.

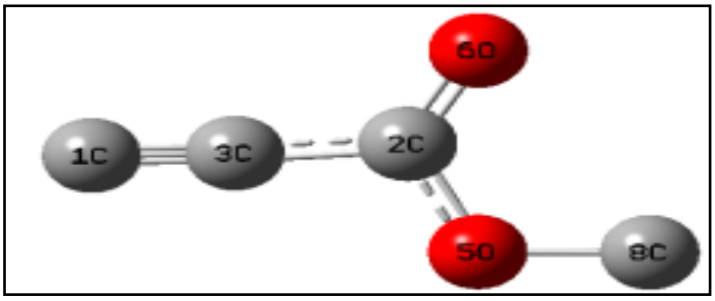


Figure 3.4: Optimized structure of methyl prop-2-ynoate.

Table 3.7: Selected bond lengths of methyl prop-2-ynoate.

| **Bond** | **Bond length (Å)** |
|---|---|
| C1-C3 triple bond | 1.19821 |
| C2-O6 | 1.20407 |
| C2-O5 | 1.34083 |
| C2-C3 | 1.44695 |

Table 3.8: Selected bond angles of methyl prop-2-ynoate.

| **Bond** | **Bond angle ($^0$)** |
|---|---|
| C1-C3-C2 | 177.072 |
| O6-C2-05 | 124.808 |

It is clear that the optimized structure is in agreement with the basic knowledge , that the ( sp CΞC) bond length is 1.19821Å which is slightly shorter than for typical alkyne (1.204 Å) (*56*). Since it is attached to the withdrawing methoxy carbonyl group which in turn stabilized the triple bond. Furthermore, the C2-C3 bond (1.44695 Å) is shortened compared to a typical single bond (1.53 Å) (*56*), indicating partially double bond, due to resonance. The C1-C3-C2 angle is $177^0$ with small deviation from linearity, and the O6-C2-O5 angle is ($124.8^0$) indicating plane geometry accompanied with the C=O $sp^2$ hybridization. IR stretching frequencies are listed in Table 3.9.

Table 3.9: Selected IR frequencies ($cm^{-1}$) for methylprop-2-ynoate.

| **Bond** | **calculated IR frequency** | **IR frequency scaled (0.9646)** |
|---|---|---|
| O5 –C8 | 1016.81 | 980.81 |
| C1- C3 (triple) | 2220.5 | 2141.90 |
| C2=O6 | 1769.97 | 1707.31 |
| C2-O5(partially double bond) | 1251.62 | 1207.31 |

### 3.2.1.3) $\eta^2$-Methyl prop-2-ynoate(pentacarbonyl)chromium

The optimized structure of $\eta^2$-methyl prop-2-ynoate(pentacarbonyl)-chromium is shown in Figure 3.5. Furthermore, selected bond lengths and bond angles are listed in Tables 3.10, and Table 3.11.

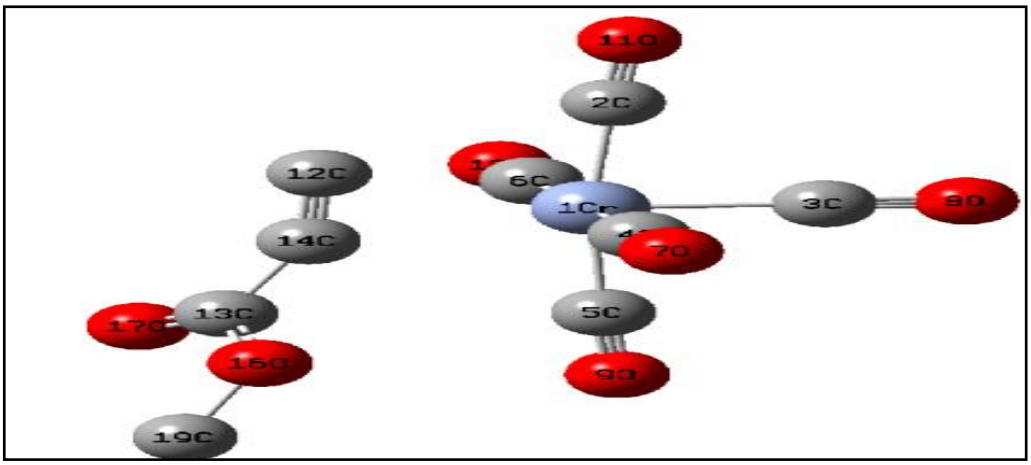


Figure 3.5: $\eta^2$-Methyl prop-2-ynoate(pentacarbonyl)chromium. (Hydrogen atoms are omitted for simplicity).

Table 3.10: Selected bond length (Å) for the ground state $\eta^2$-methyl prop-2-ynoate(pentacarbonyl)chromium and comparison with the transition state.

| Bonds | Bond length (GS)* | Bond length (TS)* |
|---|---|---|
| C12-Cr (triple bond) | 2.30330 | 2.35949 |
| C14-Cr(triple bond) | 2.31619 | 2.37840 |
| C12-C14 triple bond | 1.22773 | 1.22060 |
| C3-Cr (trans) | 1.88253 | 1.87765 |
| C3-O8 (trans carbonyl) | 1.14335 | 1.14395 |
| C2-Cr | 1.91393 | 1.91836 |
| C2-O11 | 1.14126 | 1.14091 |
| C6-Cr | 1.93611 | 1.92196 |
| C6-O10 | 1.13769 | 1.14031 |
| C4-Cr | 1.93214 | 1.92854 |
| C4-O7 | 1.13843 | 1.13945 |
| C5-Cr | 1.92330 | 1.93350 |
| C5-O9 | 1.13952 | 1.13802 |

*GS: Ground state.
*TS : Transition state.

Table 3.11 Selected calculated bond angles for the ground state $\eta^2$- methyl prop-2-ynoate(pentacarbonyl)chromium and comparison with the transition state.

| **Bond** | **BOND ANGLE ($^0$) (GS)** | **BOND ANGLE ($^0$) (TS)** |
|---|---|---|
| C2 Cr C3 | 85.780 | 88.254 |
| C5 Cr C3 | 85.815 | 88.080 |
| C12 C14 C13 | 157.373 | 161.066 |
| O17 C13 O16 | 125.249 | 125.448 |

The C12ΞC14 bond length is (1.2277Å) longer than the CΞC in methyl prop-2-ynoate (1.1982Å). C12-Cr bond length is (2.3033 Å), and C14-Cr bond length is (2.31619Å) which agree with experimental bond distance in C-Cr triple bond system (2.327Å) (*6*), (2.277-2.331Å) (*50*).

The trans C3-Cr bond length is (1.8825Å) compared to the average cis C-Cr bond length (1.9264 Å), this is accompanied by lengthening of the trans C3-O8 bond (1.4335 Å) compared to the average cis CΞO bonds (1.13922 Å). These data are also in agreement with the experimental data (*6,50,51*). These observations suggest that alkyne forms π-back bonding with the metal center, which decreases the interaction between C12-C14, accompanied by a decrease in vibration stretching as shown in Table 3.12 compared to the vibration stretching frequency C12-C14 in methyl prop-2-ynoate.

Table 3.12: Selected IR frequency ($cm^{-1}$) for the ground state $\eta^2$- methyl prop-2-ynoate(pentacarbonyl)chromium and the transition state.

| **Bond** | **IR frequency calculated (GS)** | **IR frequency scaled (0.9646) (GS)** | **IR frequency calculated (TS)** | **IR frequency scaled (0.9646) (TS)** |
|---|---|---|---|---|
| O16- C19 | 1009.46 | 973.73 | 1008.58 | 972.88 |
| O16 –C13 (partially double bond) | 1238.78 | 1194.93 | 1241.38 | 1197.44 |
| C13=O17 | 1771.64 | 1708.92 | 1771.94 | 1709.21 |
| C12-C14 (triple bond) | 2021.35 | 1949.79 | 2042.42 | 1970.12 |
| Carbonyl | 2049.68 | 1977.12 | 2052.81 | 1980.14 |
| Carbonyl | 2054.56 | 1981.83 | 2055.14 | 1982.39 |
| Carbonyl | 2066.23 | 1993.09 | 2066.6 | 1993.44 |
| Carbonyl | 2082.03 | 2008.33 | 2080.91 | 2007.25 |
| Carbonyl | 2155.55 | 2079.24 | 2153.8 | 2077.56 |

The transition state differ slightly from the ground state in geometry as shown in Figure 3.6, and Tables above, in the transition state the C12ΞC14 bond length is lowered; which indicates that the bond become stronger than in the ground state. A distortion to the ground state structure took place by the change in the dihedral angle C12C14Cr1C2 which is equal to $0.635^{o}$ in the ground state to about $45^{o}$ in the transitions state. This change might result in the loss of π-back bonding in the transition state which is supported by the fact that the trans C3-Cr  bond distance in the transition state is decreased,

while the C3-O8 bond distance is increased compared to the ground state, which only means a loss of the alkyne π-back bonding.

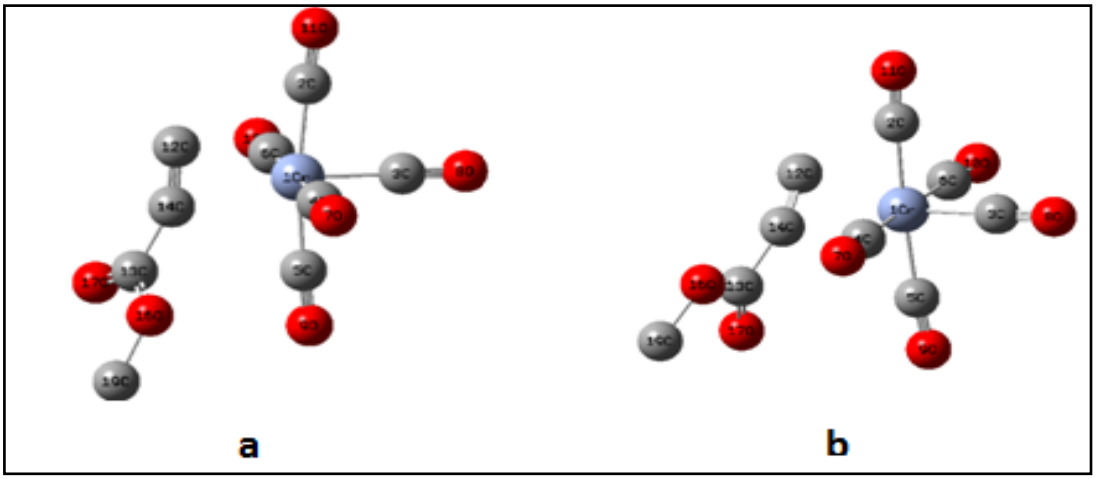


Figure 3.6: Optimized structure of methyl prop-2-ynoate(pentacarbonyl)chromium (a) ground state, (b) transition state.

The C≡O stretching frequency in the cis position remains almost the same with slight difference, while the trans carbonyl vibration is decreased.

### 3.2.1.4) 3-Diazopentane

The optimized structure of 3-diazopentane is shown in Figure 3.7, followed by selected bond length in Table 3.13 , and selected bond angles in Table 3.14.

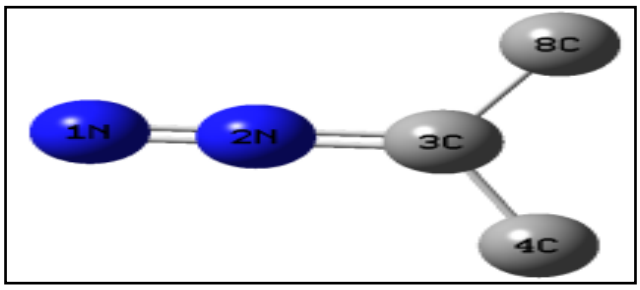


Figure 3.7: Optimized structure of 3-diazopentane

Table 3.13: Selected bond lengths of 3-diazopentane

| Bond | Bond length (Å) |
|---|---|
| N1-N2 | 1.14327 |
| N2-C3 | 1.28625 |
| C3-C4 | 1.51013 |
| C3-C7 | 1.51013 |

Table 3.14 Selected bond angles of 3-diazopentane

| Bond | Bond angle ($^0$) |
|---|---|
| N2 C3 C7 | 119.872 |
| N2 C3 C4 | 119.872 |
| C4 C3 C7 | 120.256 |
| N1 N2 C3 | 180.00 |

The 3-diazopentane optimized structure supposed to be planer structure since the carbon has $sp^2$ hybridization, the angles are around $120^0$, while nitrogen hybridization ranges between *sp* and $sp^2$ so it forms linear N-N-C system. The calculated bond lengths are almost in agreement with experimental values. The calculated C=N bond distance is (1.2863Å) compared to the experimental for a typical C=N is (~1.279Å) (*56*). The calculated N=N bond distance (1.1433 Å) is slightly shorter than the typical experimental N=N bond distance (~1.19 Å), this may be due to the resonance structure of diazoalkanes (*7*),

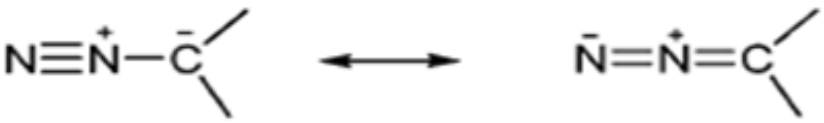

As shown in Table 3.15 the N-N stretching vibration to be (2051.4 $cm^{-1}$), is in the triple bond range, while the N-C bond is (1462.1 $cm^{-1}$) in the lower limit of double bond range.

Table 3.15: Selected IR frequencies of 3-diazopentane ($cm^{-1}$)

| Bond | IR frequency calculated | IR frequency scaled (0.9646) |
|---|---|---|
| N1=N2 | 2126.68 | 2051.4 |
| N2=C3 | 1515.76 | 1462.1 |

### 3.2.1.5) 3,3-Diethyl-5-methoxycarbonyl-3H-pyrazole

3,3-Diethyl-5-methoxycarbonyl-3H-pyrazole was optimized at its ground state, and its transition state, the optimized structures, and bond lengths, bond angles, and IR stretching frequency are listed in Figure 3.8, Tables 3.16, 3.17, 3.18 respectively.

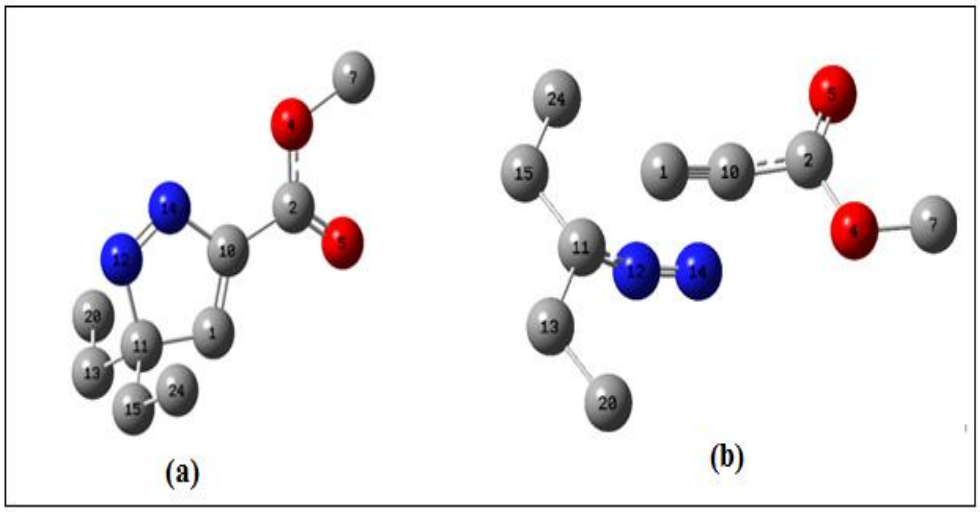


Figure 3.8: Optimized structure of 3,3-diethyl-5-methoxycarbonyl-3H-pyrazole (a) ground state (b) transition state.(Hydrogen atoms are omitted for simplicity).

Table 3.16: Bond length of 3,3-diethyl-5-methoxycarbonyl-3H-pyrazole in ground state and transition state.

| Bond | Bond length (Å) (GS) | Bond length (Å) (TS) |
|---|---|---|
| N12 –N14 | 1.24848 | 1.14060 |
| N14-C10 | 1.43954 | 2.57639 |
| C1-C10 | 1.33649 | 1.23029 |
| N12-C11 | 1.48396 | 1.33347 |
| C1-C11 | 1.48804 | 2.19081 |
| C2-C10 | 1.47971 | 1.42842 |
| C2-O5 | 1.20791 | 1.21128 |
| C2-O4 | 1.33743 | 1.35153 |
| C7-O4 | 1.43547 | 1.42942 |
| C11-C15 | 1.55254 | 1.51642 |
| C15-C24 | 1.52642 | 1.52340 |
| C11-C13 | 1.55255 | 1.51599 |
| C13-C20 | 1.52641 | 1.52336 |

Table 3.17: Selected bond angles ($^0$) of 3,3-diethyl-5-methoxycarbonyl-3H-pyrazole in ground state and transition state.

| Bond | Bond angle (GS) | Bond angle (TS) |
|---|---|---|
| O5 C2 O4 | 124.318 | 123.655 |
| C2 O4 C7 | 115.898 | 115.009 |
| O4 C2 C10 | 112.363 | 111.508 |
| C10 C2 O5 | 123.319 | 124.835 |
| C2 C10 N14 | 123.255 | 92.215 |
| C10 N14 N12 | 109.846 | 85.941 |
| N14 N12 C11 | 111.018 | 153.140 |
| N12 C11 C1 | 102.504 | 92.089 |
| C10 C1 C11 | 106.819 | 113.746 |
| C2 C10 C1 | 126.932 | 171.913 |

Table 3.18: Selected IR frequencies of 3,3-diethyl-5-methoxycarbonyl-3H-pyrazole in ground state and transition state ($cm^{-1}$).

| Bond | IR frequency calculated (GS) | IR frequency scaled (0.9646) (GS) | IR frequency calculated (TS) | IR frequency scaled (0.9646) (TS) |
|---|---|---|---|---|
| O4 –C2 | 1287.19 | 1241.62 | 1242.7 | 1198.71 |
| N12-N14 | 1535.94 | 1481.57 | 2138.13 | 2062.44 |
| C2=O5 | 1767.09 | 1704.54 | 1752.4 | 1690.37 |
| C1-C10 | 1656.15 | 1597.52 | 2055.64 | 1980.87 |

Pyrazole optimized geometry is analogous to the expected geometry in literature as in (*17,19*). The N12-N14 bond length is decreased from the ground state to the transition state as it may go from double bond to nearly triple bond. The N12-C11 bond distance is shorter in the transition state than the ground state which may be due to the fact that in the ground state it is singly bonded, while in the transition state it is doubly bonded. The C1-C10 bond is also decreased as it is returned back to triple bond in the transition state, while it is doubly bonded in the ground state. The transition state takes place by the breaking of the N14-C10, and C-C11 bonds. All of these changes are reflected in the calculated IR frequency. The stretching frequency of N12-N14 is increased from the double bond range (1481.57 $cm^{-1}$) in the ground state to the triple bond range (2062.44 $cm^{-1}$) in the transition state, the same thing happens for C-C10 stretching frequency, i.e. increased.

### 3.2.1.6)Pentacarbonyl(3,3-diethyl-5-methoxycarbonyl-3H-pyrazol-$C_2$)chromium(0)

To analyze the structure of the pentacarbonyl(3,3-diethyl-5-methoxycarbonyl-3H-pyrazol-C2)chromium(0) Figure 3.9a, it has to be divided into three parts according to the supposed transition state at which they are shown in Figure 3.9b (TS1), and Figure 3.9c (TS2).

Tables 3.18, 3.19, and 3.20 illustrate the differences in bond lengths, bond angles, and IR frequencies between the ground state and each of the transition states.

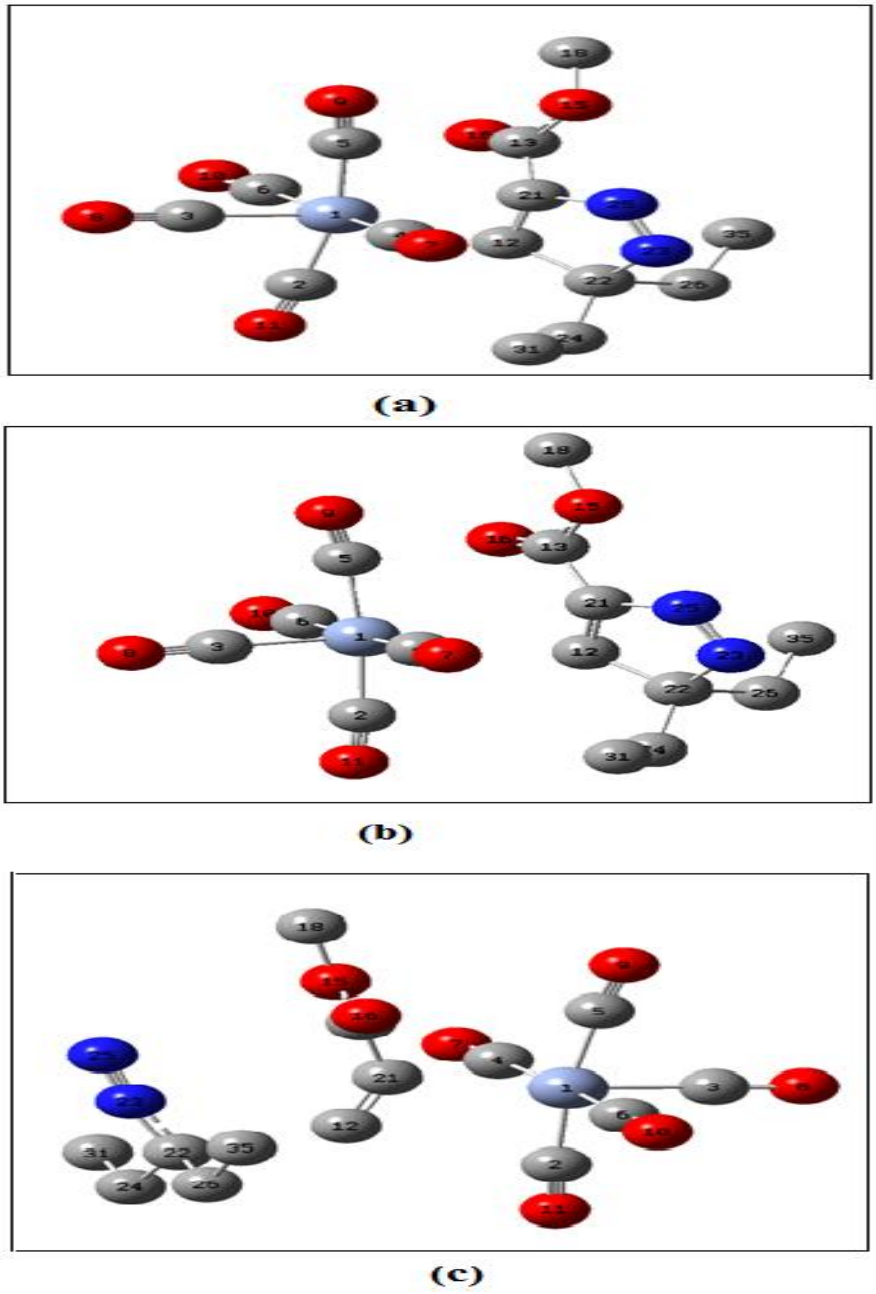


Figure 3.9: The optimized structure of pentacarbonyl(3,3-diethyl-5-methoxycarbonyl-3H-pyrazol-C2)chromium(0): (a) ground state, (b) first transition state (TS1), (c) second transition state (TS2). (Hydrogen atoms are omitted for simplicity).

Table 3.19: Selected bond lengths (Å) of pentacarbonyl(3,3-diethyl-5-methoxycarbonyl-3H-pyrazol-C2)chromium(0) in the ground state and both transition states.

| **Bond** | **Bond length (Å) (GS)** | **Bond length (Å) (TS1)** | **Bond length (Å) (TS2)** |
|---|---|---|---|
| Cr-C21 | 2.41905 | 3.09375 | 2.35604 |
| Cr-C12 | 2.49382 | 3.13298 | 2.87465 |
| C12-C21 | 1.37635 | 1.34778 | 1.25342 |
| C21-N25 | 1.45812 | 1.44645 | 3.46781 |
| N23-N25 | 1.24453 | 1.24746 | 1.12407 |
| N23-C22 | 1.48213 | 1.47855 | 1.32533 |
| C22-C12 | 1.50848 | 1.49545 | 2.18737 |
| C13-C21 | 1.49001 | 1.48848 | 1.46416 |
| C13-O16 | 1.20807 | 1.20782 | 1.20692 |
| C13-O15 | 1.33424 | 1.33218 | 1.34023 |
| O15-C18 | 1.43784 | 1.43941 | 1.43845 |
| C22-C26 | 1.58239 | 1.57640 | 1.52497 |
| C26-C35 | 1.52430 | 1.52479 | 1.52534 |
| C22-C24 | 1.54748 | 1.54991 | 1.52346 |
| C24-C31 | 1.52705 | 1.52580 | 1.52562 |
| Cr-C3 (trans) | 1.87493 | 1.85278 | 1.86254 |
| C3-O8 (trans) | 1.14356 | 1.14659 | 1.14814 |
| Cr-C2 | 1.91302 | 1.91840 | 1.90788 |
| C2-O11 | 1.14252 | 1.14247 | 1.14653 |
| Cr-C4 | 1.93090 | 1.92562 | 1.91935 |
| C4-O7 | 1.13810 | 1.13972 | 1.14187 |
| Cr-C5 | 1.92866 | 1.92098 | 1.91969 |
| C5-O9 | 1.13874 | 1.14090 | 1.14217 |
| Cr-C6 | 1.93345 | 1.93082 | 1.92089 |
| C6-O10 | 1.13766 | 1.13847 | 1.14150 |

Table 3.20: Selected bond angles ($^0$) of pentacarbonyl(3,3-diethyl-5-methoxycarbonyl-3H-pyrazol-C2)chromium(0) in the ground state and both transition states.

| **BOND ANGLES** | **B3LYP** | | |
|---|---|---|---|
| **ANGLE** | **Ground state** | **Transition state 1** | **Transition state 2** |
| C21-C12-Cr | 70.764 | 75.867 | 53.527 |
| C21-Cr-C12 | 32.493 | 24.991 | 25.328 |
| C12-C21-Cr | 76.743 | 79.133 | 101.145 |
| C12-C21-N25 | 108.396 | 109.298 | 78.264 |
| C21-N25-N23 | 110.313 | 109.869 | 64.138 |
| N25-N23-C22 | 111.761 | 111.434 | 171.534 |
| N23-C22-C12 | 102.475 | 102.495 | 99.668 |
| C22-C12-C21 | 105.702 | 106.474 | 123.904 |
| C21-C13-O16 | 123.532 | 123.164 | 123.560 |
| C2-Cr-C3 | 84.960 | 87.319 | 86.809 |
| C6-Cr-C3 | 88.706 | 90.183 | 92.660 |
| C3-Cr-C4 | 87.976 | 89.779 | 92.604 |
| C3-Cr-C5 | 85.180 | 87.517 | 85.846 |
| C5-Cr-C4 | 87.018 | 88.400 | 90.259 |
| C5-Cr-C2 | 169.797 | 174.613 | 172.655 |
| C4-Cr-C6 | 175.368 | 177.916 | 174.735 |
| C12-Cr-C3 | 159.448 | 163.118 | 161.746 |
| C21-Cr-C3 | 168.035 | 171.743 | 172.922 |

Table 3.21: IR frequency ($cm^{-1}$) of pentacarbonyl(3,3-diethyl-5-methoxycarbonyl-3H-pyrazol-C2)chromium(0) in the ground state and both transition states.

| **Bond** | **IR frequency calculated (GS)** | **IR frequency scaled (0.9646) (GS)** | **IR frequency calculated (TS1)** | **IR frequency scaled (0.9646) (TS1)** | **IR frequency calculated (TS2)** | **IR frequency scaled (0.9646) (TS2)** |
|---|---|---|---|---|---|---|
| Carbonyl | 2149.91 | 2073.80 | 2151.35 | 2075.19 | 2127.76 | 2052.437 |
| Carbonyl | 2082.74 | 2009.01 | 2073.07 | 1999.68 | 2056.79 | 1983.98 |
| Carbonyl | 2067.43 | 1994.24 | 2056.26 | 1983.47 | 2038.79 | 1966.617 |
| Carbonyl | 2049.4 | 1976.85 | 2035.48 | 1963.42 | 2019.57 | 1948.077 |
| Carbonyl | 2041.87 | 1969.59 | 2025.2 | 1953.51 | 2009.98 | 1938.827 |
| C=O | 1756.5 | 1694.32 | 1760.72 | 1698.39 | 1747.47 | 1685.61 |
| C=C | 1501.42 | 1448.27 | 1613.66 | 1556.54 | 1872.57 | 1806.281 |
| N=N | 1564.28 | 1508.90 | 1535.9 | 1481.53 | 2187.37 | 2109.937 |

a) The first transition state (TS1**):** This transition state occurs when lengthening the bond between the carbon double bond of the 3H-pyrazole and chromium of the chromium pentacarbonyl. While the distance in C12-Cr bond and C21-Cr bond become longer, the distance in C12=C21 bond is decreased as shown in Table 3.18. and the N-N bond becomes slightly longer. Furthermore, the trans CO bond is increased from 1.1436Å in the ground state to 1.1466 Å in this transition state, and trans Cr-C bond is decreased from 1.8749 Å in the ground state to the 1.5278 Å. This can only be explained by the fact that there is some back-bonding between the 3,3-diethyl-5-methoxycarbonyl-3H-pyrazol-$C_2$ and the metal center in the ground state complex. The back-bonding is lost in the transition state were the ligand becomes a donor ligand only, hence increasing the trans CO bond distance. This explanation is confirmed by the IR frequency shown in Table 3.20. There are slight differences in the cis Cr-C and the C≡O bond distances. Because the transition state may be less steric than the ground state, as also can be seen in the bond angles shown in Table 3.19. In this transition state, the structure of 3H-pyrazole

fragment is almost the same structure as the free 3H-pyrazole as discussed in section (5.2.1.5).

b) The second transition state (TS2): This transition state takes place by the cleavage of the C21-N25 bond, and the C12-N23 bond, and maintains the interaction between methyl-prop-2-ynoate and pentacarbonyl, but in a different way compared to $\eta^2$- Methyl prop-2-ynoate(pentacarbonyl)chromium. Since the C21-Cr bond become shorter than in the ground state structure, and the Cr-C12 bond becomes longer than in the ground state, the C12-C21 bond distance (1.2534 Å) still longer than the free alkyne triple bond. The trans Cr-C3 bond in the transition state is shorter than the ground state structure, while the CΞO bond is longer. The N23-N25 bond distance is decreased since it adopts the *sp* hybridization; also the N23-C22 bond becomes shorter since it goes from single bond in the ground state to partially double bond in transition state.

c) The third transition state (TS3): This transition state should involve the rearrangement in the ground state structure, which may occurs by ring rearrangement as earlier studies proposed for chromium(0) complexes with ring system like

Tricarbonyl(cyclooctatetraene)chromuim(0), the possible rearrangements for transition state are 1,2-, 1,3-, 1,4-, 1,5- ring shifts **(***57***)**. But in this study the work on this rearrangement is ongoing and requires more time.

### 3.2.2) Thermochemical analysis:

The two reaction mechanisms which are shown in Figure 3.10 can be followed in terms of changes in enthalpy, entropy, and Gibbs free energy. These thermochemistry parameters are obtained from the thermochemical analysis which is done by the frequency calculations at 298.15 K and 1 atmosphere (*21*).

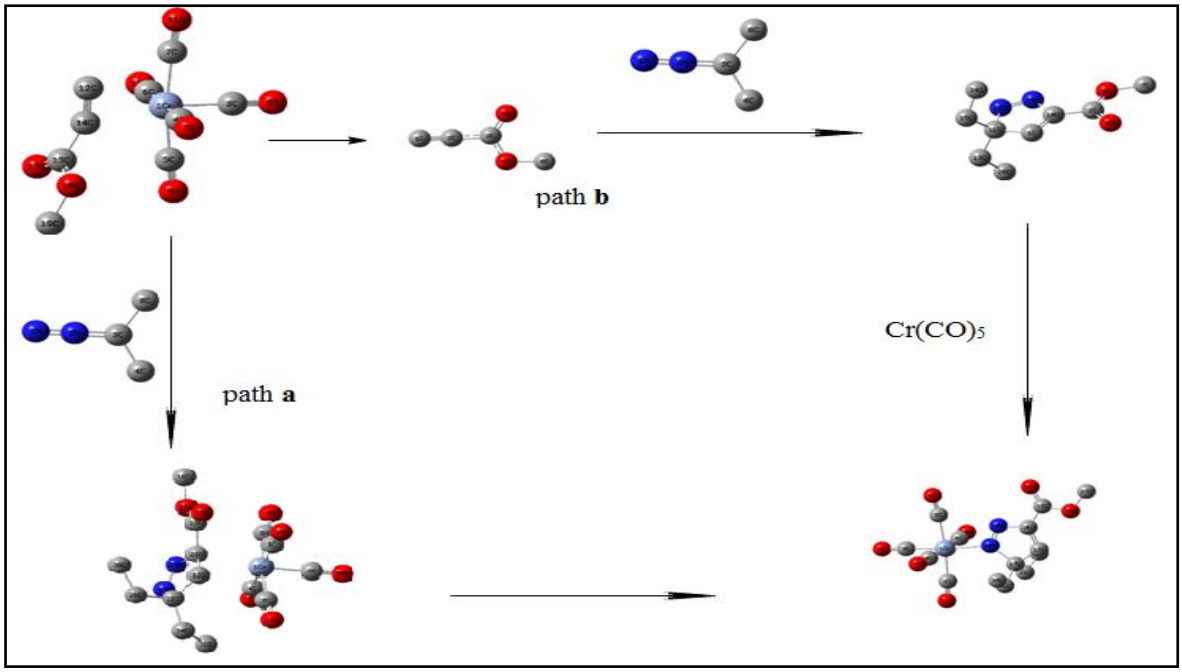


Figure 3.10: The two proposed mechanisms of the addition reaction of $\eta^2$-methyl prop-2-ynoate(pentacarbonyl)chromium to 3-diazopentane.

## 3.2.2.1) Path (a) analysis:

### 3.2.2.1.1) The addition of 3-diazopentane to $\eta^2$-methyl prop-2-ynoate(pentacarbonyl)chromium to form Pentacarbonyl(3,3-diethyl-5-methoxycarbonyl-3H-pyrazol-C2)chromium(0)

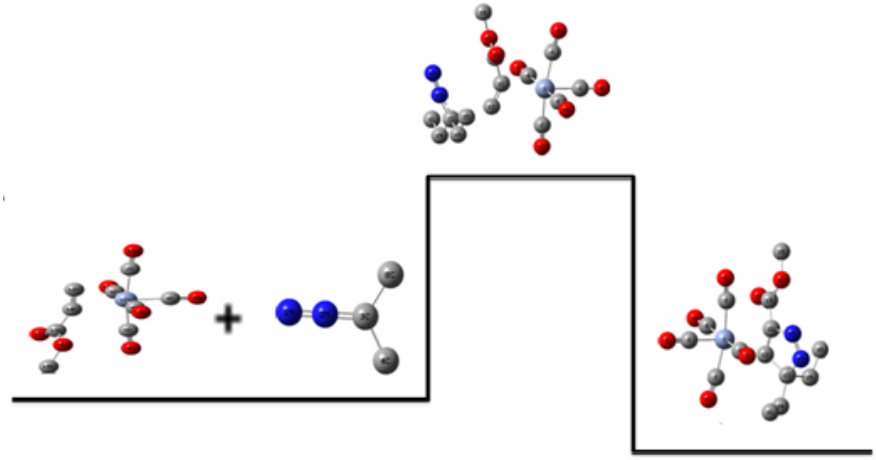

Figure 3.11: Cycloaddition 3-diazopentane to $\eta^2$-methyl prop-2-ynoate(pentacarbonyl)chromium to form pentacarbonyl(3,3-diethyl-5-methoxycarbonyl-3H-pyrazol-C2)chromium(0)

Dissociation of pentacarbonyl(3,3-diethyl-5-methoxycarbonyl-3H-pyrazol-C2)chromium(0) to $\eta^2$-methyl prop-2-ynoate(pentacarbonyl)-chromium(0), and 3-diazopentane has a $\Delta G^{\#}$ of activation equals to 34.51 kcal/mol, $\Delta S^{\#}$ of activation equals 18.97 cal/mol.K, and $\Delta H^{\#}$ of activation equals to 40.16 kcal/mol. While the forward step which involves the cycloaddition of 3-diazopentane to $\eta^2$-methyl prop-2-ynoate(pentacarbonyl)chromium to form pentacarbonyl(3,3-diethyl-5-methoxycarbonyl-3H-pyrazol-C2)chromium(0)

has a $\Delta G^{\#}$ of activation equals to 24.59 kcal/mol, $\Delta S^{\#}$ of activation equals -45.08 cal/mol.K, and $\Delta H^{\#}$ of activation equals to 11.16 kcal/mol. Since this is the bulkiest transition state it was verified by intrinsic reaction path (IRC) calculations. Energy of each optimized geometry for the six steps (forward and backward) in Hartree (1Hartree = 627.51kcal/mol) is plotted versus the IRC reaction coordinate as shown in Figure 3.12. The maximum is the calculated geometry of the transition state, which confirms that this is true transition state.

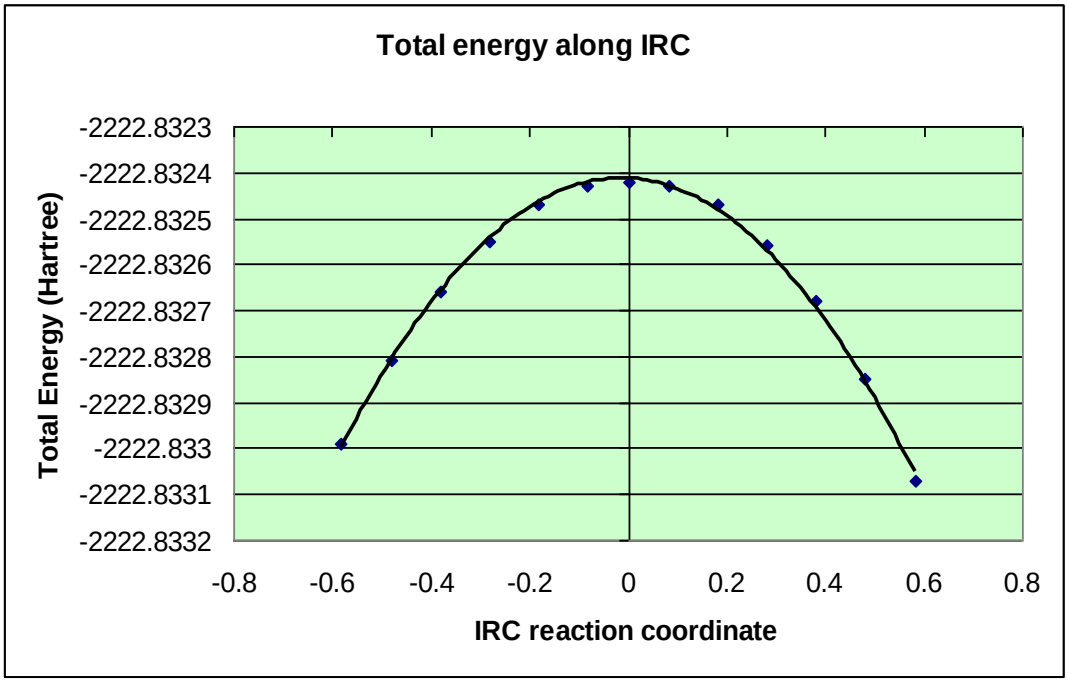


Figure 3.12: Results of IRC calculation

### 3.2.2.1.2) Rearrangement of pentacarbonyl(3,3-diethyl-5-methoxycarbonyl-3H-pyrazol-C2)chromium(0) to give pentacarbonyl(3,3-diethyl-5-methoxycarbonyl-3H-pyrazol-$N_2$)chromium (0)

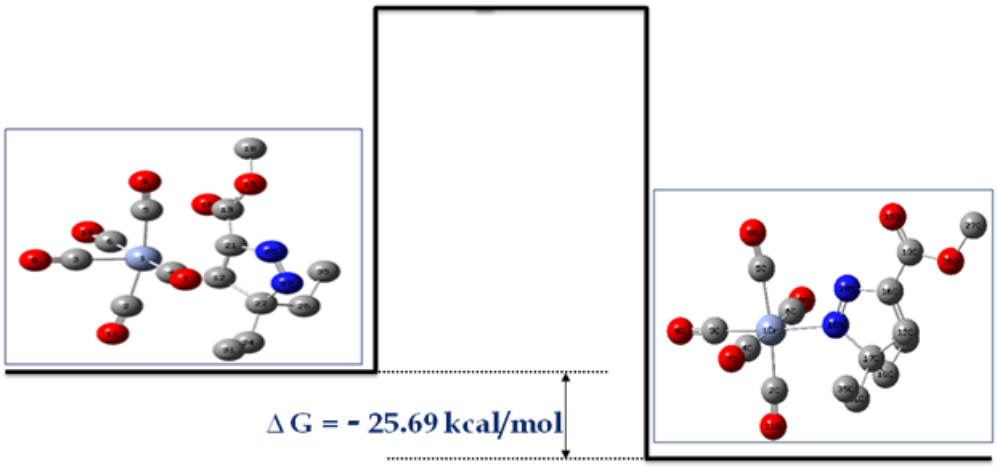


Figure 3.13: Rearrangement of pentacarbonyl(3,3-diethyl-5-methoxycarbonyl-3H-pyrazol-C2)chromium(0) to give pentacarbonyl(3,3-diethyl-methoxycarbonyl-3H-pyrazol-$N_2$)chromium (0)

This step may occur either by rearrangement of ground state or by breakage of the (Cr- C double bond) of pentacarbonyl(3,3-diethyl-5-methoxycarbonyl-3H-pyrazol-C2)chromium(0). Rearrangement transition state is not clear since it could not be obtained till now. But analogy to the rearrangement activation energies of Tricarbonyl(cyclooctatetraene)chromuim(0) which has these values (6.3,0.6, 10.0, and 11.6 kcal/mol) for the 1,2-, 1,3-,1,4-, and 1,5- ring shifts respectively (*57*), the preferred shift is 1,3-shift since it is the

lowest activation energy, which is in agreement with their experiment (*57*).

The other possible path that could lead to the formation of Pentacarbonyl(3,3-diethyl-5-methoxycarbonyl-3H-pyrazol-$N_2$) chromium (0) is by the dissociation of the 3H-pyrazol from the pentacarbonyl(3,3-diethyl-5-methoxycarbonyl-3H-pyrazol-C2)chromium (0) as shown in Figure 3.14, which has a small activation energy $\Delta G^{\#}$ = 0.32 kcal/mol, then recombination to form

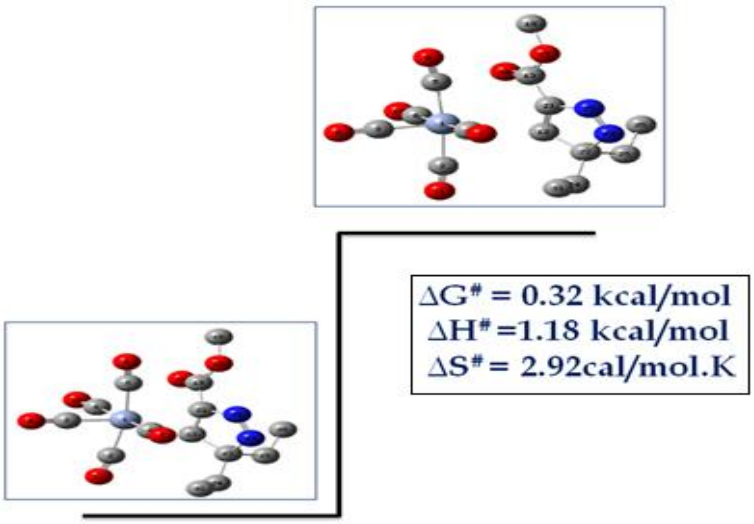


Figure 3.14: Dissociation of the 3H-pyrazol from pentacarbonyl(3,3-diethyl-5-methoxycarbonyl-3H-pyrazol-C2)chromium(0)

pentacarbonyl(3,3-diethyl-5-methoxycarbonyl-3H-pyrazol-$N_2$)chromium(0). The transition state is not clearly identified, but the certain thing is that pentacarbonyl(3,3-diethyl-5-methoxycarbonyl-3H-pyrazol-C2)chromium(0) will go to pentacarbonyl(3,3-diethyl-5-

methoxycarbonyl-3H-pyrazol-N2)chromium(0), since pentacarbonyl(3,3-diethyl-5-methoxycarbonyl-3H-pyrazol-N2)chromium (0) is more stable.

### 3.2.2.2) Path (b) analysis:

### 3.2.2.2.1): The disociation of the $\eta^2$-Methyl prop-2-ynoate(pentacarbonyl)chromium

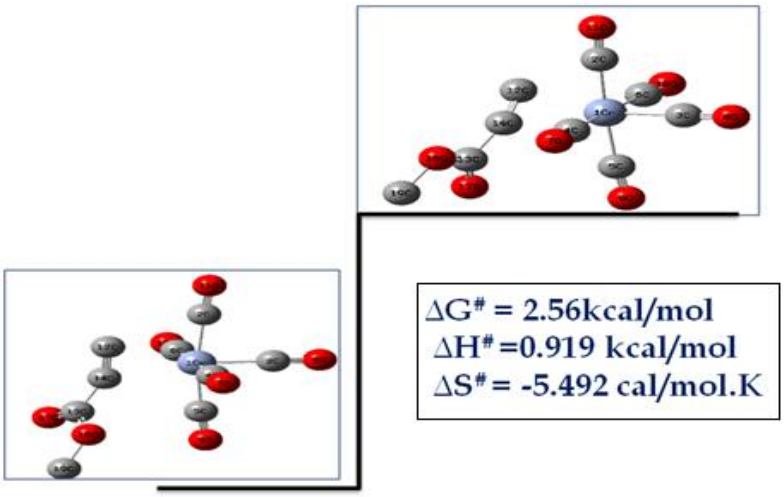


Figure 3.15: The disociation of the $\eta^2$-Methyl prop-2-ynoate(pentacarbonyl)chromium

The activation energy for the dissociation of the η2- Methyl prop-2-ynoate(pentacarbonyl)chromium is small (2.56kcal since the interaction is weak as the enthalpy shows 0.9187 kcal/mol. $\Delta S^{\#}$ is negative while it is expected to be positive, and there is no obvious explanation for this!

### 5.2.2.2.2) The cycloadditon of the alkyne to the 3-diazopentane

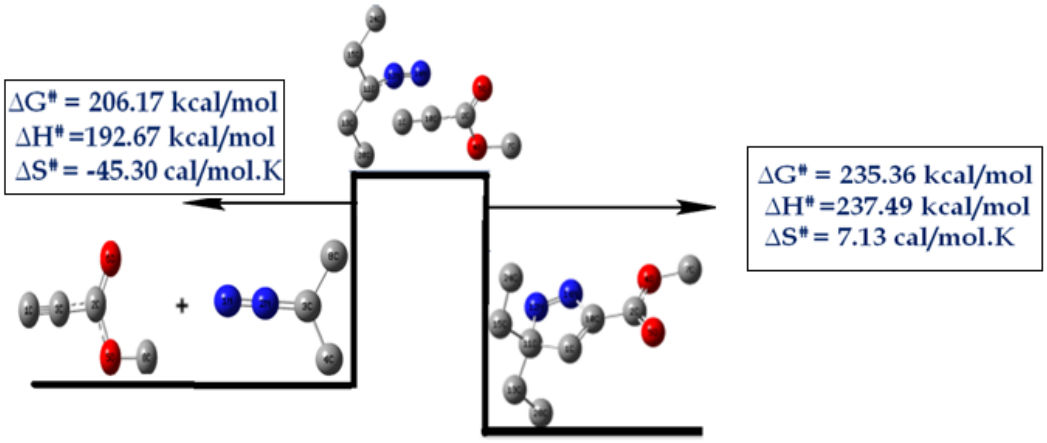


Figure 3.16: The cycloadditon of the alkyne to the 3-Diazopentane.

The activation energy for both sides of the reaction is very high which means that it is very difficult to pass this energy barrier. The bonds in 3,3-Diethyl-5-methoxycarbonyl-3H-pyrazole are strong, it is a stable compound; the bond dissociation enthalpy is high (237.49 kcal/mol). Hence, higher energy is needed for the dissociation to occur, while the association reaction of methyl prop-2-ynoate and 3-diazopentane is also has higher activation energy but it is still lower than the dissociation process. Association reaction is associated with negative entropy of activation which is in this case is very high ($\Delta S^{\#}$ = -45.305 cal/mol.k), and with $\Delta H^{\#}$ = 192.67 kcal/mol.

### 3.2.2.2.3) The Cr-N bond brakeage in pentacarbonyl (3,3-diethyl-5-methoxycarbonyl-3H-pyrazol-$N_2$)chromium(0).

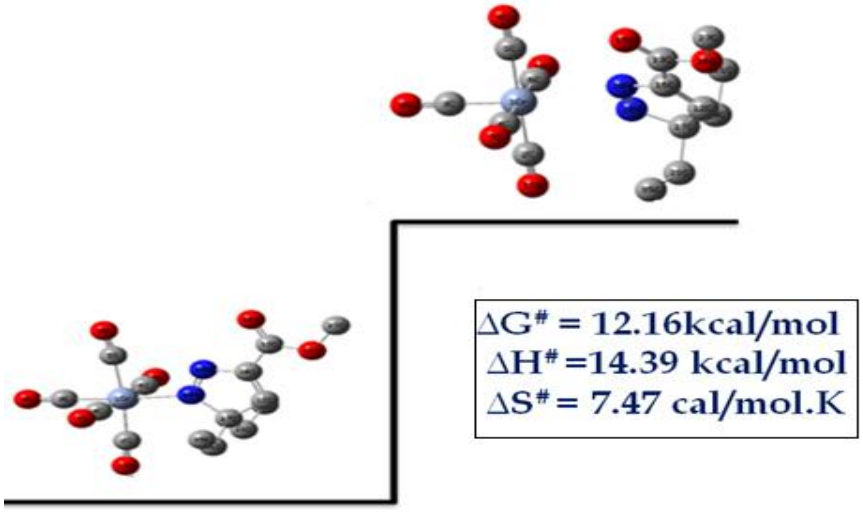


Figure 3.17: The Cr-N bond brakeage in pentacarbonyl (3,3-diethyl-5-methoxycarbonyl-3H-pyrazol-$N_2$)chromium(0).

The bond strength between the chromium carbonyl and pyrazole (Cr-N bond) is determined by bond dissociation enthalpy which is (14.39 kcal/mol), breaking this bond needs energy of (12.164 kcal/mol), the positive $\Delta S^{\#}$ confirms a dissociation process.

According to the above information about bonds strength and activation energies, it can be concluded that since the energy of activation of the pyrazole formation step is high, one can reject path **b** compared to path **a** which has an overall low activation barrier

# CHAPTER FOUR

# CONCLUSION AND RECOMENDATIONS

In this study, the structural and electronic properties were analyzed for all the compounds that may be obtained by the two mechanisms proposed by Abd-Elzaher et al. of the cycloaddition reaction of 3-Diazopentane to $\eta^2$-Methylprop-2-ynoate(pentacarbonyl)chromium(0) to form 3H-pyrazole complex. There is a good agreement between the experimental and the calculated bond length, bond angles and IR data.

On the basis of the obtained results, it was concluded that preparation of 3H-pyrazol complexes occurs via the addition of the diazoalkane to the coordinated alkyne followed by either ring rearrangement or by breaking of the Cr-C double bond, followed by formation of Cr-N bond in 3H-pyrazole complex, So path **a** is preferred thermodynamically. On the other hand, Path **b** is rejected since the cycloaddition step of diazoalkane to the non-coordinated alkyne is higher in energy than the addition of diazoalkanes to the coordinated-alkyne by a factor of 8. Hence, this result agrees with the proposed path by Abd-Elzaher et al., but disagrees with the

explanation. The author suggested that the displacement step of the coordinated alkyne by the solvent is the slower step, while it seems according to the obtained results that the displacement of alkyne requires low energy. Moreover, the same author suggested that the addition step of the diazoalkane to the non-coordinated alkyne is a fast step, which again disagrees with the obtained results since this step needs sufficient energy to proceed; $\Delta G^{\#}$ = 206.17 kcal/mol. As a result, the chromium carbonyl can play a catalyst role in this reaction, since it lowers the energy barrier by its coordination with the alkyne that will undergo the cycloaddition reaction.

Through studying the two mechanisms, it was noticed that three types of ligands (L) are attached to the chromium carbonyl, methyl prop-2-ynoate via carbon-carbon triple bond (C≡C), and pentacarbonyl(3,3-diethyl-5-methoxycarbonyl-3H-pyrazol-N2)chromium(0) via nitrogen atom (N), and pentacarbonyl(3,3-diethyl-5-methoxycarbonyl-3H-pyrazol-C2)chromium(0) via carbon-carbon double bond (C=C). Bonding of these ligands with chromium are expected to consist of both ligand to metal σ-donation, and metal to ligand π-back donation. This conclusion is based on the results obtained for the bond distances of the trans C≡O bond and the trans

Cr-C bond. Comparison of the bond length of the trans CO and the trans C-Cr to the attached ligand (L) in the transition state compared to the ground state complexes. The CO bond is longer and the C-Cr is shorter in the transition state than in the ground state. This means that the Cr is back bonding with L in the ground state this back bonding is lost in the transition state and L becomes more electron donor.

It is recommended to do further studies using different computational methods to compare with the method used in this study (B3LYP).

It is also recommended to look at the bonding nature of orbitals by computing the natural bond orbital (NBO) and the electron density for each complex. And to look deeply at the rearrangement step.

## REFERENCES


1) Wikipedia, The Free Encyclopedia, Computational chemistry. http://en.wikipedia.org/wiki/Computational_chemistry (December 8, 2010).
2) Young, D. *Computational Chemistry: A Practical Guide for Applying Techniques to Real-World Problems*; John Wiley & Sons: 2001.
3) Lewars, E. *COMPUTATIONAL CHEMISTRY Introduction to the Theory and Applications of Molecular and Quantum Mechanics*; Kluwer Academic Publishers: 2004.
4) Collman, J.P.; Hegedus, L. S.; Norton,J. R.; Finke,R.G. *Principles and Applications of organotransition chemistry;* University science books: Mill Valley,CA,1987.
5) Crabtree, R. H. *The organometallic chemistry of the transition metals; Wiley:* New York, 2005.
6) CedenÕ, D. L.; Weitz, E. *J.Am.Chem.Soc.* **2001,**123 , 12857-12865.
7) Kissane, M.; Maguire, A. R. *Chem. Soc. Rev.* **2010**, 39, 845–883.
8) Gilchrist, T. *Heterocyclic Chemistry*, 3rd ed.; Longman, 1997.

9) Barluenga, J.; Rodríguez, F.; Fañanás, F.; Flórez, J. *Topics Organomet. Chem.***2004**, 13, 59-12.

10) Yang, S.; Lin, X.; Sun, C.; Fang, D. *J. Mol. Struct.-THEOCHEM*. **2007**, 815, 127-133.

11) Baldoli, C.; Buttero, P.; Licandro, E.; Maiorana, S.; Papagni, A.; Zanotti-Gerosa, A.*J. Organomet. Chem.***1994**, 476, 27-29.

12) Padwa, A.; Pearson, W. Synthetic Applications of 1,3-Dipolar CycloadditionToward Heterocyclic And Natural Products, JOHN WILEY &SONS,INC, 2003.

13) Abd-Elzaher, M. M.; Weibert, B.; Fischer, H. *J. Organomet. Chem*. **2003**, 669, 6 -13.

14) Szécsényi, K. M.; Leovac, V.M., Jaimovi, K.; Pokol,G. *J.Therm. Anal. Calorim.***2003**, 74, 943-952.

15) Yet, L. *Comprehensive Heterocyclic Chemistry III*, Chapter 4.01, Albany Molecular Research, Inc:Albany, NY, USA, 2008, 1-141.

16) Elguero, J. *Comprehensive Heterocyclic Chemistry II*, Chapter 3.01, Instituto de QufmicaMedica, CSIC:Madrid, Spain, 1996, 1-75.

17) Suschitzky, H.; Suschitzky, J.*The Chemistry of Heterocycle, structure, reaction, synthesis, and application*, 2nd ed.; WILEY-VCH, 2003.

18) Badea, M.; Emandi, A.; Marinescu, D.; Cristurean, E.; Olar, R.; BraileanuA.; Budrugeac P.; Segal E. *J. Therm. Anal.Calorim.***2003**, 72, 525-531.

*19)* Acheson, R.*An Introduction to the Chemistry of Heterocyclic Compounds*, 3rd ed.; Wiley-Intersciencepublication : New York, 1977.

20) Mcquarrie, D.; Simons, J. *Physical Chemistry: A Molecular Approach*, University Science Books: California, 1997.

*21)* Foresman, J.; Frisch, A. *Exploring Chemistry with Electronic Structure*,2nd ed.; Gaussian, Inc.: USA, 1996.

22) Magnasco, V. *Elementary Methods of Quantum Mechanics*, Elsevier, 2006.

23) Levine, I. *Quantum Chemistry*, 5th ed.; Prentice Hall: New Jersey, 2000.

24) Mcquarrie, D. *Quantum Chemistry*, 1st ed.; University Science Books: California,1983.

*25)* Mueller, M. *Fundamental of Quantum ChemistryMolecular Spectroscopyand Modern Electronic Structure Computations*, Kluwer Academic Publishers: New York, 2002.

*26)* Sherrill, C. D. A *Brief Review of Elementary Quantum Chemistry*, Georgia Institute of Technology, 2006. http://vergil.chemistry.gatech.edu/notes/quantrev/node28.html. (December 12, 2010).

27) Lowe, J. *Quantum Chemistry*, Academic Press: London, 1978.

*28)* Cramer, C. *Essentials of Computational Chemistry Theories and Models*, 2nd ed.; John Wiley & Sons, Ltd: USA, 2004.

29) Friedman, R. S.; Atkins, P.W. *Molecular Quantum Mechanics*, 4th ed.; Oxford University Press Inc.: New York, 2005.

30) Simons, J.; Nichols, J. *Quantum Mechanics in Chemistry: Topics in Physical Chemistry*, Oxford University Press Inc.: New York, 1997.

*31)* Sherrill, C. D. A *Brief Review of Elementary Quantum Chemistry*, Georgia Institute of Technology, 2006. http://vergil.chemistry.gatech.edu/notes/quantrev/node27.html. (December 13, 2010).

*32)* Ramachandran, K. I.; Deepa, G.; Namboori, K. *Computational Chemistry and Molecular Modeling*, Springer: Verlag Berlin Heidelberg, 2008.

33) Jensen, F. *Introduction to Computational Chemistry*, 2nd ed.; John Wiley & Sons, Ltd: USA, 2007.

*34)* Quinn, C. *Computational quantum chemistry: an interactive guide to basis set theory*, Academic Press, 2002.

35) Simons, J. *An Introduction to Theoretical Chemistry*, Cambridge University Press, 2003.

36) Basis Set, https://www.wiki.ed.ac.uk/download/attachments/.../basissets.pdf?...1. (December 19, 2010).

37) Basis Sets, http://www.gaussian.com/g_tech/g_ur/m_basis_sets.htm. (December 19, 2010).

*38)* Koch, W.; Holthausen, M. A *Chemist's Guide to Density Functional Theory*, 2nd ed.; Wiley-VCH Verlag GmbH, 2001.

39) Lawrance, G. A. *Introduction to Coordination Chemistry*, John Wiley & Sons Ltd., 2010.

40) Miessler, G. L.; Tarr, D. A. *Inorganic Chemistry*, 3rd ed.; Pearson Education International, 2004.

41) Hill, A. F. *Organotransition Metal Chemistry*, Royal Society of Chemistry, 2002.

42) Housecroft, C. E.; Sharpe, A. G. Inorganic Chemistry, 3rd ed.; Prentice Hall, 2008.

*43)* Basolo, F.; Pearson, R. G. Prog. Inorg. Chem.**1962**, 4, 381-453.

*44)* Cotton, F. A.; Wilkinson, G., *Advanced Inorganic Chemistry: A Comprehensive Text*, 3rd ed.; John Wiley & Sons, Inc.: USA, 1972.

*45)* Zumdahl, S.; Drago, R. *J. Am. Chem. Soc.***1968**, 90, 6669-6675.

46) Coe, B. J.; Glenwright, S. J. *Coord. Chem. Rev.***2000**, 203, 5-80.

*47)* Atwood, J.D.; Wovkulich, M. J.; Sonnenberger, D. C. *Acc. Chem. Res*, **1983**, 16, 350-355.

48) Szymafiska-Buzar, T.; Downs, A. J.; Greene, T. M.; Marshall, A. S. *J. Organomet. Chem.***1995**, 495, 149- 161.

49) Omae. I. *Appl. Organometal. Chem.***2008**, 22, 149-166.

*50)* Nechaev, M. S.; Rayon, V. M.; Frenking, G. *J. Phys. Chem. A* **2004**, 108, 3134 - 3142.

51) Grevels, F.; Jacke, J. *Organometallics***2005**, 24, 4613-4623.

52) Szymańska-Buzar, T.; Kern, K. *J. Organomet. Chem.***2001**, 622, 74-83.

53) BRUCE, M. I. *Chem. Rev.*,**1991**, 91, 197-257.

54) Gaussian 03, Revision E.01 , Frisch, M. J.; Trucks, G. W.; Schlegel, H. B.; Scuseria, G. E.; Robb, M. A.; Cheeseman, J. R.; Montgomery, Jr., J. A.; Vreven, T.; Kudin, K. N.; Burant, J. C.; Millam, J. M.; Iyengar, S. S.; Tomasi, J.; Barone, V.; Mennucci, B.; Cossi, M.; Scalmani, G.; Rega, N.; Petersson, G. A.; Nakatsuji, H.; Hada, M.; Ehara, M.; Toyota, K.; Fukuda, R.; Hasegawa, J.; Ishida, M.; Nakajima, T.; Honda, Y.; Kitao, O.; Nakai, H.; Klene, M.; Li, X.; Knox, J. E.; Hratchian, H. P.; Cross, J. B.; Bakken, V.; Adamo, C.; Jaramillo, J.; Gomperts, R.; Stratmann, R. E.; Yazyev, O.; Austin, A. J.; Cammi, R.; Pomelli, C.; Ochterski, J. W.; Ayala, P. Y.; Morokuma, K.; Voth, G. A.; Salvador, P.; Dannenberg, J. J.; Zakrzewski, V. G.; Dapprich, S.; Daniels, A. D.; Strain, M. C.; Farkas, O.; Malick, D. K.; Rabuck, A.D.; Raghavachari, K.; Foresman, J. B.; Ortiz, J. V.; Cui, Q.; Baboul, A. G.; Clifford, S.; Cioslowski, J.; Stefanov, B. B.; Liu, G.; Liashenko, A.; Piskorz, P.; Komaromi, I.; Martin, R. L.; Fox,

D. J.;Keith, T.; Al-Laham, M. A.; Peng, C. Y.; Nanayakkara, A.; Challacombe, M.; Gill, P. M. W.; Johnson, B.; Chen, W.; Wong, M.W.; Gonzalez, C.; and Pople, J. A.; Gaussian, Inc., Wallingford CT, 2004.

55) Palusiak, M. *J. Organomet. Chem.* **2007**, 692, 3866-3873.

*56)* Pauling, L. *The nature of the chemical bond and the structure of molecules and crystals: an introduction to modern structural chemistry* ,Cornell University Press, 1960.

57) Lawless, M.; Marynick, D. *J. Am. Chem. Soc.***1991**, 113, 7513-7521.

# APPENDIX

# SOFTWARE PACKAGES FOR ELECTRONIC STRUCTURE CALCULATIONS

## Gaussian 03w

Gaussian software was first established by John Pople in 1970 (1), it has been continuously updated, and has various versions labeled by year of release (Gaussian 70,…, Gaussian 92, Gaussian 94, Gaussian 98,…, Gaussian 09) (*1*,*2*,*3*). It includes all common ab-initio methods, some semiemperical methods, and molecular mechanics (*2*,*4*). Gaussian can optimize geometries, predict the energy, calculate vibrational frequencies, IR spectra, thermodynamic properties, search for transition states, and a wide range of molecular properties that can be computed (*2*,*4*,*5*).

Computation can be carried out on systems in the gas phase or in solution, and in their ground state or in excited state (*5*). Each Gaussian job requires an input file, specifying the type of calculation, basis set, and molecular specification of the input data. Input files contain ASCII text only and are prepared using a text editor. Gaussian input files require a filename with a .gjf extension (*5*). And after running, it gives an output file with a filename extension .out which

contains the result of calculations (*5*). Gaussian can be used separately, or in conjunction with Gaussian View.

**Gaussian view 3.07**

Gaussian View is a graphic interface for use with the Gaussian program. It can be used to build molecules, set up the options in the input file, run a calculation, and display results.

Instead of typing the coordinates, method, basis set, etc., Gaussian View is used by opening the program icon. Then the calculation is specified by pointing and clicking to build the molecule, and using pull-down menus to select the calculation type, level of theory and basis set, then Gaussian input file is generated, and can be run, after Gaussian finish the job, Gaussian View reads Gaussian output files and visualize the results (*4*).

The next section will illustrate how these two programs work, and shows the steps for running them is the best way.

**Running Gaussian 03 and Gaussian view**

Before the facility of Gaussian view, Gaussian was used by itself.

So we will show an example of running Gaussian with, and without Gaussian view.

**1) Running Gaussian without the use of Gaussian view**

The following steps are necessary to run Gaussian in windows:

1) The program is started by choosing its icon; the main window of Gaussian is opened.

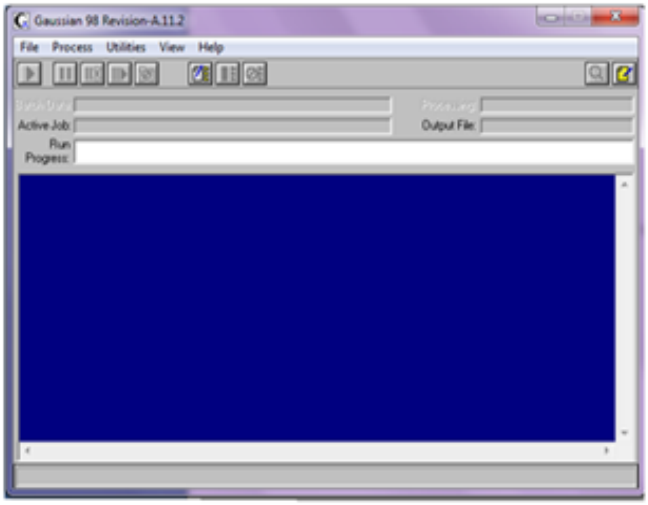


Figure 1: Main program window.

2) To create a new input file the job entry window is opened. This window is divided into sections; each one holds a different part of the Gaussian input (*5*). The sections are,

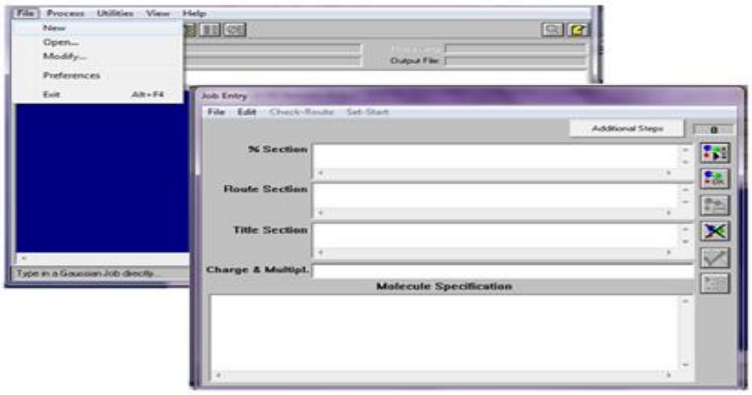


Figure 2: Job entry window.

**2.a)** % Section: used to specify the memory and number of processors used, and to locate and name scratch files. Checkpoint file is one of Gaussian scratch files that contains results in a machine readable file (*5,6*). The % Chk command specifies the name for the checkpoint file, and tells the program to save the file after the job finishes (*5*). Saved checkpoint files can be used to retrieve calculation results to use it in subsequent calculation, and to restart a failed job (*5*).

**2.b)** Route section: is used to specify the kind of job calculations, theoretical method, basis set, and may contain additional keywords to describe additional options. It is started by # sign, # alone requests normal output, #T request terse output, #P requests the maximum details in output (*5*).

**2.c)** Title section: is used to give a brief description of the job.

**2.d)** Charge & multiple : this section holds the charge on the molecule, and its spin multiplicity which is given by $2S + 1$, where S is total spin for the molecule, paired electrons have no contribution, while unpaired electrons contribute. In the case of a single unpaired electron ($\pm\frac{1}{2}$) it has a spin multiplicity of 2, and so on (*5*).

**2.e)** Molecule specification: the structure of the molecular system is obtained either by construction (Z- matrix or Cartesian coordinates or

mix of them) or by coordinates generated by or converted from a drawing program (such Gaussian view in the following section) (*5*).

**2.e.1)** Cartesian coordinate input: consists of series of lines of the form

Atomic-symbol X-coordinate Y-coordinate Z-coordinate

For example, water input file is given (*5*).

| Atomic-symbol | X-coordinate | Y-coordinate | Z-coordinate |
|---|---|---|---|
| O | -0.464 | 0.177 | 0.0 |
| H | -0.464 | 0.137 | 0.0 |
| H | 0.441 | -0.143 | 0.0 |

**2.e.2)** Z-matrix: specifies the location and bonds between atoms using bond length (in angstroms), bond angles (in degrees), and dihedral (torsion) angles, construction Z-matrix (*7*), it is in the form

| Atom Number | Atom Name | Atom Connect | Bond Distance | Angle Connect | Bond Angle | Dihedral Connect | Dihedral Angle |
|---|---|---|---|---|---|---|---|

There are steps to Construct Z-matrix, it will be shown as example of Hydrogen peroxide $H_2O_2$ (*5*,*8*):

- An atom in the molecule is chosen as starting atom, and placed at the origin in 3-d space. The left oxygen is assigned as O1.

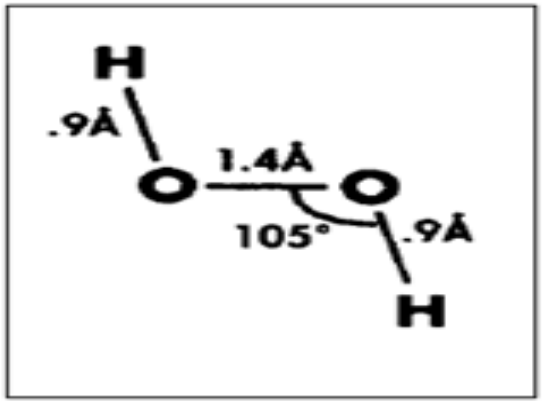


Figure 3: Hydrogen peroxide structure (*5*).

- Another atom bonded to the first is chosen and placed along z-axis, length of the bond connecting them is specified.

O1

H1 O1 0.9

- A third atom bonded to either one of the previous two atoms, bond angle formed by the two bonds, and bond length are specified

O1

H1 O1 0.9

O2 O1 1.4 H1 105.0

- A fourth atom is chosen, bond length, bond angle, and a dihedral angle are specified.

O1

H1 O1 0.9

O2 O1 1.4 H1 105.0

H2 O2 0.9 O1 105.0 H1 120

Dihedral angle describes the angle that the fourth atom makes with respect to the plane formed by the other three (0-360$^0$), it is visualized by Newman projection.

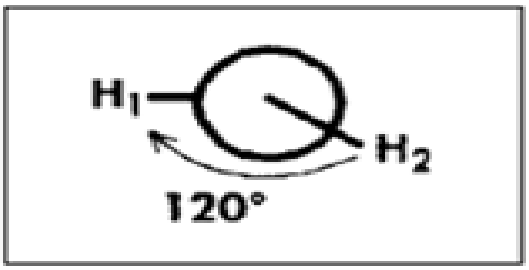


Figure 4: Newman projection for hydrogen peroxide (*5*).

3) After all required informations are filled in the job entry window, run bottom is pressed, and the file is saved.

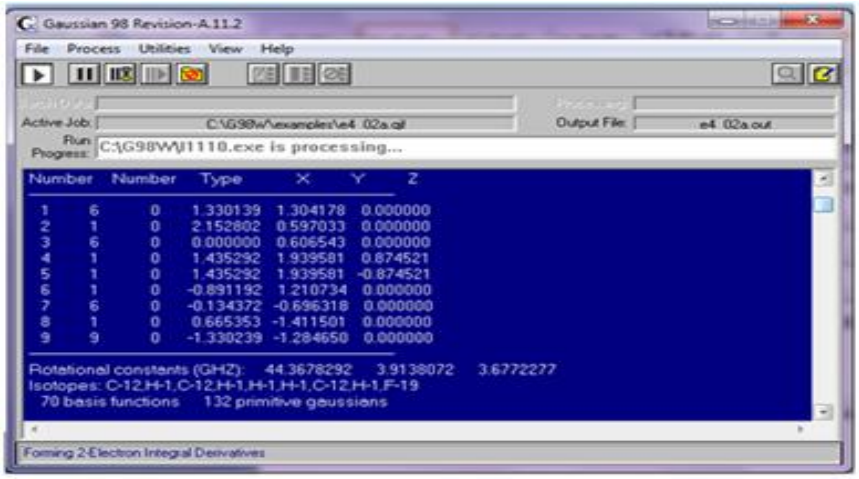


Figure 5: Program in process.

4) When the job is finished, it will display an argument. The output file is saved as text file, and the results should be examined (*5*).

**2) Running Gaussian by using the Gaussian view**

In running Gaussian via Gaussian view, one mainly wroks with Gaussian view, which in turn will order Gaussian to do the calculation. The following steps are used.

1) When Gaussian view program is opened, two windows are opened; one contains the toolbars and builder while the second displays the structure being built.

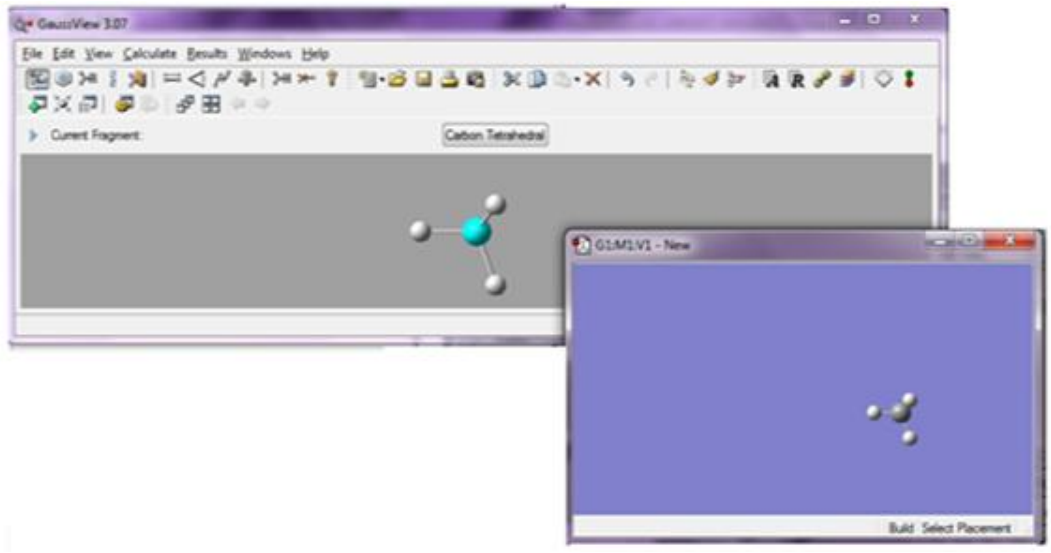


Figure 6: The two windows of Gaussian view 3.07.

2) Building Molecule

By using the construction windows one can choose any element, any hybridization, any group, and build the molecule, by clicking on the second window (*9*). After the structure is built, then calculation options should be chosen (*9*).

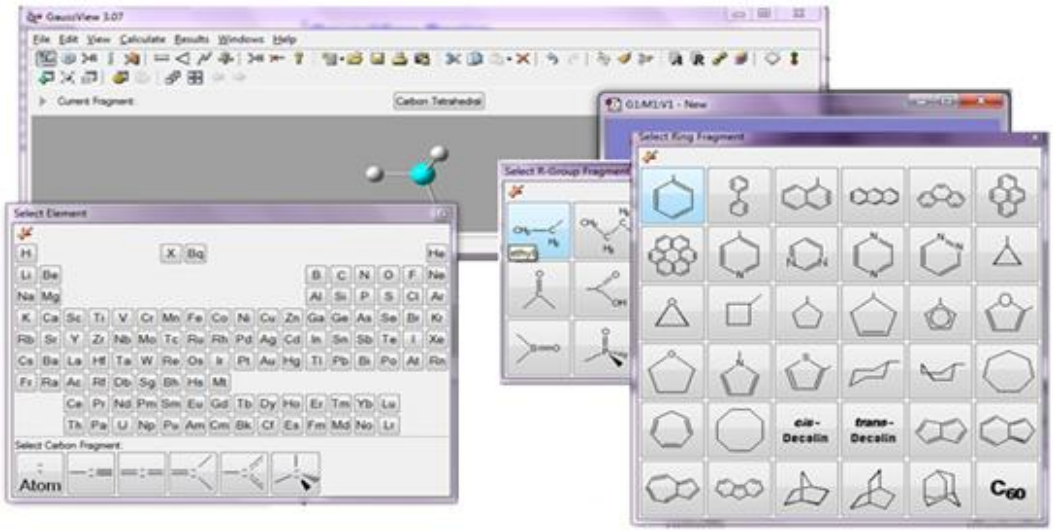


Figure 7: The windows that help construct molecules.

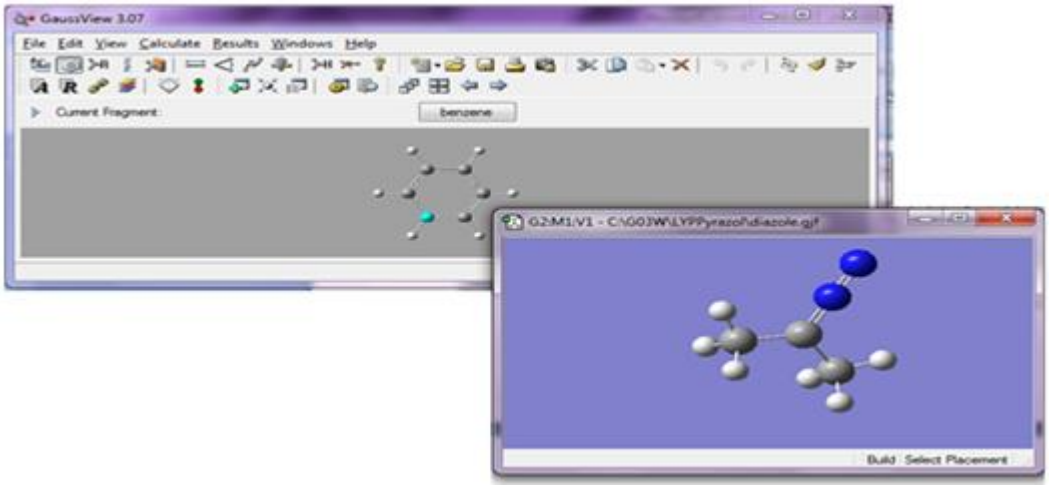


Figure 8: A constructed structure.

3) Gaussian calculation setup window is now opened, it has many tabs corresponding to different element of the calculation, and the first is job type, at which the type of calculations is selected. The types of calculations are energy, optimization, frequency, NMR, IRC, and others (*9*).

4) A method and the basis sets are selected from the method tab; this is the most important tab, since the basic options are chosen from it (*9*).

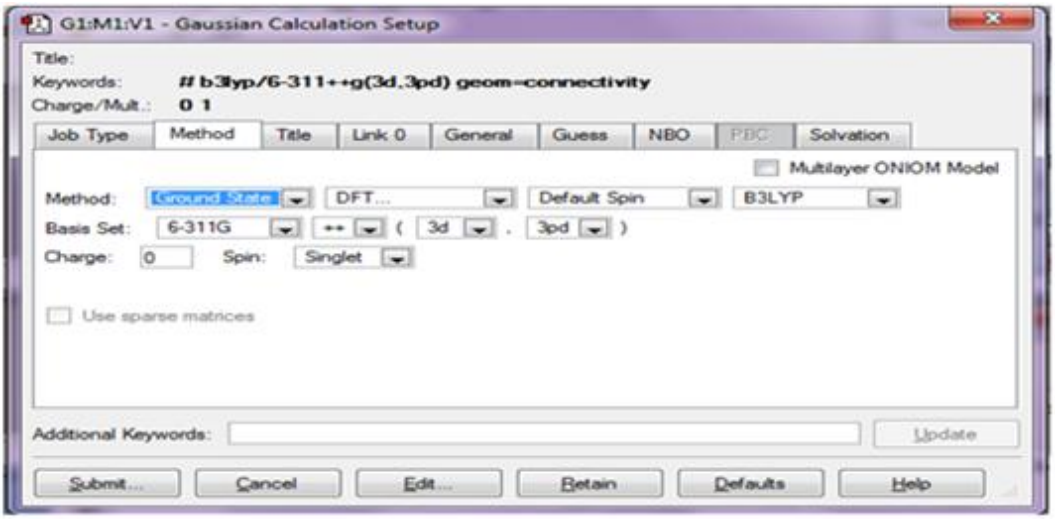

Figure 9: Method options.

5) The Title Panel holds a field used for the Gaussian title section designed to contain a brief description of the job. The Link 0 Panel is used for entering Link 0 commands for the job, this panel specifies a

name for the checkpoint file and also the amount of memory to use for this job (*9*).

6) The Guess, NBO, and Solvation are:

* General panel allows selecting some commonly used general calculation options (*9*).

* Guess panel contains settings related to the initial guess (*9*).

* NBO panel is used to select NBO analysis at the conclusion of the Gaussian job (Natural Bond Orbital) (*9*).

* Solvation panel allows specifying that the calculation is to be performed in solution rather than in the gas phase (*9*).

7) Gaussian View promotes to view the output file (.out). The output file contain the resulst that one request the program to calculate. In performing optimization and frequency calculation, Gaussian will first optimize the structure then it will compute vibrational frequencies using the optimized structure (*9*).

8) Results can be viewed from the result tab. Summary, vibrations, surfaces, charges, NMR, optimized structure, NBO, and all output file as text file.

8.a) Summary of results, show file type, calculation type, method, and basis set, the calculated energy, the point group, the dipole moment, and the time needed to finish the job.

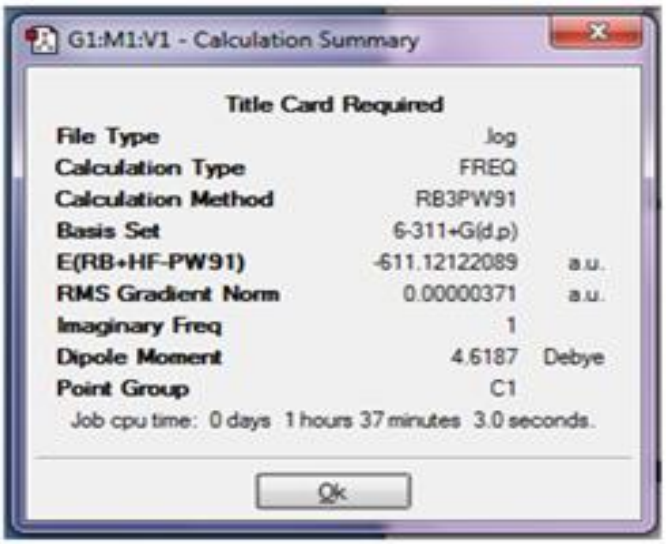


Figure 10: Summary of calculation parameters.

8.b) Display vibrations and vibrational spectrum

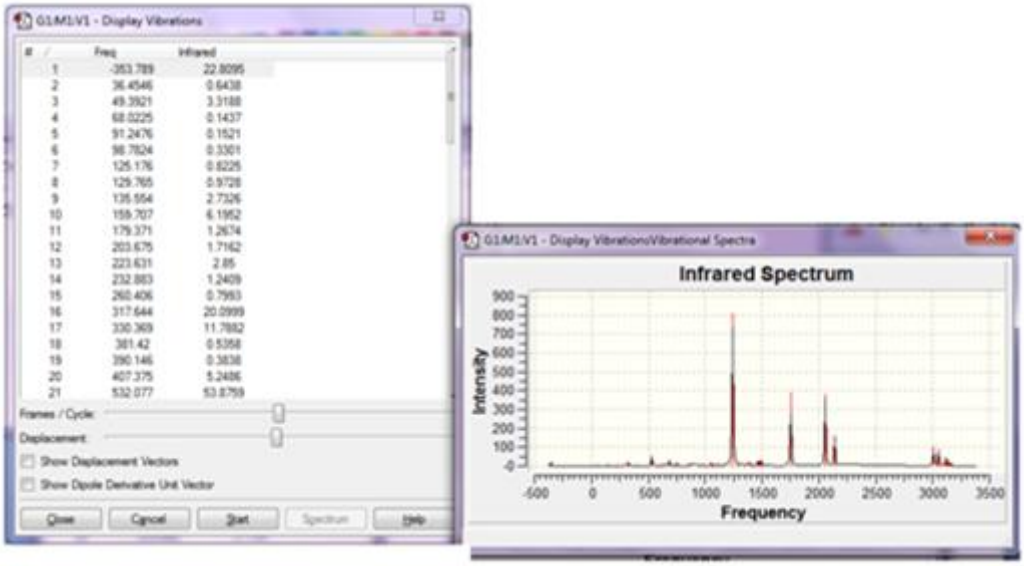


Figure 11: Vibrations and vibrational spectra.

8.c) View detailed output file as text file. Output files differ from each other according to the calculation type. However, all types are similar in many parts:

- Copyright for Gaussian 03.
- Official citation for the Gaussian 03.
- The version of Gaussian 03.
- The route section, title section, and molecular specification from the input file.
- CPU time and others.

**Job types of computational calculations**

There are several job types that can be carried out in computational. Such as:

a) Single point energy calculations.

b) Geometry optimization.

c) Frequency calculations

d) Intrinsic Reaction Coordinate (IRC) calculations (*5*).

**a) Single point energy calculations**

A single point energy (SPE) calculation is a prediction of the wavefunction and energy, and related properties for a molecule of a particular geometric structure (*5,10*). It is performed at a single and

fixed point. This calculation is performed for a new molecule to obtain basic information which could be used as starting point for an optimization, or for an optimized molecule to get accurate results, or if it is the only way to analyze a system of interest (*5*). Single point calculation can be done with any level of theory and with any level of basis set (*5*).

**b) Geometry optimization**

One of the job types of Gaussian is geometry optimization at which the best geometry of the molecule with minimum energy (*11*). Since the energy variation of molecular structure is in small change, at which called potential energy surface (PES), then the geometry optimization of the structure seeks to minimize this (PES) at stationary point (*5*). PES displays the energy of a molecule as a function of its geometry. PES is represented as 3-D plot like in Figure12.

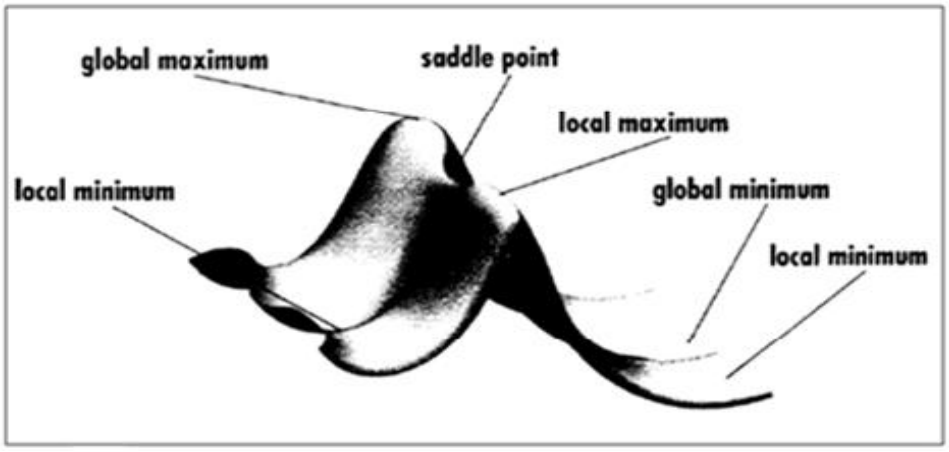


Figure 12: Model of potential energy surfaces (PES) (*5*).

There are many points at which it is low energy (local minimum), but there is one point at which it is the lowest energy (global minimum), which is assigned to has the optimized structure. If the structure to be optimized is a transition structure, then it would be the highest point on the lowest energy path (*5*,*12*).

The general procedure for optimizing a structure of a molecule, is to start with guess of a structure in the input file at which it is believed to resemble the optimized structure, then submitting it to Gaussian algorithm that systematically (iteratively) changes the geometry in such a way that the energy decrease until minimum energy is achieved , and this occurs when the convergence tests are attained (*5*,*11*,*12*).

The input file for optimization structure job contains the keyword (opt), the optimization is done by using the chosen level of theory and basis set (*5*). After the structure reaches its stationary point, the final optimized structure appears as in Figure 13 (*5*).

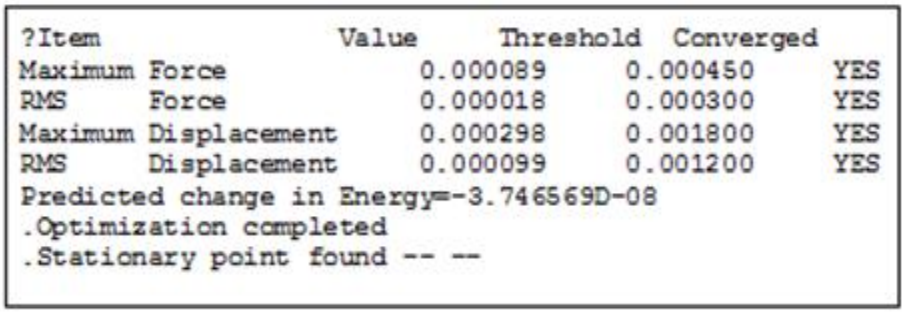

```
?Item               Value     Threshold  Converged
Maximum Force            0.000089     0.000450     YES
RMS     Force            0.000018     0.000300     YES
Maximum Displacement     0.000298     0.001800     YES
RMS     Displacement     0.000099     0.001200     YES
Predicted change in Energy=-3.746569D-08
.Optimization completed
.Stationary point found -- --
```

Figure 13: Convergence test.

**c) Frequency calculations**

Frequency calculations predict the IR spectra of molecules in their ground and excited states, compute force constants, and compute the zero-point vibration and thermal energy corrections and thermodynamic quantities such as enthalpy and entropy (*5*). Frequency calculations are valid only at stationary points on potential energy surface. Thus, it must be done just for optimized structure (*5*). So it is convenient in an output file to choose the job type (opt+ freq), first optimization occur then frequency calculation (*5*).

Frequency calculations output include thermochemical analysis carried out at 298.15K and 1 atmosphere of pressure (*5*). Thermochemical analysis consists of two parts, one lists the predicted thermodynamic quantities including the thermal energy correction, heat capacity and entropy as shown in Figure 14, the second part gives the zero-point energy for the system (*5,13*). The zero-point energy is a correction to the electronic energy of the molecule to account for the effects of the molecular vibrations (*5,13*). Figure 15 shows the zero-point and thermal energy-corrected properties.

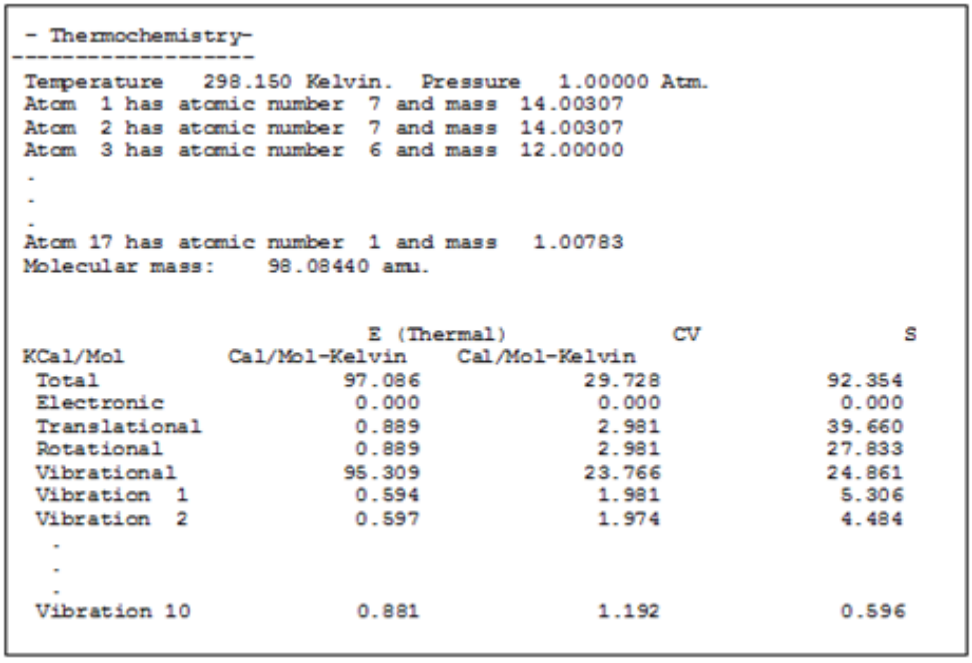

```
 - Thermochemistry-
 -------------------
 Temperature   298.150 Kelvin.  Pressure   1.00000 Atm.
 Atom  1 has atomic number  7 and mass  14.00307
 Atom  2 has atomic number  7 and mass  14.00307
 Atom  3 has atomic number  6 and mass  12.00000
  .
  .
  .
 Atom 17 has atomic number  1 and mass   1.00783
 Molecular mass:    98.08440 amu.


                          E (Thermal)             CV                S
 KCal/Mol        Cal/Mol-Kelvin    Cal/Mol-Kelvin
  Total                  97.086            29.728            92.354
  Electronic              0.000             0.000             0.000
  Translational           0.889             2.981            39.660
  Rotational              0.889             2.981            27.833
  Vibrational            95.309            23.766            24.861
  Vibration  1             0.594             1.981             5.306
  Vibration  2             0.597             1.974             4.484
    .
    .
    .
  Vibration 10             0.881             1.192             0.596
```

Figure 14: Thermodynamic quantities presented in output file of frequency calculations.

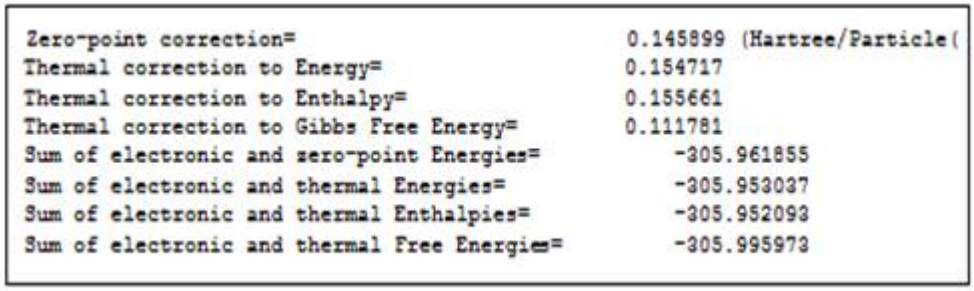

```
 Zero-point correction=                          0.145899 (Hartree/Particle(
 Thermal correction to Energy=                   0.154717
 Thermal correction to Enthalpy=                 0.155661
 Thermal correction to Gibbs Free Energy=        0.111781
 Sum of electronic and zero-point Energies=          -305.961855
 Sum of electronic and thermal Energies=             -305.953037
 Sum of electronic and thermal Enthalpies=           -305.952093
 Sum of electronic and thermal Free Energies=        -305.995973
```

Figure 15: Zero-point and thermal energy-corrected proporties in output file.

Where,

$$Sum\ of\ electronic\ and\ ZPE(E_0) = E_{electr} + ZPE \qquad (1)$$

$$Sum\ of\ electronic\ and\ thermal\ Energies(E) = E_0 + E_{vib} + E_{rot} + E_{transl} \quad (2)$$

$$Sum\ of\ electronics\ and\ thermal\ Enthalpies(H) = E + RT \quad (3)$$

$$Sum\ of\ electronic\ and\ thermal\ free\ Energies(G) = H - TS \quad (4)$$

(*5*,*13*).

Computed raw frequency values contain systematic errors resulting in data overestimate. Therefore, an empirical factor is used to scale frequencies predicted by computational methods (*5*). This factor depends on the method and size of basis sets used in calculations, it is about 0.8929 for HF method and it ranges between 0.9613 for B3LYP/6-31G(d) and 0.9679 for B3LYP/6-311++G(3df,3pd) (*5*,*14*), assuming that B3LYP/6-311++G(3df,pd) lies in this range, then the factor can be taken at 0.9646.

**d) Intrinsic Reaction Coordinate (IRC) calculations**

Completing a transition structure optimization does not mean that a right transition structure is obtained (*5*). The way to determine it is

using Intrinsic Reaction Coordinate (IRC) procedure, at which the calculation starts from the saddle point and follows the path in both directions from the transition state, optimizing the geometry of the molecular system at each point along the path, so the two minima on potential energy surface are connected by a path that passes the transition state (*5*). IRC calculations require both an optimized transition structure and the corresponding force constants (*5*). The used keyword which is written in route section to request the reaction path is IRC (*5*).

- Appendix References**:**

1) Pople, J. *J. Comput. Chem.***2004**, 25, fmv–viii.

2) Levine, I. *Quantum Chemistry*, 5th ed.; Prentice Hall: New Jersey, 2000.

3) Gaussian 09, http://www.gaussian.com/g_prod/g09.htm. (December 29, 2010).

4) Young, D. *Computational Chemistry: A Practical Guide for Applying Techniques to Real-World Problems*; John Wiley & Sons: 2001.

*5)* Foresman, J.; Frisch, A. *Exploring Chemistry with Electronic Structure*,2nd ed.; Gaussian, Inc.: USA, 1996.

6) Young, D. Using Gaussian Checkpoint Files, http://www.ccl.net/cca/documents/dyoung/topics-orig/checkpoint.html. (December 30, 2010).

7) Shodor Education Foundation, Inc., Z-Matrix to Cartesian Coordinate Conversion Page, 2000. http://www.shodor.org/chemviz/zmatrices/babel.html. (December 30, 2010).

8) A Brief introduction to Gaussian, H2O: A Sample Run. http://chemlabs.nju.edu.cn/.../Gaussian/Lecture%20for%20Gaussian/gaussian_tut. Pdf( December 30,2010).

9) Help, Gaussian view 3.07, Gaussian Inc.; 2003.

10) Cheung, D. Structures and Properties of Liquid Crystals and Related Molecules from Computer Simulation. PH.D. Thesis, University of Durham, October 2002. http://cmt.dur.ac.uk/sjc/thesis_dlc/thesis.html (December 31, 2010).

11) Bachrach, S. *Computational Organic Chemistry*, John Wiley & Sons, Inc: New Jersey, 2007.

12) Lewars, E. *COMPUTATIONAL CHEMISTRY Introduction to the Theory and Applications of Molecular and Quantum Mechanics*; Kluwer Academic Publishers: 2004.

13) Ochterski, J. Thermochemistry in Gaussian, Guassian, Inc.; 2000.

14) Andersson, M. P.; Uvdal, P. *J. Phys. Chem. A***2005**, 109, 2937-2941.